

# 1 **Highlights on mantle deformation beneath the Western Alps with** 2 **seismic anisotropy using CIFALPS2 data**

3 Pondrelli Silvia<sup>1</sup>, Salimbeni Simone<sup>1</sup>, Confal Judith M.<sup>1</sup>, Malusà Marco G.<sup>2</sup>, Paul Anne<sup>3</sup>, Guillot  
4 Stephane<sup>3</sup>, Solarino Stefano<sup>4</sup>, Eva Elena<sup>4</sup>, Aubert Coralie<sup>3,2</sup>, Zhao Liang<sup>5</sup>

5 <sup>1</sup> Istituto Nazionale di Geofisica e Vulcanologia, Sezione di Bologna, Bologna, Italy

6 <sup>2</sup> Department of Earth and Environmental Sciences, University of Milano-Bicocca, Piazza della Scienza 4, 20126 Milan, Italy

7 <sup>3</sup> Univ. Grenoble Alpes, Univ. Savoie Mont Blanc, CNRS, IRD, UGE, ISTerre, Grenoble, France

8 <sup>4</sup> Istituto Nazionale di Geofisica e Vulcanologia, ONT, Genova, Italy

9 <sup>5</sup> State Key Laboratory of Lithospheric Evolution, Institute of Geology and Geophysics, Chinese Academy of Sciences,  
10 Beijing, China

11

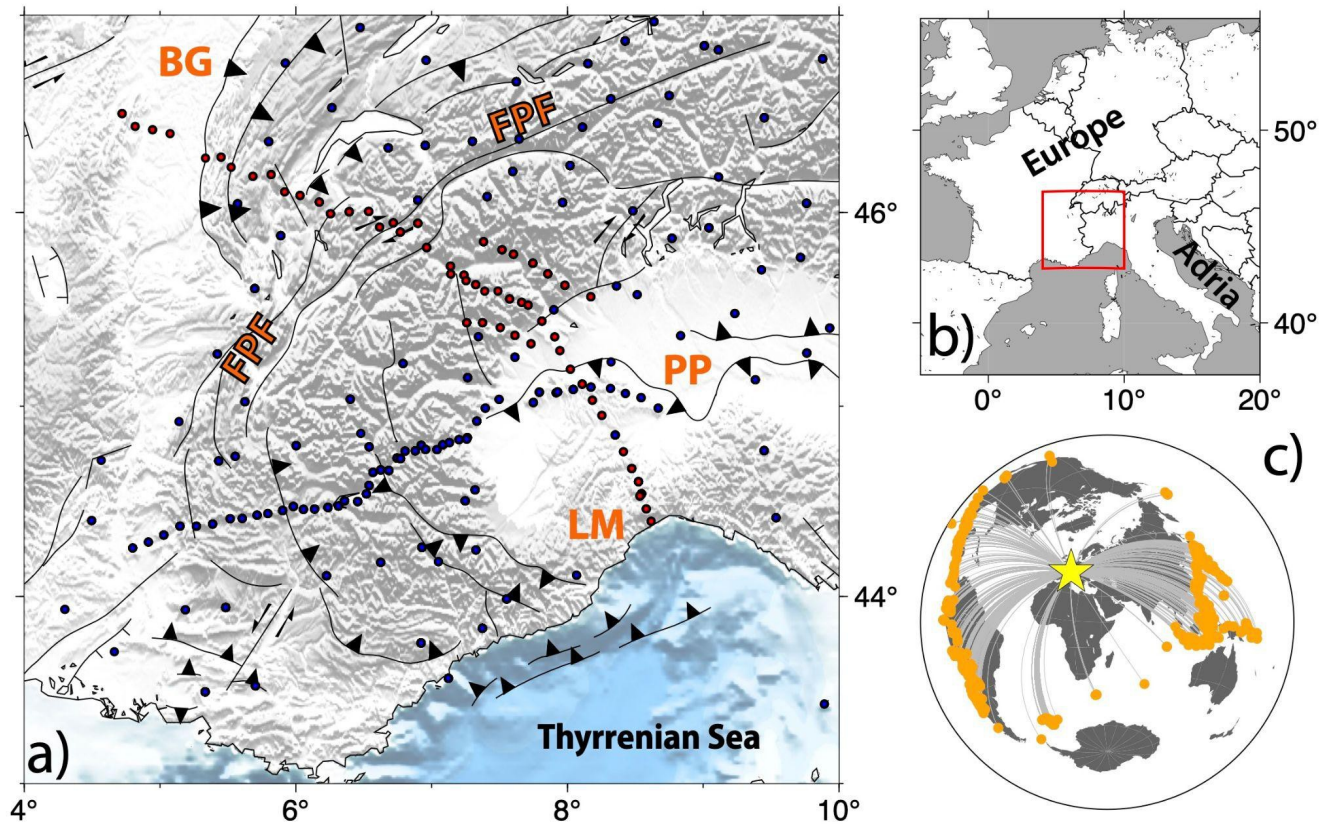
12 *Correspondence to:* Silvia Pondrelli (silvia.pondrelli@ingv.it)

13 **Abstract.** There are still open questions about the deep structure beneath the Western Alps. Seismic velocity tomographies  
14 show the European slab subducting beneath the Adria plate, but all these images did not clarify completely the possible  
15 presence of tears, slab windows, or detachments. Seismic anisotropy, considered as an indicator of mantle deformation and  
16 studied using data recorded by dense networks, allows a better understanding of mantle flows in terms of location and  
17 orientation at depth. Using the large amount of shear wave splitting and splitting intensity measurements available in the  
18 Western Alps, collected through the CIFALPS2 temporary seismic network, together with already available data, some new  
19 patterns can be highlighted and gaps left by previous studies can be filled. Instead of the typical seismic anisotropy pattern  
20 parallel to the entire arc of the Western Alps, this study supports the presence of a differential contribution along the belt,  
21 only partly related to the European slab steepening. A nearly NS anisotropy pattern beneath the external Western Alps, a  
22 direction that cuts the morphological features of the belt, is clearly found with the new CIFALPS2 measurements. It is  
23 however confirmed that the asthenospheric flow from Central France towards~~about the possible presence of tears, slab~~  
24 ~~windows or detachments. Seismic anisotropy, addressed as an indicator of mantle deformation and studied using data~~  
25 ~~recorded by dense networks, may shed some light about the location and orientation of mantle flow at depth. Using the large~~  
26 ~~amount of shear wave splitting and splitting intensity measurements available in the Western Alps, collected through the~~  
27 ~~CIFALPS2 temporary seismic network, together with already available data, highlight some new patterns, filling the gaps~~  
28 ~~left by previous studies. Instead of the typical seismic anisotropy pattern parallel to the entire arc of the Western Alps, this~~  
29 ~~study supports the presence of a differential contribution along the belt, only partly related to the European slab retreat. A~~  
30 ~~nearly NS anisotropy pattern beneath the external Alps, direction that cuts the morphological features of the belt, is clearly~~

31 found with the new CIFALPS2 measurements. It is however confirmed that the asthenospheric flow from Central France  
32 toward the Tyrrhenian Sea, is turning around the southern tip of the European slab.

## 33 1 Introduction

34 Seismic anisotropy has become a convincing study tool, mainly in the areas where recent and past geodynamic evolution  
35 have left their marks in the mantle deformation and its patterns (e.g. Long and Silver, 2009; Long, 2013 for a complete  
36 review). Several methods exist to measure seismic anisotropy. Depending on the used seismic phase, signal, and frequency,  
37 it is possible to measure seismic anisotropy at different depths and relate it to different parts of the Earth's structure, last but  
38 not least with seismic anisotropy tomography (e.g. Zhao et al., 2023). Local seismicity and surface waves are used to  
39 measure crustal seismic anisotropy, usually attributed to fractures or/and the state of stress of crustal depths (i.e. Crampin  
40 and Peacock, 2008; Okaya et al., 2018). Using seismic signals that travel deeper, it is possible to sample the deformation at  
41 lithospheric-asthenospheric depths. For instance, Pn phases record the seismic anisotropy immediately below the Moho in  
42 the lithospheric mantle (i.e. Diaz et al., 2013). On the other hand, using core phases (SKS, SKKS, etc) that record  
43 information on the receiver branch of their path, we can sample areas where recent and past geodynamic evolution have left  
44 their marks in the mantle deformation and its patterns (e.g. Long and Silver, 2009; Long, 2013 for a complete review).  
45 Several methods exist to measure seismic anisotropy. Depending on the used seismic phase, the kind of signal and  
46 frequency, it is possible to measure seismic anisotropy at different depths and relate it to different parts of the Earth's  
47 structure, last but not least with seismic anisotropy tomography (e.g. Zhao et al., 2023). Local seismicity and surface waves  
48 are used to measure crustal seismic anisotropy, usually attributed to fractures or/and the state of stress of crustal depths (i.e.  
49 Crampin and Peacock, 2008; Okaya et al., 2018). Using seismic signals that travel deeper, it is possible to sample the  
50 deformation at the lithospheric-asthenospheric depths. For instance, Pn phases record the seismic anisotropy immediately  
51 below the Moho in the lithospheric mantle (i.e. Diaz et al., 2013). On the other hand, using core phases (SKS, SKKS, etc)  
52 that record information on the receiver branch of their path, we can sample the seismic anisotropy that is thought to be  
53 mainly concentrated in the upper mantle.



54  
55  
56  
57  
58

**Figure 1 - a)** Map of the study region, focusing on the Western Alps. In red are indicated the CIFALPS2 stations, while in blue are permanent and previous temporary stations (i.e. CIFALPS and AlpArray). FPF = Frontal Pennine Fault, BG = Bresse Graben, PP = Po Plain, LM = Ligurian Mountains; b) the red square is the study area reported in a); c) map of all seismic events used in this study, with the star centered in the study region.

59

60 The azimuth of the fast velocity direction and the delay time, the two parameters that commonly result  
 61 from shear wave splitting analysis of core phases, are interpreted respectively as the direction assumed  
 62 by olivine crystals, the principal mineral component of the upper mantle when mantle undergoes  
 63 deformation, and the amount of anisotropy crossed by a seismic ray. ~~Azimuth of the fast velocity~~  
 64 ~~direction and delay time, the two parameters that commonly result from shear wave splitting analysis of~~  
 65 ~~core phases, are interpreted respectively as the direction assumed by olivine crystals, the principal~~  
 66 ~~mineral component of the upper mantle, when mantle undergoes deformation, and the amount of~~  
 67 ~~anisotropy crossed by a seismic ray.~~

68 In the Alps these kinds of measurements improved immensely with recent temporary experiments such  
69 as AlpArray (Hetényi et al., 2018) or CIFALPS and CIFALPS2 in the western sector of the chain (Zhao  
70 et al., 2015; 2016; 2018), which complemented the permanent seismic networks operating in the region.

71

72 The European Alps originated in the late Cretaceous from the oblique subduction of the Alpine Tethys  
73 under the Adria microplate. The subduction evolved in a continental collision during the late Cenozoic  
74 (e.g., Handy et al., 2010, 2013 and references therein). In the Western Alps, the tectonic lineament that  
75 worked as the suture accommodating the shortening between the two plates is the Frontal Pennine Fault  
76 (FPF, Fig. 1). Even though the geological history of this belt is one of the best studied and well known  
77 in the world, the geodynamic evolution of the European slab, in terms of position and possible presence  
78 of slab break off, is still poorly understood  
~~Figure 1 – a) Map of the study region, focusing on the  
Western Alps. In red are indicated the CIFALPS2 stations, while in blue are permanent and previous  
temporary stations (i.e. CIFALPS and AlpArray). FPF = Frontal Pennine Fault; b) the red square is the  
study area reported in a); c) map of all seismic events used in this study, with the star centered in the  
study region.~~  
82

83

84 All travel time tomographic studies identified at mantle depth the presence of seismic velocity heterogeneities interpreted  
85 as the European slab subducting beneath the Adria plate (e.g. Piromallo and Morelli, 2003; Lippitsch et al., 2003; Kissling et  
86 al., 2006; Giacomuzzi et al., 2011; Paffrath et al., 2021; Rappisi et al., 2022). However, the existence of possible slab  
87 detachments, windows or tears is debated, for instance beneath the Western Alps (e.g., Zhao et al., 2016). The first CIFALPS  
88 experiment (see Malusà et al., 2021 and references therein) clarified several points, starting from the first seismic evidence  
89 of subducted European continental lithosphere beneath the Adria lithosphere (Zhao et al., 2015), to a tomographic model  
90 with a continuous slab beneath this region (Zhao et al., 2016). In addition, recent seismic anisotropy analyses of the Western  
91 to the Central Alps shed additional light on potential discontinuities of the slabs, thanks to the possible mapping of mantle  
92 flows that would occur through them (Petrescu et al., 2020; Salimbeni et al., 2018).

93 The additional contribution of CIFALPS2, a temporary experiment deployed for 14 months from 2018 to 2019 (Zhao et al.,  
94 2018), on mantle seismic anisotropy mapping and interpretation, was expected to fill a gap in the northwestern part of the  
95 Alpine arc (red dots in Figure 1). Receiver function and ambient-noise tomography studies have underlined the north-south  
96 differences in the lithospheric structure along the belt strike (Paul et al., 2022). Therefore, there is a need for measuring  
97 additional seismic anisotropy in the mantle from CIFALPS2 data and to compare them to previous results.

98 | ~~In the Alps these kinds of measurements had a large improvement with recent temporary experiments such as AlpArray~~  
99 | ~~(Hetényi et al., 2018) or CIFALPS and CIFALPS2 in the western sector of the chain (Zhao et al., 2015; 2016; 2018), that~~  
100 | ~~complemented the permanent seismic networks operating in the region. The main interest in the Alps is related to the still~~  
101 | ~~open questions concerning the deep structure and geodynamic evolution of this orogenic belt.~~

102 | ~~All travel time tomographic studies identified the presence at mantle depth of seismic velocity heterogeneities interpreted as~~  
103 | ~~the European slab subducting beneath the Adria plate (e.g. Piromallo and Morelli, 2003; Lippitsch et al., 2003; Kissling et~~  
104 | ~~al., 2006; Giacomuzzi et al., 2011; Paffrath et al., 2021; Rappisi et al., 2022). However, the existence of possible slab~~  
105 | ~~detachments, windows or tears is still debated, for instance beneath the Western Alps (e.g., Zhao et al., 2016). The first~~  
106 | ~~CIFALPS experiment (see Malusà et al., 2021 and references therein) clarified several points, starting from the first seismic~~  
107 | ~~evidence of subducted European continental lithosphere beneath the Adria lithosphere (Zhao et al., 2015) to a tomographic~~  
108 | ~~model with a continuous slab beneath this region (Zhao et al., 2016). In addition, recent seismic anisotropy analyses of the~~  
109 | ~~Western to the Central Alps shed additional light on potential discontinuities of the slabs, thanks to the possible mapping of~~  
110 | ~~mantle flows that would occur through them (Petrescu et al., 2020; Salimbeni et al., 2018).~~

111 | ~~The additional contribution of CIFALPS2, the temporary experiment deployed for 14 months from 2018 to 2019 (Zhao et~~  
112 | ~~al., 2018), on mantle seismic anisotropy mapping and interpretation, was expected to fill a gap in the northwestern part of the~~  
113 | ~~Alpine arc (red dots in Figure 1). Receiver function and ambient noise tomography studies have underlined the north-south~~  
114 | ~~differences in the lithospheric structure along the belt strike (Paul et al., 2022). Therefore, there is a need for measuring~~  
115 | ~~seismic anisotropy in the mantle from CIFALPS2 data and compare it to previous results.~~

116 |

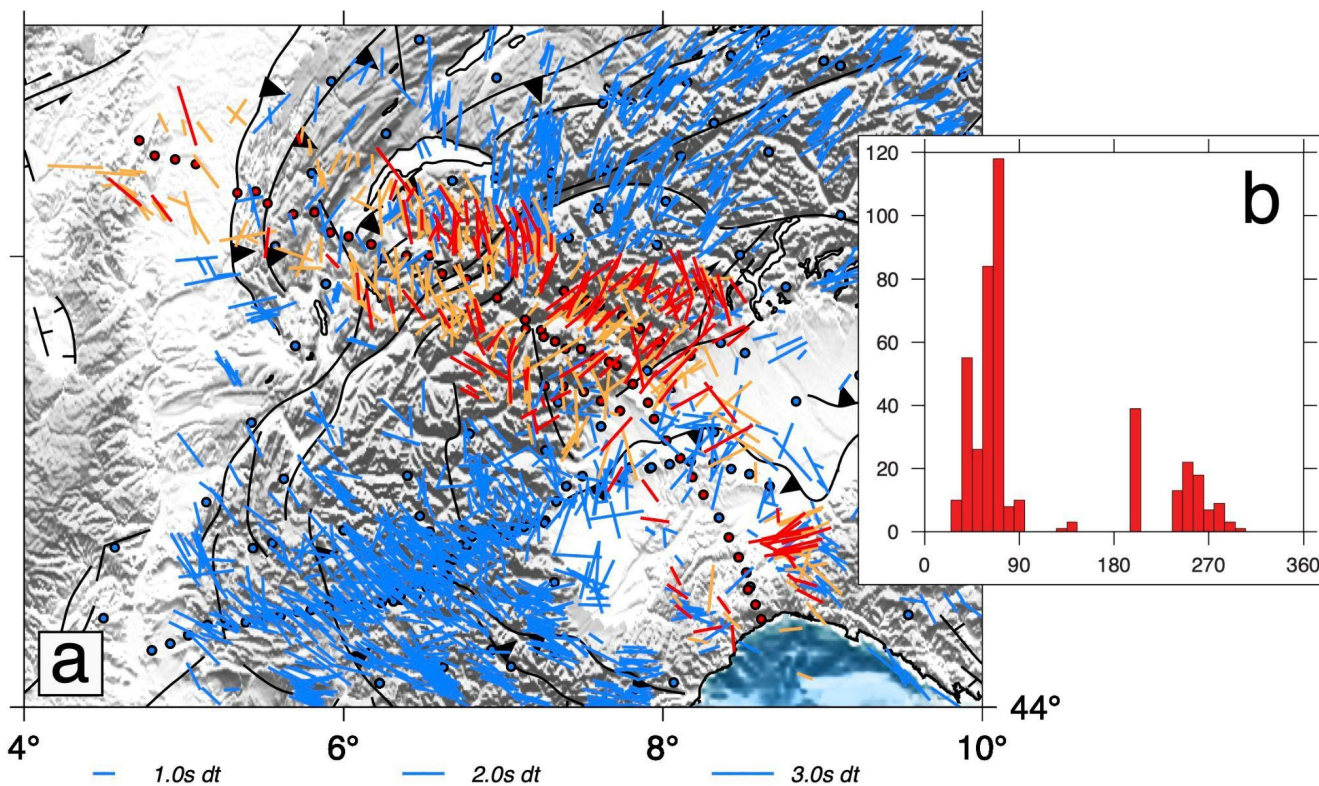
117 | ~~In this study, we present the results of the analysis of data recorded by CIFALPS2, -describing them in an integrated view~~  
118 | ~~with previous shear wave splitting measurements (SWS) to identify new features in the mantle and draw hypotheses on their~~  
119 | ~~origin.~~

## 120 | **2 Data and Methods**

121 | ~~Data used for the analysis are the recordings at CIFALPS2 stations (Figure 1; Zhao et al., 2018; doi:~~  
122 | ~~10.15778/RESIF.XT2018) of teleseismic earthquakes with a magnitude  $M > 6.0$ , that occurred between June 2018 and~~  
123 | ~~December 2019 and are located at a distance interval from the network between  $88^\circ$  and  $120^\circ$ , typical to guarantee well~~  
124 | ~~isolated SKS phases in the waveforms. 80 to 150 events for each of the 56 temporary stations have been analyzed~~  
125 | ~~located at a distance interval from the network between  $88^\circ$  and  $120^\circ$ , typical to guarantee well isolated SKS~~  
126 | ~~phases in the waveforms. 80 to 150 events for each of the 56 temporary stations have been selected~~  
127 | ~~(Figure 1).~~

128 |

129 The entire SWS analysis has been conducted using the code SplitRacer (Reiss and Rumpker, 2017), based on the Silver and  
 130 Chan (1991) method and thus on the minimization of the energy on the transverse component. Different filters have been  
 131 applied according to the amount of noise at the various sites. For most of them, located in the Alps or Ligurian mountains, a  
 132 bandpass filter between 7 and 20 s worked well, while for instance sites in the Po Plain needed different choices, i.e. 5-30 s.  
 133 The signal to noise ratio (SNR) was also used to avoid noisy waveforms; initially, the threshold was 3, but where the amount  
 134 of events to be analyzed was scarce we decreased it down to 1.5, again mainly for sites located in or close to the Po Plain. It  
 135 is worth noticing that SWS analysis recovers fast-velocity directions, assuming a single layer of horizontal anisotropy.  
 136 Moreover, the depth at which this anisotropy is located is difficult to define, that a single layer is anisotropic, and  
 137 characterized by horizontal anisotropy. Moreover, the depth at which this anisotropy is located is difficult to define but it is  
 138 classically assumed that most measured anisotropy is in the upper mantle (Savage, 1999). Thus, it is common to visualize  
 139 any lateral variation by plotting results at the piercing point of the incident ray at 150 km depth (Figure 2a).



140 **figure 2 - a) Map of single SWS measurements for the study region, plotted at the location of the piercing point of the ray at 150 km**  
 141 **depth. In red and orange are good and fair measurements from CIFALPS2 stations (red circles) respectively. In the background,**  
 142 **in light blue, previous SWS measurements and stations; b) histogram of back azimuths of events used in the analysis.**  
 143

144 To improve the resolution of the data to be discussed and interpreted, splitting intensity (SI)  
 145 measurements have been performed on the same CIFALPS2 recordings used for SWS measures (Table

146 S2 in Supplementary Material). Splitting intensity is measured by projecting the transverse component  
147 on the radial component derivative; it is related to the variations of the amplitude of the transverse  
148 component with the back azimuth (Chevrot, 2000; Monteiller and Chevrot, 2010). A routine based on  
149 Kong et al. (2015) and Confal et al. (2023) was used to calculate splitting intensity values from  
150 waveforms with a cut-off of 15 s before and 30 s after the supposed SKS arrival. A dominant period of  
151 12 s is used for the Wiener filtering. To filter out low quality waveforms in this automatic process a  
152 cross-correlation coefficient of |0.7| and splitting intensities values and error threshold of |2.0| and 0.5  
153 respectively were used (Baccheschi et al., under revision). With splitting measurements from at least  
154 four different 10° bins of back azimuths, the classical evaluation of the anisotropy parameters, i.e. the  
155 azimuth of the fast direction phi and the delay time dt, is obtained by fitting a sinusoid to the back  
156 azimuthal dependence of splitting intensity values (Chevrot, 2000). In particular, the sinusoid amplitude  
157 and phase give dt and phi respectively (see Figure S1 in Supplementary M1 in Supplementary  
158 Material). Splitting intensity is measured by projecting the transverse component on the radial  
159 component derivative; it is related to the variations of the amplitude of the transverse component with  
160 the back azimuth (Chevrot, 2000; Monteiller and Chevrot, 2010). A routine based on Kong et al. (2015)  
161 and Confal et al. (2023) was used to calculate splitting intensity values from the waveform with a cut-  
162 off of 15 s before and 30 s after the supposed SKS arrival. A dominant period of 12 s is used for the  
163 Wiener filtering. To filter out low quality waveforms in this automatic process a cross-correlation  
164 coefficient of |0.7| and splitting intensities values and error threshold of |2.0| and 0.5 respectively were  
165 used (Baccheschi et al., under revision). With splitting measurements from at least four different 10°  
166 bins of back azimuths, the classical evaluation of the anisotropy parameters, i.e. the azimuth of the fast  
167 direction phi and the delay time dt, is obtained by fitting a sinusoid to the back azimuthal dependence of  
168 splitting intensity values (Chevrot, 2000). In particular, the sinusoid amplitude and phase give dt and  
169 phi respectively (see Figure S2 in supplementary material as an example).

170 Figure 2— a) Map of single SWS measurements for the study region, plotted at the location of the piercing point of the ray at 150  
171 km depth. In red and orange are good and fair measurements from CIFALPS2 stations (red circles) respectively. In the  
172 background, in light blue, previous SWS measurements and stations; b) histogram of back azimuths of events used in the analysis.

### 174 | 3 Shear wave splitting results

175 | From SWS analysis we obtained more than 400 pairs of splitting parameters ( $\phi$  and  $\Delta t$ ) if we consider together good (170)  
176 | and fair (241) results (Figure 2a, good in red, fair in orange; all results are available at <https://osf.io/nqxxk4>, Pondrelli et al.,  
177 | 2023). The quality assignment is given following the SplitRacer criteria (Reiss and Rumpker, 2017), considering the  
178 | visibility of the phase, the ellipticity of the initial particle motion and its linearity in the final stage, and the errors associated  
179 | with  $\phi$  and  $\Delta t$  values. In Figure S2 of the Supplementary Material some measurement examples are shown. In addition,  
180 | nearly 600 null measurements have been obtained (Figure S3 in Supplementary Material), where a null is considered when  
181 | no split appears in the signal (i.e. no energy in the transversal component). This is due either to the absence of anisotropy or  
182 | to the initial polarization being parallel to the fast or slow anisotropic direction. A high percentage of good and fair results  
183 | were obtained for events with a NE back azimuth, so it should be taken into account that this direction is oversampled  
184 | (Figure 2b). fast polarization direction  $\phi$  and delay time  $\Delta t$ ) if we consider together good and fair results (Figure 2a, good in  
185 | red, fair in orange; all results are available at <https://osf.io/nqxxk4>, Pondrelli et al., 2023). The quality assignment is given  
186 | following the SplitRacer criteria (Reiss and Rumpker, 2017), considering the visibility of the phase, the ellipticity of the  
187 | initial particle motion and its linearity in the final stage, and the errors associated with  $\phi$  and  $\Delta t$  values.

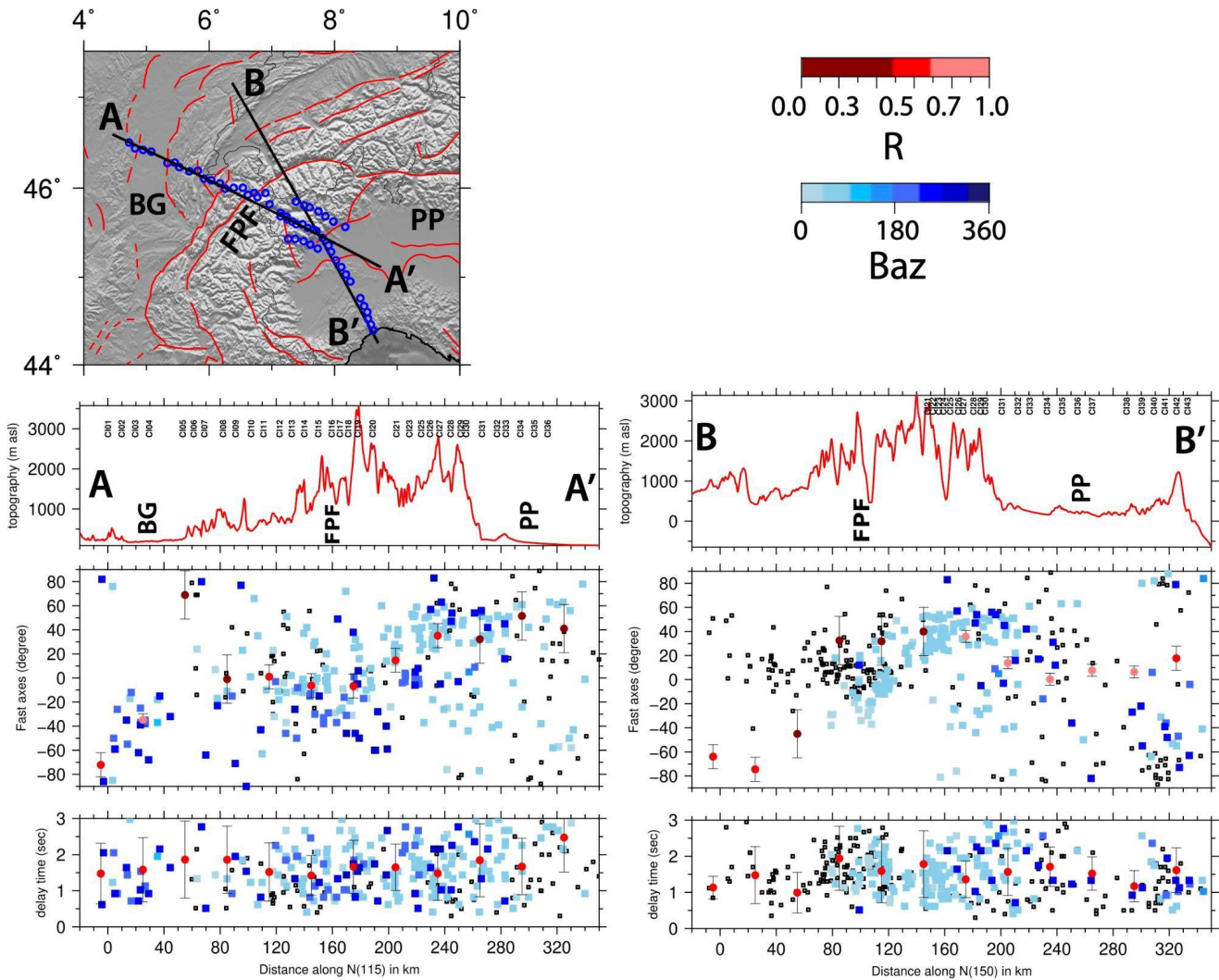
188 | ~~More than 600 null measurements have been obtained (Figure S1 in Supplementary Material), where a null is considered~~  
189 | ~~when no split appears in the signal (i.e. no energy in the transversal component). This is due either to the absence of~~  
190 | ~~anisotropy or to the initial polarization being parallel to the fast or slow anisotropic direction. A high percentage of good and~~  
191 | ~~fair results were obtained for events with a NE back azimuth, so it should be taken into account that this direction is~~  
192 | ~~oversampled.~~

193

194 | This new dataset fills the region between the north-western external Alps and the Ligurian Sea. The anisotropy directions of  
195 | no-nulls and nulls mostly agree with previous measurements (Figures 2 and 3, Figure S3 in Suppl. Material). Along the  
196 | part of the transect crossing the Alps (transect AA' in Figure 3), NE-SW direction dominates in the internal part of the belt,  
197 | between the FPF and the boundary of the Po Plain (see average values, red dots in Figure 3). In the western part of  
198 | the AA' transect, measurements are more scattered, with a coexistence of NE-SW and NS to NNE-SSW directions. In the  
199 | outer part of the Alpine belt and in the Bresse Graben, the prevailing directions are NS to NNE-SSW. Anisotropy in this  
200 | region is weaker, but fast velocity directions remain constant toward the NW end of the transect, confirmed also by null  
201 | measurements (Fig.S3 in Supplementary Material). These two patterns, one NE-SW parallel to the Alps strike and the other  
202 | nearly NS, and their location along the transect are well visible in Figure 3, mainly following average values (reddish  
203 | dots) mostly agree with previous measurements (Figures 2 and 3). Along the part of the transect crossing



204 the Alps (transect AB in Figure 3), NE-SW direction dominates in the internal part of the belt, between  
205 the Frontal Penninic Fault (FPF) and the western boundary of the Po Plain. In the western part of the  
206 transect, measurements are more scattered, with a coexistence of NE-SW and NS to NNE-SSW  
207 directions. In the outer part of the Alpine belt and in the Bresse Graben, NW of the FPF, the prevailing  
208 directions are NS to NNE-SSW. Anisotropy in this region is weak, but fast velocity directions remain  
209 constant toward the NW end of the transect. These two patterns, one NE-SW parallel to the Alps strike  
210 and the other nearly NS, and their location along the transect are well visible in Figure 3, mainly  
211 following average values of transect AB.



212 **figure 3 - Distribution of splitting parameters along the two sections of the CIFALPS2 region. For each section topography (upper),**  
 213 **fast axes direction (middle) and delay time (lower) distributions along a swath box of 30 km are displayed. In the fast axes and**  
 214 **delay time panels, every single measurement is represented by a square; the results of CIFALPS2 are blueish and color coded in**  
 215 **agreement with the back azimuth of the events analyzed, while the results of previous works are represented by smaller empty**  
 216 **squares. In the fast axes panel, circles represent the average values calculated using a basic circular arithmetic mean inside the**  
 217 **swath box with 30-km-step increment; they are coloured in agreement with the spreading distribution around the mean value**  
 218 **( $R=0$  distribution completely scattered,  $R=1$  distribution completely aligned with the mean direction). In the delay time panels, red**  
 219 **dots are the average value and its error, calculated with arithmetic mean and standard deviation. FPF = Frontal Penninic Fault;**  
 220 **BG = Bresse Graben; PP = Po Plain.**

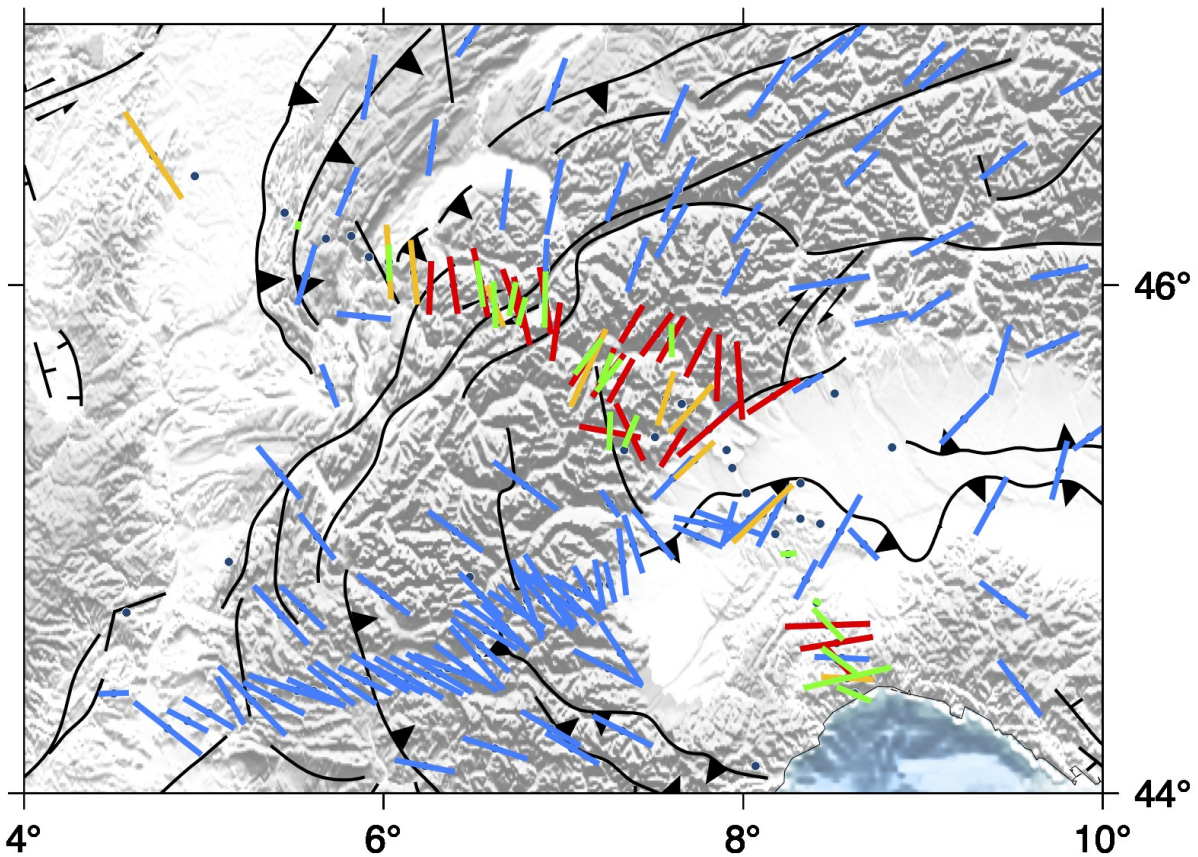
222

223 In the Po Plain, measurements appear scattered, similar to previous studies (e.g. Salimbeni et al., 2018;  
 224 Petrescu et al., 2020; Figures 2 and 3). In the transition between the belt and the plain, the typical NE-

225 SW Alpine direction prevails. Even if measurements are scarce, this direction appears also in the center  
226 of the Po Plain, together with a few NW-SE directions located southeast, close to the Ligurian Alps.  
227 However section BB' in Figure 3 shows that anisotropy directions are diverse, resulting in a strong  
228 dispersion of average values computed along the section. In the Ligurian part of the transect, several  
229 directions are detected, ENE-SSW and NW-SE (Apenninic) on the eastern side with a few weaker  
230 (lower dt) NNE-SSW measurements in the western side. Apenninic directions located southeast, close  
231 to Ligurian Alps. However section CD in Figure 3 shows that anisotropy directions are diverse,  
232 resulting in a strong dispersion of average values computed along the section (dark green symbols, i.e.  
233 low R).

234 In general, we do not find any particular pattern in the delay time measurements. Average values  
235 computed along the sections (Figure 3) are mostly constant, around 1.5 s with a large range in single  
236 measurement values.

237



238

239 **Figure 4 - Maps of average SWS measurements (red, yellow and blue) and anisotropy parameters obtained using SI measurements**  
 240 **(green). In red average values for CIFALPS2 stations obtained with more than 3 measurements, in yellow averages obtained with**  
 241 **less than 3 values; in light blue, average measurements from previous works. Dots represent stations.**

242 In the Ligurian part of the transect, several directions are detected, ENE-SSW and NW-SE (Apenninic) on the eastern side  
 243 with a few weaker (lower dt) NNE-SSW measurements in the western side.

244 In general, we do not find any particular pattern in the delay time measurements. Average values computed along the  
 245 sections (Figure 3) are mostly constant, around 1.5 s.

246

247

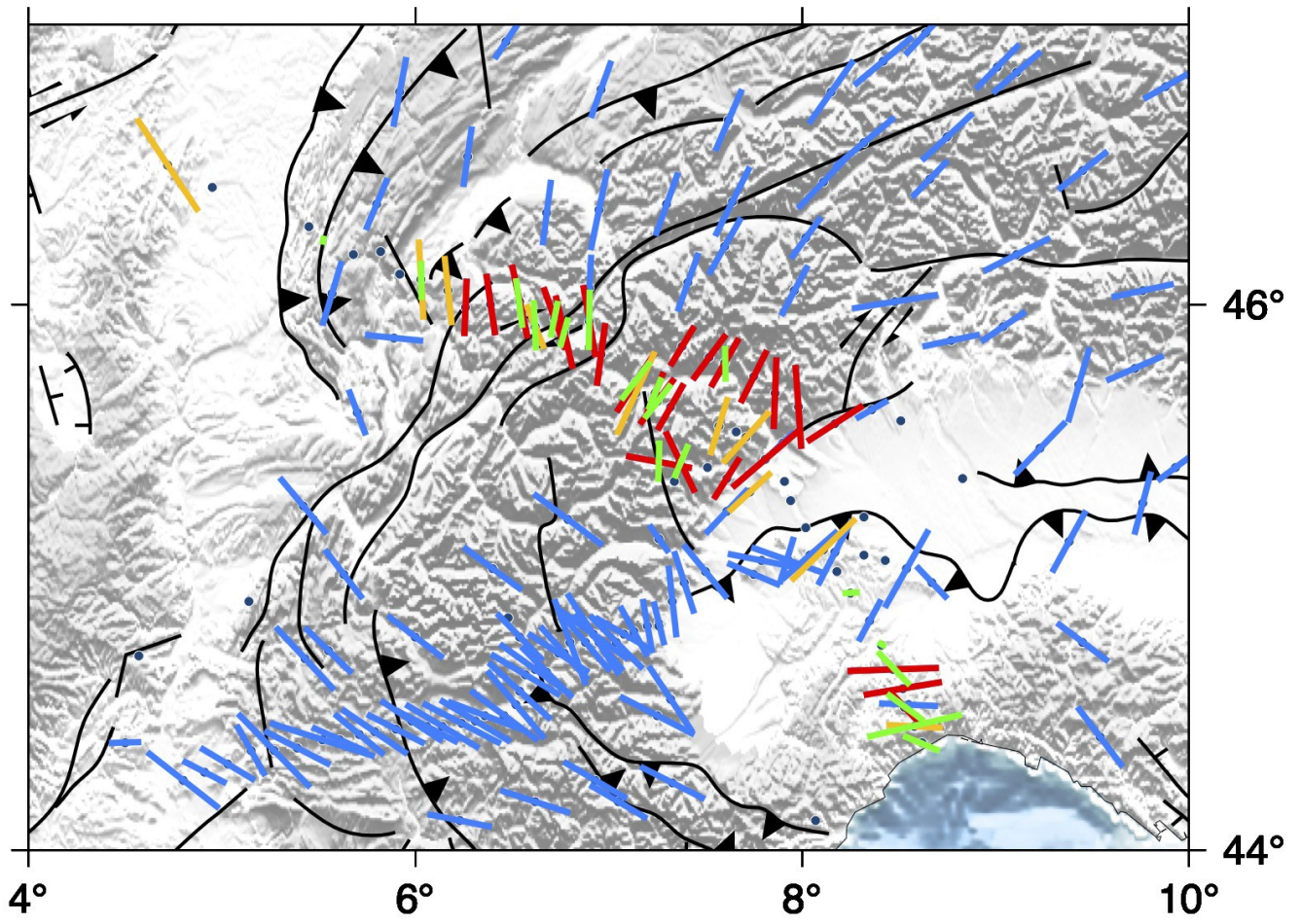
248 In Figure 4, average SWS values for each station are mapped together with anisotropy values obtained by splitting intensity  
 249 (SI) measurements (Table S1 in Supplementary Material). The first observation is that average SWS and SI data are very  
 250 similar, mainly at sites where the single measurement results are more homogeneous, while differences are present where  
 251 back azimuthal variations in fast direction are more evident, for instance in the southernmost part of the transect, in the  
 252 Ligurian Mountains.

251 ~~CIFALPS2 region. For each section topography (upper), fast axes (middle) and delay time (lower)~~  
252 ~~distributions along a swath box of 30 km are displayed. In the fast axes and delay time panels, every~~  
253 ~~single measurement is represented by a square; the results of CIFALPS2 are blueish and color coded in~~  
254 ~~agreement with the back azimuth of the events analyzed, while the results of previous works are~~  
255 ~~represented by empty squares. In the fast axes panel, circles represent the average values calculated~~  
256 ~~inside the swath box with 30 km step increment and are coloured in agreement with the spreading~~  
257 ~~distribution around the mean value (R=0 mean distribution completely scattered, R=1 distribution~~  
258 ~~completely aligned with the mean direction). In the delay time panels, the average value and its error are~~  
259 ~~calculated with arithmetic mean and standard deviation.~~

260

261 ~~In general, it is clear that CIFALPS2 results are coherent with the average distribution of the anisotropy from previous~~  
262 ~~measurements. The main Alpine pattern that follows the belt arc, here NE-SW, is represented in most of the averaged values~~  
263 ~~for sites located in the transition between the Po Plain and the FPF. From the FPF to the NW endpoint of the~~  
264 ~~transect, the main direction is close to NS, a direction that does not find an agreement with the orogen~~  
265 ~~trend, still NE-SW. Figure 4, average SWS values for each station are mapped together with anisotropy~~  
266 ~~values obtained by splitting intensity (SI) measurements (Table S2 in Supplementary Material). The~~  
267 ~~first observation is that average SWS and SI data are very similar, mainly at sites where the results are~~  
268 ~~more homogeneous, while differences are present where detections at the east and the west of the~~  
269 ~~transect are more evident, for instance in the southernmost part of the transect, close to the Ligurian~~  
270 ~~Sea. In general, it is clear that CIFALPS2 results are coherent with the average distribution of the~~  
271 ~~anisotropy from previous measurements. The main Alpine pattern that follows the belt arc, here NE-~~  
272 ~~SW, is represented in most of the averaged values for sites in the transition between the Po-~~

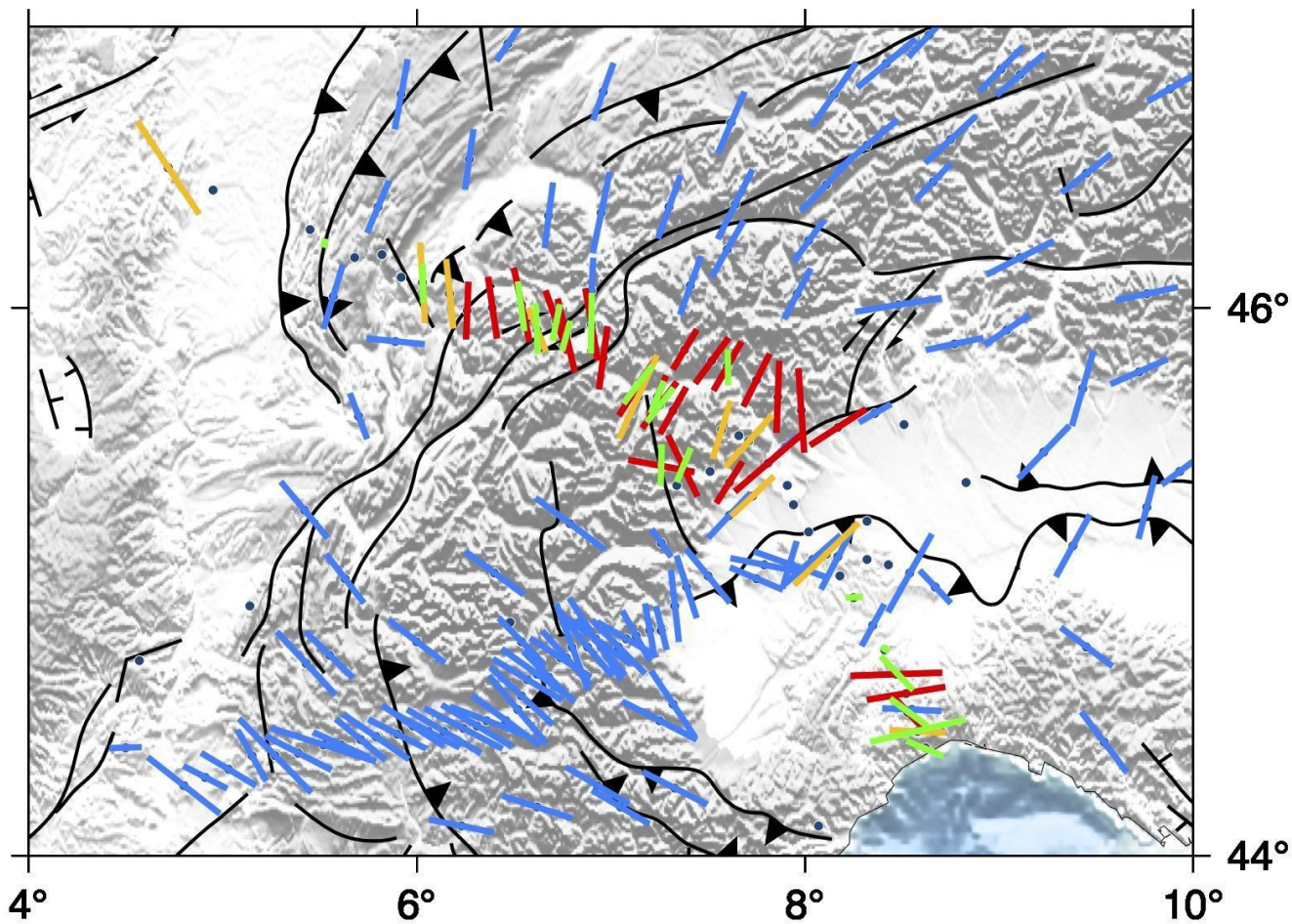
273 ~~Figure 4— Maps of average SWS measurements (red, yellow and blue) and anisotropy parameters obtained using SI measurements~~  
274 ~~(green). In red average values from CIFALPS2 stations obtained with more than 3 measurements, in yellow averages obtained~~  
275 ~~with less than 3 values and in light blue averaged measurements from previous works.~~



277 In order to extract as much information as possible, we split the dataset into groups according to the  
 278 main morphological features: a) External zone to the west of the FPF; b) Internal zone between the FPF  
 279 and the western boundary of the Po plain, c) the Po Plain, and d) the Ligurian Alps. By plotting a rose  
 280 diagram for all good and fair measurements obtained for the stations of each group, taking into account  
 281 the influence of back azimuths, we get an overview of the main features and lateral changes of the  
 282 anisotropy detected through these SWS measurements.

283 Plain and the FPF thrust. From the FPF to the NW endpoint of the transect, the main direction is close to NS,  
 284 direction that does not find an agreement with the orogen trend, still NE-SW.

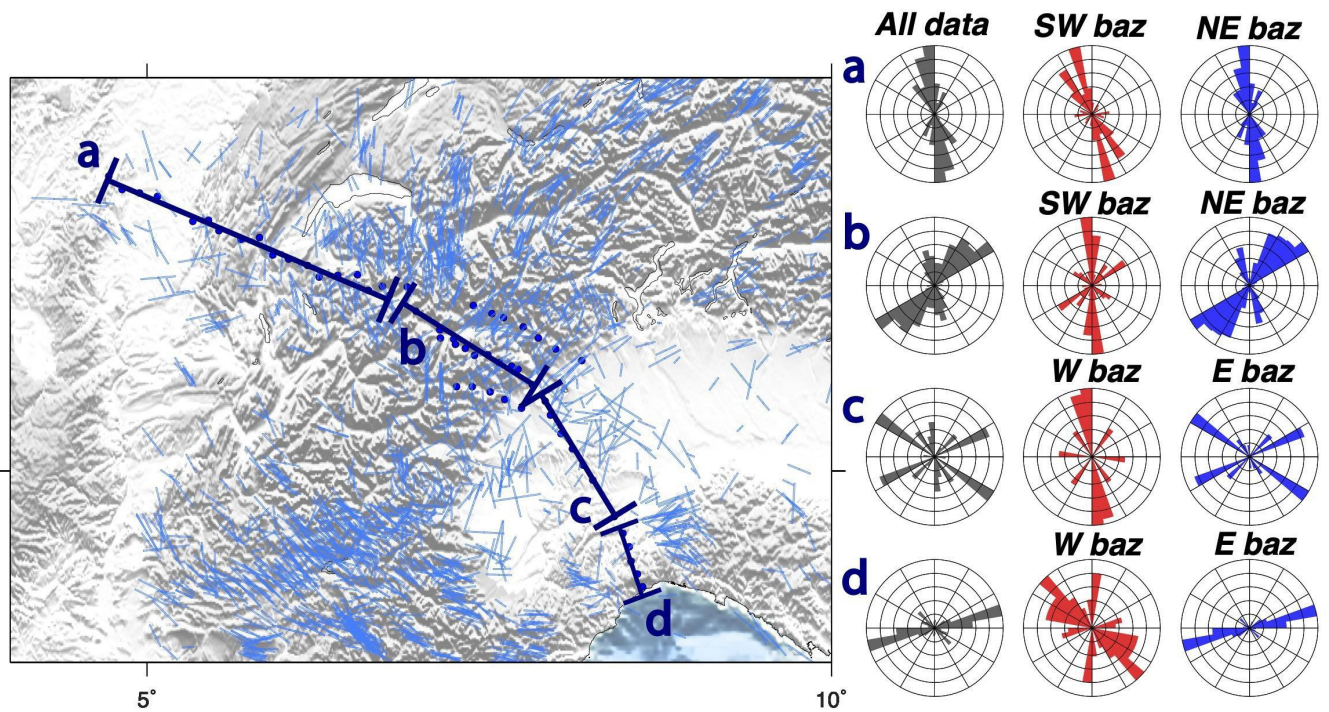
285



286 In Figure 5, the rose diagrams show evident differences along the CIFALPS2 transect, somewhere underlined by different  
287 patterns with respect to back azimuths. Only in group a), in the External zone, the N-S dominant direction remains,  
288 regardless of the amount of measurements or separation into opposite back azimuths (red and blue rose diagrams). For all  
289 other groups, there is a clear difference depending on the back azimuth. In group b) the entire dataset shows a main trend in a  
290 NE-SW direction, in agreement with the Alps strike in this region; the same direction is observed for events coming from  
291 NE (blue rose diagram). On the contrary, measurements obtained from events with a SW back azimuth are dominated by a  
292 nearly NS direction, quite similar to that shown by group a). The entire dataset for the Po Plain (c) and the subgroup with  
293 east back azimuths show a clear bimodal distribution, with both the Alpine NE-SW and the Apenninic NW-SE typical  
294 directions; west back azimuth events show instead N to NNW directions, very similar to those obtained in previous work at  
295 the first CIFALPS transect (e.g. Salimbeni et al., 2018) and again similar to group a) and SW back azimuth measurements of  
296 group b). In the Ligurian Alps, in the group d), opposite back azimuths show different results. It is worth noticing that in the  
297 group d) the ENE-WSW direction is dominant both in the all data plot and in the east back azimuth plot, while the west  
298 back azimuth plot shows a wide dispersion with a NW-SE direction prevailing. order to extract as much information as  
299 possible, we split the dataset into groups according to the main morphological features: a) External zone to the west of the  
300 FPF; b) Internal zone between the FPF and the western boundary of the Po plain, c) the Po Plain part and d) the Ligurian  
301 Alps. By plotting a rose diagram for all good and fair measurements obtained for the stations of each group, taking into  
302 account the influence of back azimuths, we get an overview of the main features and lateral changes of the anisotropy  
303 detected through these SWS measurements.

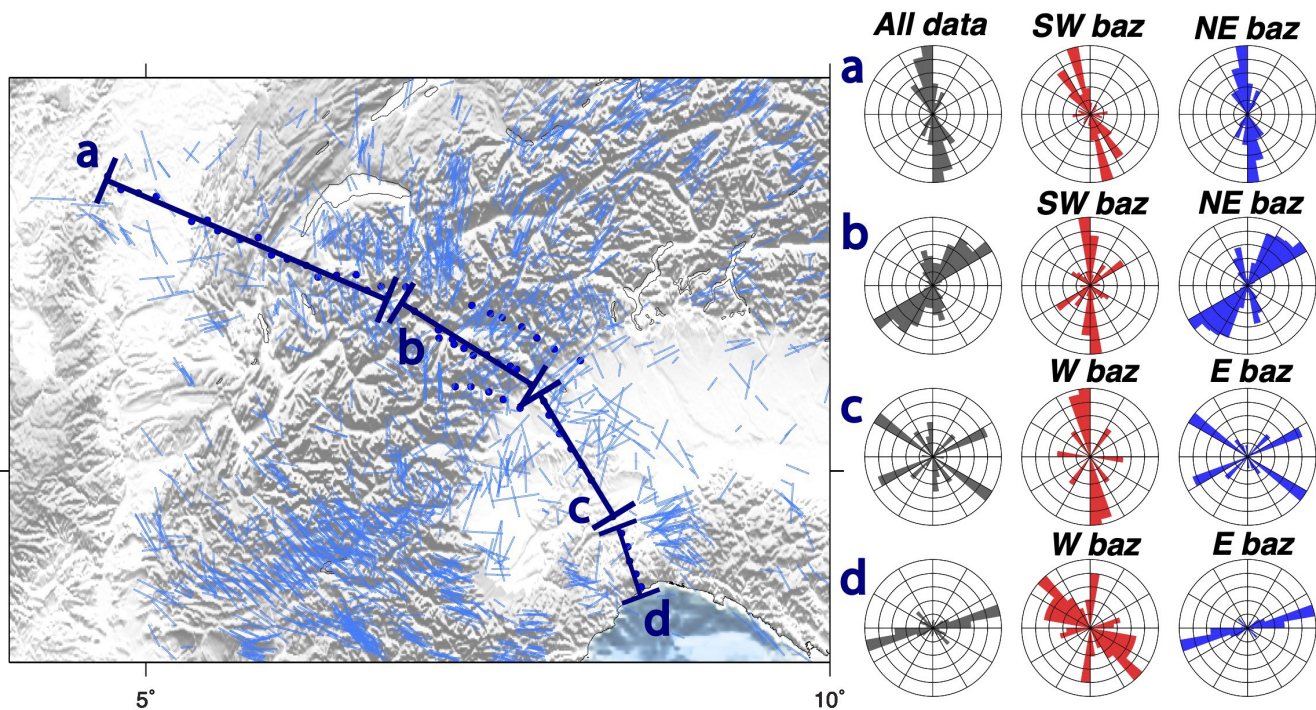
304 **Figure 5 - Normalised rose diagrams produced for groups of stations along the profile, a) External zone with respect to FPF; b)**  
305 **Internal zone with respect to FPF; c) Po Plain; d) the Ligurian Alps. Grey rose diagrams: all data; Red: events with SW (a,b) or W**  
306 **(c,d) back azimuths, blue: events with NE (a,b) or E (c,d) back azimuths.**





307 In Figure 5, the rose diagrams show evident differences along the CIFALPS2 transect, somewhere underlined by different  
 308 patterns with respect to back azimuths. Only in group a), in the External zone, the N-S dominant direction remains  
 309 independently if all the dataset is used or if measurements are separated with respect to opposite back azimuths (red and blue  
 310 rose diagrams). For all other groups, there is a clear difference depending on the back azimuth. In the group b) the entire  
 311 dataset shows a main trend in a NE-SW direction, in agreement with the Alps strike in this region; the same direction is  
 312 observed for events coming from NE (blue rose diagram). On the contrary, measurements obtained from events with a SW  
 313 back azimuth are dominated by a nearly NS direction, quite similar to that shown by group a). The entire dataset for the Po  
 314 Plain (c) and the subgroup with east back azimuths show a clear bimodal distribution, with both the Alpine NE-SW and the  
 315 Apenninic NW-SE typical directions; west back azimuth events giving instead N to NNW directions, very similar to those  
 316 obtained in previous work (e.g. Salimbeni et al., 2018) and again similar to group a) and SW back azimuth measurements of  
 317 group b). In the Ligurian Alps, in the group d), opposite back azimuths show different results. It is worth noticing that the  
 318 ENE-WSW direction is dominant both in the all data plot and in the E back azimuth plot, while the W back azimuth plot  
 319 shows a wide dispersion with a NW-SE direction prevailing.

320 **Figure 5** – Normalised rose diagrams produced for groups of stations along the profile, a) External zone with respect to FPF; b)  
 321 Internal zone with respect to FPF; c) Po Plain; d) the Ligurian Alps. Grey rose diagrams: all data; Red: events with SW (a,b) or W  
 322 (c,d) back azimuths, blue: events with NE (a,b) or E (c,d) back azimuths.



#### 323 | 4 Discussion and hypotheses

324 CIFALPS2 SWS measurements clearly provide new information since they cover large areas where no seismic station is  
 325 currently deployed or has been operating in the past. They allow us or has been operating in the past. They allow to fill data  
 326 gaps and draw conclusions on the seismic anisotropy pattern and mantle deformation beneath the Western Alps.

327

328 A large-scale summary, prepared using the average values to avoid the scatter of single SWS measurements, is shown in  
 329 Figure 6. ENE-WSW fast velocity directions, parallel to the strike of the Alps, are present from the Central to the Western  
 330 Alps, in the transition between Po Plain and the belt, and terminate where the European slab and the belt are bending (double  
 331 headed arrows in the inset sketch of Figure 6). At this point anisotropy directions do not strictly follow the chain strike, as  
 332 they rather cut the main tectonic and morphological features. In the same zone (highlighted by the green circle A, Figure 6)  
 333 converges a mantle flow that strikes from NE-SW to NS, in a coherent direction that however cuts the arcuate shape of the  
 334 belt (yellow lines in the northern part of study region, Figure 6); this pattern is different from those described in previous  
 335 anisotropy studies of the Western Alps (Barruol et al., 2004; Lucente et al., 2006; Barruol et al., 2011; Salimbeni et al.,  
 336 2018) where anisotropy has always been described as rotating with the belt direction. The discrepancy between the direction  
 337 of tectonic lines and the nearly NS fast velocity is in agreement with a deep source of the anisotropy, in the mantle. Link and  
 338 Rumpker (2023) in a recent analysis found that a similar nearly NS pattern would be mostly located in a shallower part of the  
 339 mantle, and in part also present in a lower layer. They consider it as a shallow asthenospheric contribution. Link and

340 Rumpker (2023) in a recent analysis found that this pattern is mostly located in a shallower layer, but being also present in  
341 the lower layer and being close to the tectonic sutures, they consider it as a shallow asthenospheric contribution. The NW-SE  
342 asthenospheric flow identified from SE France toward the Ligurian Sea, which culminates in a flow around the southern tip  
343 of the European slab, is instead in agreement with previous studies. This flow apparently originates beneath Central France,  
344 in the Massif Central region (Barruol et al., 2004), and it seems that the NS mantle flow merges with it (left green circle,  
345 Figure 6) and then, flowing around the southern tip of the European slab, moves to the Tyrrhenian Sea.

346 On the contrary, the NW-SE asthenospheric flow identified from SE France toward the Ligurian Sea, which culminates in a  
347 flow around the southern tip of the European slab, is in agreement with previous studies. This flow apparently originates  
348 beneath Central France, in the Massif Central region (Barruol et al., 2004), and it seems that the NS mantle flow merges with  
349 it (left green circle, Figure 6) and then, flowing around the southern tip of the European slab, moves to the Tyrrhenian Sea.

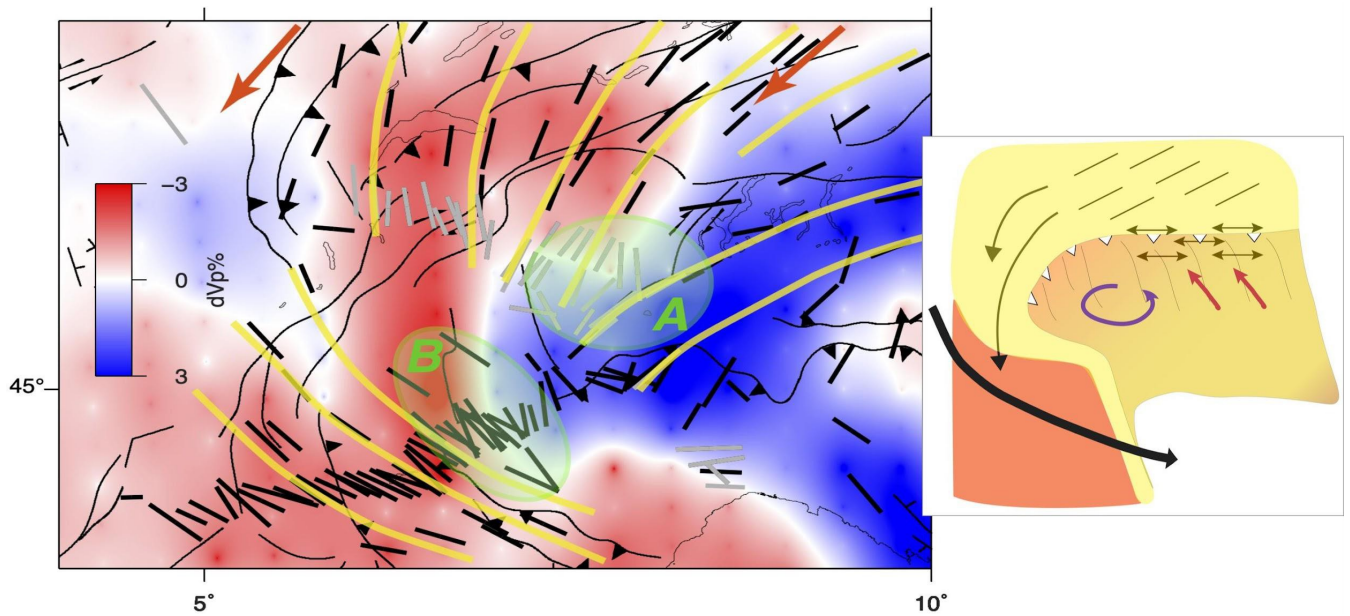
350  
351 The overlap with the teleseismic travel time tomographic image at 150 km depth by Zhao et al. (2016) indicates that all these  
352 fast velocity directions correspond to mantle deformation below the European slab. The mantle close to the slab has a NE-  
353 SW seismic anisotropy direction because it is deformed by the slab steepening. This feature is visible only in a narrow  
354 stripe, in the transition between Western and Central Alps, probably because in this place the slab steepening was favored  
355 by the plate motion direction (e.g. Adria anticlockwise rotation, Figure 6). Moving north, in the outer part of the belt, the  
356 anisotropy directions are those of an undeformed mantle, substantially parallel to the APM direction (orange arrows in  
357 Figure 6). Moving (south)westward, the deflection from NE-SW to NS may be related to the mantle being squeezed by the  
358 retreating European slab and moved toward the south where the retreat process was weakening or probably already ended.  
359 Indeed, in the Western Alps, the arcuate shape of the trench and slab, together with the (upper) Adria plate rotating in  
360 anticlockwise direction with a rotation pole more or less located in the western Po Plain (e.g. Serpelloni et al., 2016; Le  
361 Breton et al., 2017), may have been less favorable to the retreat of the slab. Such differences between the northern and  
362 southern Western Alps, in particular in the European Moho geometry, have been also identified by comparing CICALPS and  
363 CICALPS2 receiver function sections (Paul et al., 2022). The European Moho is strongly dipping down deformed by the slab  
364 retreat. This feature is visible only in a narrow stripe, in the transition between Western and Central Alps, probably because  
365 in this place the slab retreat was favored by the plate motion direction (e.g. Adria anticlockwise rotation, Figure 6). Moving  
366 north, in the outer part of the belt, the anisotropy directions are those of an undeformed mantle, substantially parallel to the  
367 APM direction (orange arrows in Figure 6). Moving (south)westward, the deflection from NE-SW to NS may be related to  
368 the mantle being squeezed by the retreating European slab that moved toward the south where however the retreat process  
369 was weakening or probably already ended. Indeed, in the Western Alps, the arcuate shape of the trench and slab, together  
370 with the (upper) Adria plate rotating in anticlockwise direction with a rotation pole more or less located in the western Po  
371 Plain (e.g. Serpelloni et al., 2016; Le Breton et al., 2017), may have been less favorable to the retreat of the slab, which was  
372 less effective with respect to other locations. Such differences between the northern and southern Western Alps, in particular

373 in the European Moho geometry, have been also identified by comparing CIFALPS and CIFALPS2 receiver function  
 374 sections (Paul et al., 2022). The European Moho is strongly dipping to ~75 km depth along CIFALPS section, while its dip is  
 375 much weaker in CIFALPS2 section. Moreover, the absence of slab retreat in the Western Alps has been described also by  
 376 Malusà et al. (2015), studying the mechanisms for exhumation of (U)HP terranes along the Cenozoic Adria-Europe plate  
 377 boundary.

378 The mantle flow from beneath the Central Alps converges with the asthenospheric flow coming from SE France where  
 379 Western Alps subduction, precisely a continental subduction (Malusà et al., 2021; Paul et al., 2022) runs out. In the region,  
 380 the European slab is almost vertical (Zhao et al., 2016) and is no more affected by slab retreat. Substantially a differential  
 381 behaviour of slab movement along the chain is at the base of the anisotropy pattern variation from Central to the entire  
 382 Western Alps.

383 In the Po Plain, the image is patchy and complex, with very few good quality measurements and some  
 384 really low values of dt. This does not necessarily mean that the mantle is isotropic, but that anisotropy  
 385 may be multilayered or fast velocity directions are verticalFigure 6—Top left: Zhao et al. (2016)  
 386 tomography (dVp in %)—layer at 150 km depth—overlapped with average SWS measurements: results  
 387 from CIFALPS2 data in light grey and from previous studies in black. Orange arrows on top represent  
 388 the absolute European plate motion from GSRM v2.1 model (calculated from Plate Motion Calculator |  
 389 Software | GAGE). Yellow traces simulate average mantle deformation directions and green areas A  
 390 and B highlight points where directions converge. Bottom right: a sketch of this part of alpine  
 391 subduction, where, in light yellow is the European plate, the double-headed arrows represent the only  
 392 anisotropy of the study region related to European slab retreat (whose direction is represented by the red  
 393 arrows), thin black lines are the anisotropy parallel to the APM, the thick black arrow represents the SE  
 394 France asthenospheric mantle flow, the purple circular arrow represents the Adria plate rotation.

395  
 396 Figure 6 - Left: Zhao et al. (2016) tomography (dVp in %) - layer at 150 km depth - overlapped with average SWS measurements:  
 397 results from CIFALPS2 data in light grey and from previous studies in black. Orange arrows on top represent the absolute  
 398 European plate motion from GSRM v2.1 model (calculated from Plate Motion Calculator | Software | GAGE). Yellow traces  
 399 simulate average mantle deformation directions and green areas A and B highlight points where directions converge. Right: a  
 400 sketch of this part of alpine subduction, where, in light yellow is the European plate, the double-headed arrows represent the only  
 401 anisotropy of the study region related to European slab retreat (whose direction is represented by the red arrows), thin black lines  
 402 are the anisotropy parallel to the APM, the thick black arrow represents the SE France asthenospheric mantle flow, the purple  
 403 circular arrow represents the Adria plate rotation.



405 | ~~In the Po Plain, the image is patchy and complex, with very few good quality measurements and some really low values of~~  
 406 | ~~dt. This does not necessarily mean that the mantle is isotropic, but that anisotropy may be multilayered or fast velocity~~  
 407 | ~~directions vertical.~~ It is worth noting that beneath the Po basin, the European slab is nearly vertical (e.g., Zhao et al. 2016;  
 408 | Paffrath et al., 2021) and the space for the mantle above is really narrow. With such a complex mantle structure, it is not  
 409 | surprising that a unique and significant pattern of anisotropy cannot be identified. In the Ligurian Alps, our measurements  
 410 | show different orientations east and west of the transect with, in general, a prevailing EW direction (Figure 5d), but a minor  
 411 | NNE-SSW set of measurements from the western back azimuths. These results are certainly intriguing but not sufficient to  
 412 | support any new hypothesis.

### 413 | 5 Conclusions

414 | New data collected by the CIFALPS2 project clearly fills the gap that has forced the interpolation between more sparse  
 415 | information in the past. The pattern of seismic anisotropy shown here, is not entirely parallel to the belt, as it is in the Central  
 416 | Alps and in the transition to the Western Alps, up to the point this portion of belt is arcuate. Indeed, in the central part of the  
 417 | study region, a nearly NS pattern coming from central Europe cuts all principal morphologic features of the belt. It  
 418 | converges with the part of the mantle deformed by the retreating slab in the point where the retreat is less favored or ended.  
 419 | The arcuate shape of the belt and of the slab, added to the Adria plate rotation with respect to Eurasia around a pole here  
 420 | particularly close to the boundary, reduce the effectiveness of a slab retreat. The NS mantle flow is then interpreted as the

421 European mantle moving south to merge with the large asthenospheric flow that from beneath Central France moves toward  
422 the Tyrrhenian Sea turning around the southern tip of the European slab.

#### 423 **Data availability**

424 All shear wave splitting measurements from this work have been included and are available in the Italian shear wave  
425 splitting collection <https://osf.io/nqxxk4> (Pondrelli et al., 2023).

#### 426 **Author contribution**

427 PS, SS and CJM made measurements and analyses. PS prepared the manuscript with the contribution of all co-authors. All  
428 authors designed the [CIFALPS2 experiment](#)~~experiments~~ ~~CIFALPS2~~ and carried it out.

#### 429 **Competing interests**

430 The authors declare that they have no conflict of interest.

#### 431 **Acknowledgements**

432 This research is funded by the National Natural Science Foundation of China and by NEWTON (NEW Window inTO Earth's  
433 iNterior), ERC StG funded project (grant ID:758199).

434 |

435 |

436 |

437 |

438 |

439 |

#### 440 **References**

441 Barruol, G., Bonnin, M., Pedersen, H., Bokelmann, G., Tiberi, C.: Belt-parallel mantle flow beneath a halted continental  
442 collision: the Western Alps, *Earth Planet. Sci. Lett.* 302, 429–438, 2011.

443 Barruol, G., Deschamps, A., Coutant, O.: Mapping upper mantle anisotropy beneath SE France by SKS splitting indicates a  
444 Neogene asthenospheric flow induced by the Apenninic slab rollback and deflected by the deep Alpine roots, *Tectonophys.*,  
445 394, 125–138, 2004.

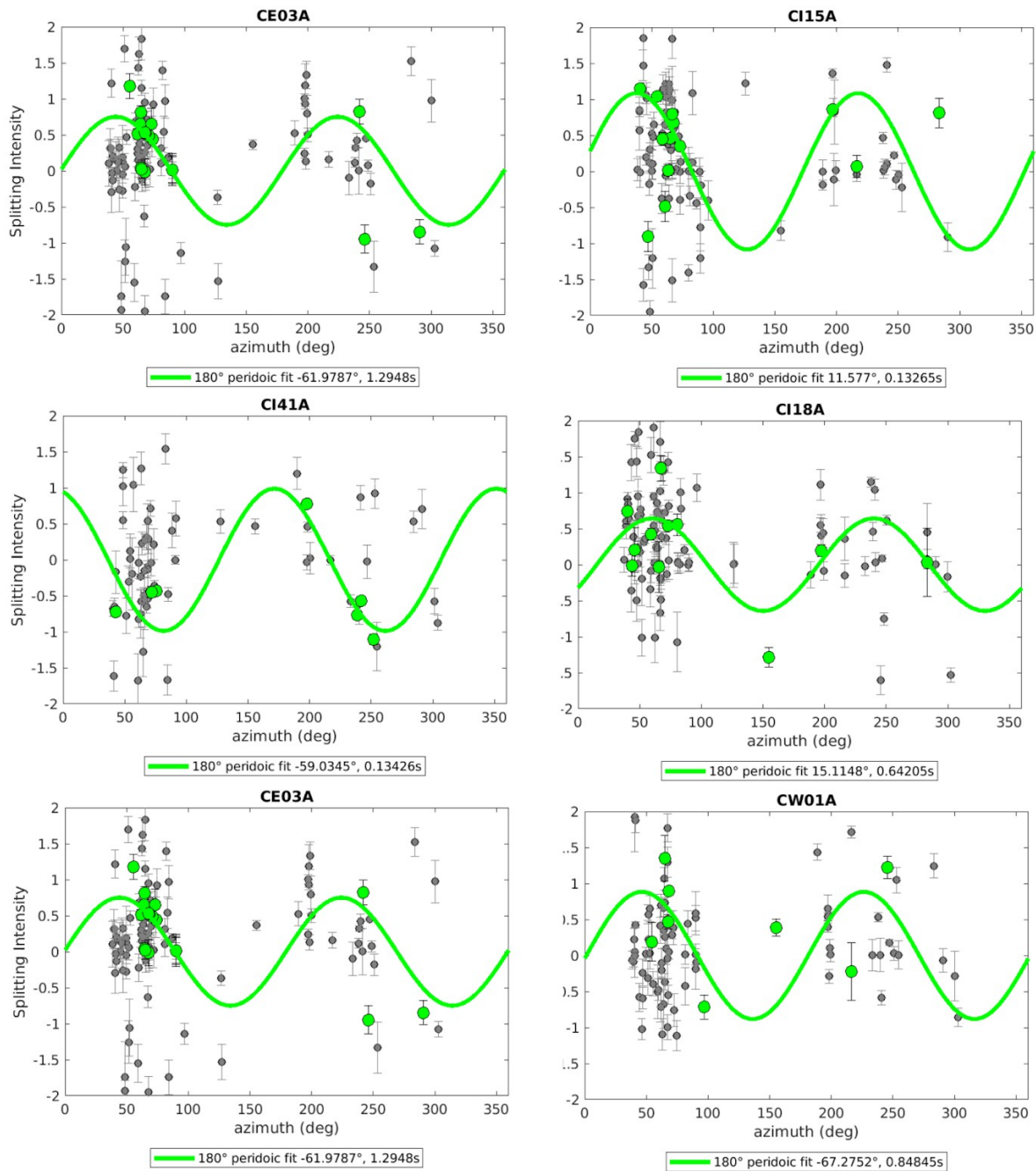
- 446 Barruol, G. and M. Granet: A Tertiary asthenospheric flow beneath the southern French Massif Central related to the west  
 447 Mediterranean extension evidenced by upper mantle seismic anisotropy, *Earth Plan. Sci. Lett.*, 202, 31-47, 10.1016/S0012-  
 448 821X(02)00752-5, 2002.
- 449 Chevrot, S.: Multichannel analysis of shear wave splitting, *J. Geophys. Res. Solid Earth*, 105(B9), 21579-21590, 2000.
- 450 Confal, J. M., Baccheschi, P., Pondrelli, S., Karakostas, F., VanderBeek, B. P., Huang, Z., Faccenda, M.: Reproducing  
 451 Complex Anisotropy Patterns at Subduction Zones from Splitting Intensity Analysis and Anisotropy Tomography, *Geophys.*  
 452 *J. Int.*, 235, 1725–1735, <https://doi.org/10.1093/gji/ggad329>, 2023.
- 453 Crampin, S. and Peacock S.: A review of the current understanding of seismic shear-wave splitting in the Earth's crust and  
 454 common fallacies in interpretation, *Wave Mot.*, 45 (2008), pp. 675-722, 10.1016/j.wavemoti.2008.01.003, 2008.
- 455 Díaz, J., Gil, A., and Gallart, J.: Uppermost mantle seismic velocity and anisotropy in the Euro-Mediterranean region from  
 456 Pn and Sn tomography, *Geophys. J. Int.*, 192(1), 310-325, 2013.
- 457 Monteiller, V., and Chevrot, S.: How to make robust splitting measurements for single-station analysis and three-  
 458 dimensional imaging of seismic anisotropy, *Geophys. J. Int.*, 182(1), 311-328, 2010.
- 459 Giacomuzzi, G., Chiarabba, C., and De Gori, P.: Linking the Alps and Apennines subduction systems: New constraints  
 460 revealed by high-resolution teleseismic tomography, *Earth and Plan. Science Lett.*, 301(3–4), 531–543, 2011.
- 461 Hetényi G., I. Molinari, J. Clinton et al.: The AlpArray Seismic Network: a large-scale European experiment to image the  
 462 Alpine orogeny, *Surv. Geophysics*, 39, 1009-1033. doi:10.1007/s10712-018-9472-4, 2018.
- 463 Kissling, E., Schmid, S. M., Lippitsch, R., Ansorge, J., and Fügenschuh, B.: Lithosphere structure and tectonic evolution of  
 464 the Alpine arc: New evidence from high-resolution teleseismic tomography, *Geological Society, London, Memoirs*, 32, 129–  
 465 145, 2006.
- 466 Kong, F., Gao, S. S., and Liu, K. H.: Applicability of the multiple-event stacking technique for shear-wave splitting analysis,  
 467 *Bull. Seism. Soc. Am.*, 105(6), 3156-3166, 2015.
- 468 Le Breton, E., Handy, M. R., Molli, G., and Ustaszewski, K.: Post-20 Ma motion of the Adriatic plate: New constraints from  
 469 surrounding Orogens and implications for crust-mantle decoupling, *Tectonics*, 36, 3135–3154. doi:10.1002/ 2016TC004443,  
 470 2017.
- 471 Lippitsch, R., Kissling, E., and Ansorge, J.: Upper mantle structure beneath the Alpine orogen from high-resolution  
 472 teleseismic tomography, *J. Geophys. Res.: Solid Earth*, 108(B8). <https://doi.org/10.1029/2002JB002016>, 2003.
- 473 Long, M.: Constraints on subduction geodynamics from seismic anisotropy. *Rev. Geophys.*, 51, 76–112,  
 474 <https://doi.org/10.1002/rog.20008>, 2013.
- 475 Long, M.D., and Silver, P. G.: Shear Wave Splitting and Mantle Anisotropy: Measurements, Interpretations, and New  
 476 Directions, *Surv Geophys* 30, 407–461, <https://doi.org/10.1007/s10712-009-9075-1>, 2009.
- 477 Malusà, M. G., C. Faccenna, S. L. Baldwin, P. G. Fitzgerald, F. Rossetti, M. L. Balestrieri, M. Danišik, A. Ellero, G. Ottria,  
 478 and C. Piromallo: Contrasting styles of (U)HP rock exhumation along the Cenozoic Adria-Europe plate boundary (Western  
 479 Alps, Calabria, Corsica), *Geochem. Geophys. Geosyst.*, 16, 1786–1824, doi:10.1002/2015GC005767, 2015.

- 480 Malusà, M. G., Guillot, S., Zhao, L., Paul, A., Solarino, S., Dumont, T., Schwartz, S., Aubert, C., Baccheschi, P., Eva, E.,  
481 Lu, Y., Lyu, C., Pondrelli, S., Salimbeni, S., Sun, W., & Yuan, H.: The deep structure of the Alps based on the CIFALPS  
482 seismic experiment: A synthesis, *Geochem. Geophys. Geosyst.*, 22(3), e2020GC009466, 2021.
- 483 Okaya, D., S.S. Vel, W.J. Song, S.E. Johnson: Modification of crustal seismic anisotropy by geological structures  
484 (“structural geometric anisotropy”), *Geosphere*, 15, pp. 146-170, 10.1130/GES01655, 2018.
- 485 Paffrath, M., Friederich, W., Schmid, S. M., Handy, M. R., and AlpArray and AlpArray-Swath D Working Group: Imaging  
486 structure and geometry of slabs in the greater Alpine area—A P-wave travel-time tomography using AlpArray Seismic  
487 Network data, *Solid Earth*, 12, 2671-2702, doi: 10.5194/se-12-2671-2021, 2021.
- 488 Paul, A., M.G. Malusà, S. Solarino, S. Salimbeni, E. Eva, A. Nouibat, S. Pondrelli, C. Aubert, T. Dumont, S. Guillot, S.  
489 Schwartz, L. Zhao: Along-strike variations in the fossil subduction zone of the Western Alps revealed by the CIFALPS  
490 seismic experiments and their implications for exhumation of (ultra-) high-pressure rocks, *Earth Plan. Science Lett.*, 598,  
491 117843, <https://doi.org/10.1016/j.epsl.2022.117843>, 2022.
- 492 Piromallo, C., and Morelli, A.: P wave tomography of the mantle under the Alpine-Mediterranean area, *J. Geophys. Res.:*  
493 *Solid Earth*, 108(B2). <https://doi.org/10.1029/2002JB001757>, 2003.
- 494 Pondrelli S., S. Salimbeni, P. Baccheschi, J. M. Confal, L. Margheriti (2023). Peeking inside the mantle structure beneath the  
495 Italian region through SKS shear wave splitting anisotropy: a review, *Ann. Geophys.*, 66, 2, doi:1044.01/ag-8872.
- 496 Rappisi, F., VanderBeek, B. P., Faccenda, M., Morelli, A., Molinari, I.: Slab geometry and upper mantle flow patterns in the  
497 Central Mediterranean from 3D anisotropic P-wave tomography, *J. Geophys. Res.: Solid Earth*, 127, e2021JB023488. doi:  
498 10.1029/2021JB023488, 2022.
- 499 Reiss, M. C. and G. Rumpker: SplitRacer: MATLAB Code and GUI for Semiautomated Analysis and Interpretation of  
500 Teleseismic Shear-Wave Splitting, *Seism. Res. Lett.*, 88, 2A, 392-409, doi: <https://doi.org/10.1785/0220160191>, 2017.
- 501 Salimbeni, S., M. G. Malusà, L. Zhao, S. Guillot, S. Pondrelli, L. Margheriti, A. Paul, S. Solarino, C. Aubert, T. Dumont, S.  
502 Schwartz, Q. Wang, X. Xu, T. Zheng and R. Zhu: Active and fossil mantle flows in the western Alpine region unravelled by  
503 seismic anisotropy analysis and high-resolution P wave tomography, *Tectonophys.*, 731-732, 35-47,  
504 doi:10.1016/j.tecto.2018.03.002, 2018.
- 505 Serpelloni, E., G. Vannucci, L. Anderlini, and R.A. Bennett: Kinematics, seismotectonics and seismic potential of the eastern  
506 sector of the European Alps from GPS and seismic deformation data, *Tectonophys.*,  
507 <https://doi.org/10.1016/j.tecto.2016.09.026>, 2016.
- 508 Silver, P. G. and W. W. Chan: Shear wave splitting and subcontinental mantle deformation, *J. Geophys. Res.: Solid Earth*,  
509 96, B10, 16429-16454, 1991.
- 510 Zhao, L., Paul, A., Guillot, S., Solarino, S., Malusà, M.G., Zheng, T.Y., Aubert, C., Salimbeni, S., Dumont, T., Schwartz, S.,  
511 Zhu, R.X., Wang, Q.C.: First seismic evidence for continental subduction beneath the Western Alps, *Geology* 43, 815–818,  
512 2015.



- 513 Zhao, L., Paul, A., Malusà, M. G., Xu, X., Zheng, T., Solarino, S., Guillot, S. Schwartz, S., Dumont, T., Salimbeni, S.,  
514 Aubert, C., Pondrelli, S., Wang, Q., and Zhu, R.: Continuity of the Alpine slab unraveled by high-resolution P wave  
515 tomography, *J. Geophys. Res.*, 121, 8720–8737, 2016.
- 516 Zhao, L., Paul, A., Solarino, S., RESIF: Seismic network YP: CIFALPS temporary experiment (China-Italy-France Alps  
517 seismic transect) [Data set]. RESIF - Réseau Sismologique et géodésique Français, <https://doi.org/10.15778/RESIF.YP2012>, 2016.
- 519 Zhao, L., Paul, A., Solarino, S., RESIF: Seismic network XT: CIFALPS-2 temporary experiment (China-Italy-France Alps  
520 seismic transect #2) [Data set]. RESIF - Réseau Sismologique et Géodésique Français, <https://doi.org/10.15778/RESIF.XT2018>, 2018.
- 521 ~~seismic transect #2 [Data set]. RESIF - Réseau Sismologique et géodésique Français, <https://doi.org/10.15778/RESIF.XT2018>, 2018.~~
- 522 ~~https://doi.org/10.15778/RESIF.XT2018, 2018.~~
- 523 Zhao D., Liu X., Wang Z. and Gou T.: Seismic Anisotropy Tomography and Mantle Dynamics, *Surv. Geophys.*, 44, 947–  
524 982, <https://doi.org/10.1007/s10712-022-09764-71>, 2023.





526

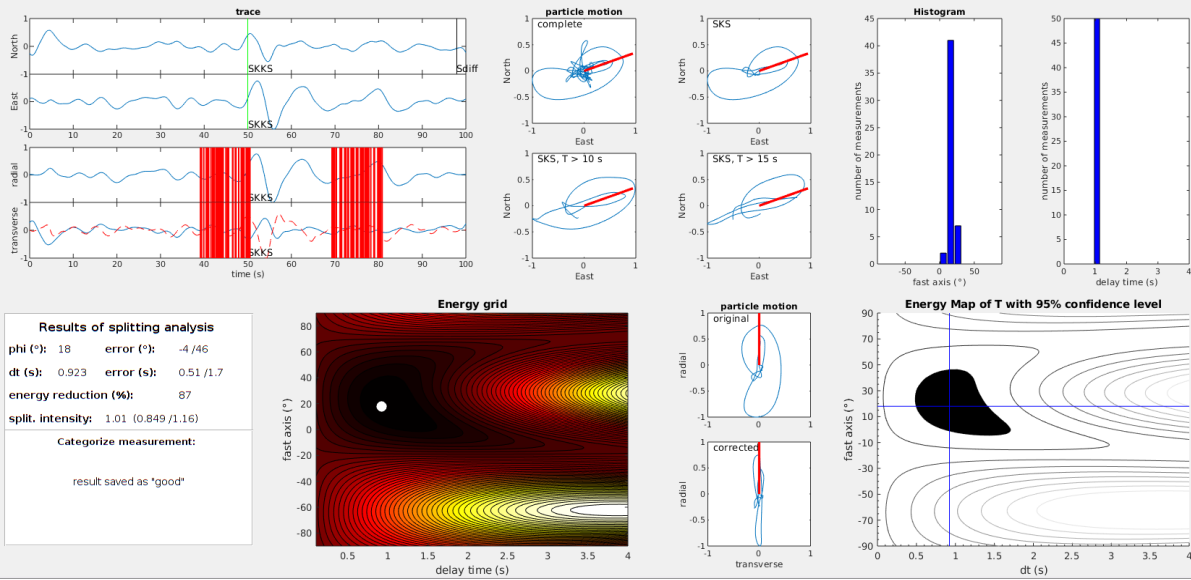
527

528

Figure S1 - Splitting intensity measurements for a few example stations. Gray dots: all measurements; green circles: only measurements that fit the criteria and the sinusoidal curve (fast polarization direction and time delay written below).

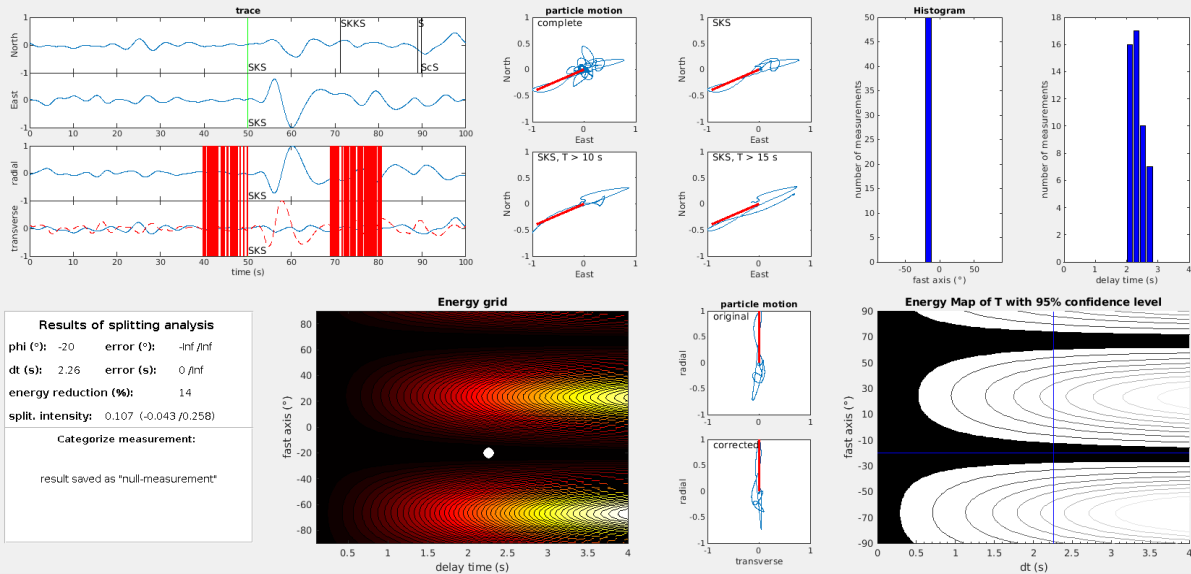
529

Station: CI23, date: 24-Jun-2019 02:53:39, BAZ: 70.6°, distance: 116.59°



530

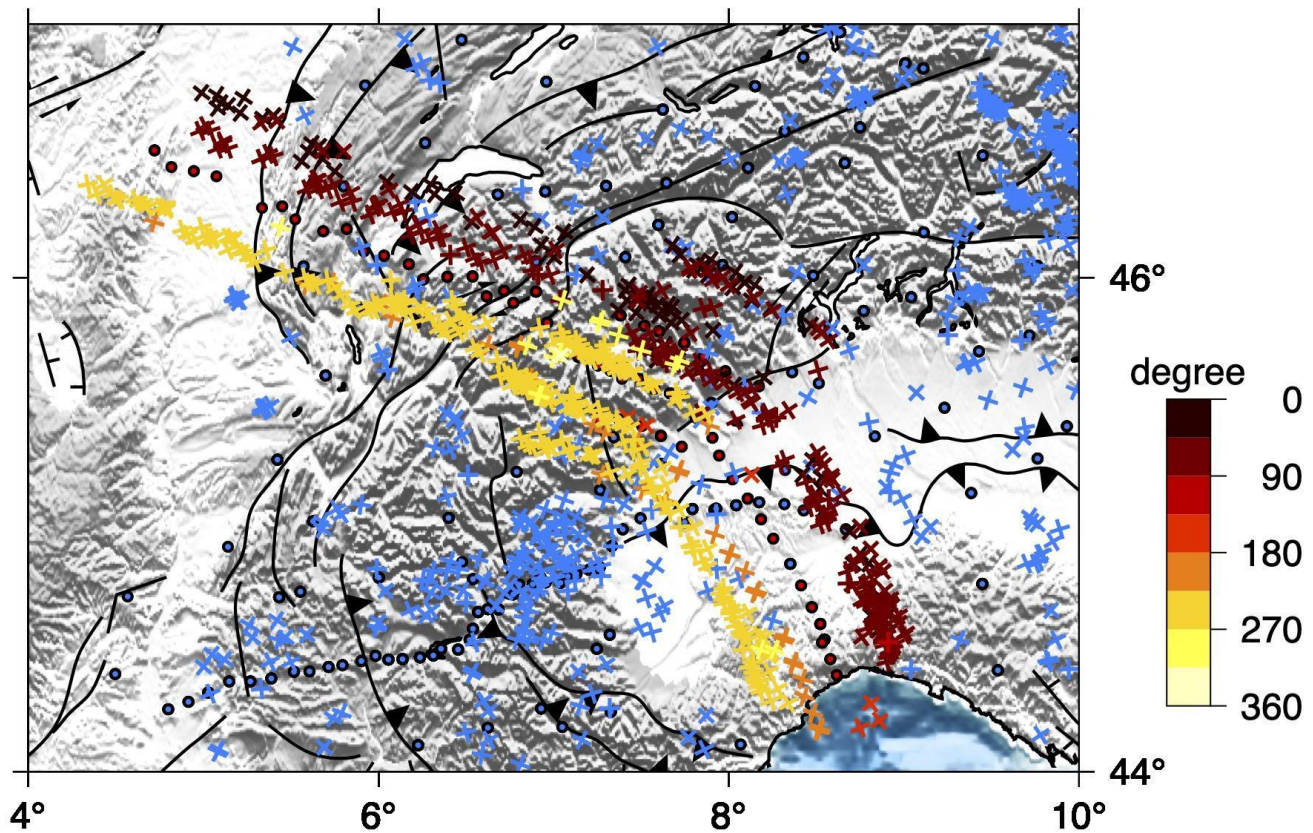
Station: CI21, date: 01-Nov-2018 22:19:51, BAZ: 246.9°, distance: 94.73°



531

532 [Figure S2 - Examples of measurements. Upper panel: a good shear wave splitting measurement at](#)  
 533 [station CI23. Lower panel: a null measurement at station CI21.](#)

534



535

E

536 figure S3 – Map of null measurements plotted at the piercing point of 150 km depth, marked with  
 537 crosses rotated in the back azimuth direction and coloured following the color scale on the right,  
 538 depending on the back azimuth; in light blue all previous data.

539

540

541

542

543

544

545

546

547

550 Table S1 - Good single Splitting Intensity (SI) measurements. Header: Station | Station latitude | Station  
 551 longitude | Earthquake ID (YYMMDDhhmm) | back-azimuth | SI |SI error

<u>Station</u>	<u>Lat</u>	<u>Lon</u>	<u>EQ ID</u>	<u>BAZ</u>	<u>SI</u>	<u>SI error</u>
<u>CE01</u>	<u>45.85</u>	<u>7.38</u>	<u>1809281002</u>	<u>73.70</u>	<u>0.56</u>	<u>0.04</u>
<u>CE01</u>	<u>45.85</u>	<u>7.38</u>	<u>1812290339</u>	<u>64.00</u>	<u>0.06</u>	<u>0.09</u>
<u>CE01</u>	<u>45.85</u>	<u>7.38</u>	<u>1901061727</u>	<u>66.54</u>	<u>0.65</u>	<u>0.04</u>
<u>CE01</u>	<u>45.85</u>	<u>7.38</u>	<u>1901171506</u>	<u>52.65</u>	<u>0.75</u>	<u>0.26</u>
<u>CE01</u>	<u>45.85</u>	<u>7.38</u>	<u>1901260812</u>	<u>66.06</u>	<u>-0.16</u>	<u>0.18</u>
<u>CE01</u>	<u>45.85</u>	<u>7.38</u>	<u>1903150503</u>	<u>245.84</u>	<u>0.39</u>	<u>0.15</u>
<u>CE01</u>	<u>45.85</u>	<u>7.38</u>	<u>1904121140</u>	<u>72.66</u>	<u>0.44</u>	<u>0.07</u>
<u>CE01</u>	<u>45.85</u>	<u>7.38</u>	<u>1904230537</u>	<u>61.60</u>	<u>0.43</u>	<u>0.06</u>
<u>CE01</u>	<u>45.85</u>	<u>7.38</u>	<u>1905141258</u>	<u>46.67</u>	<u>1.24</u>	<u>0.09</u>
<u>CE01</u>	<u>45.85</u>	<u>7.38</u>	<u>1905311012</u>	<u>64.11</u>	<u>0.31</u>	<u>0.13</u>
<u>CE01</u>	<u>45.85</u>	<u>7.38</u>	<u>1907071508</u>	<u>68.18</u>	<u>0.24</u>	<u>0.23</u>
<u>CE01</u>	<u>45.85</u>	<u>7.38</u>	<u>1907140943</u>	<u>67.84</u>	<u>-0.40</u>	<u>0.38</u>
<u>CE01</u>	<u>45.85</u>	<u>7.38</u>	<u>1909190706</u>	<u>83.83</u>	<u>0.62</u>	<u>0.06</u>
<u>CE01</u>	<u>45.85</u>	<u>7.38</u>	<u>1909211953</u>	<u>69.62</u>	<u>0.01</u>	<u>0.17</u>
<u>CE01</u>	<u>45.85</u>	<u>7.38</u>	<u>1909252346</u>	<u>69.16</u>	<u>0.32</u>	<u>0.17</u>
<u>CE01</u>	<u>45.85</u>	<u>7.38</u>	<u>1910290104</u>	<u>64.96</u>	<u>1.83</u>	<u>0.16</u>
<u>CE01</u>	<u>45.85</u>	<u>7.38</u>	<u>1911141617</u>	<u>67.24</u>	<u>1.11</u>	<u>0.06</u>
<u>CE02</u>	<u>45.81</u>	<u>7.52</u>	<u>1809281025</u>	<u>74.30</u>	<u>1.92</u>	<u>0.28</u>
<u>CE02</u>	<u>45.81</u>	<u>7.52</u>	<u>1901212359</u>	<u>81.62</u>	<u>-0.54</u>	<u>0.23</u>

<u>CE02</u>	<u>45.81</u>	<u>7.52</u>	<u>1902121234</u>	<u>40.73</u>	<u>-0.08</u>	<u>0.28</u>
<u>CE02</u>	<u>45.81</u>	<u>7.52</u>	<u>1904121140</u>	<u>72.78</u>	<u>0.74</u>	<u>0.36</u>
<u>CE02</u>	<u>45.81</u>	<u>7.52</u>	<u>1906240253</u>	<u>70.77</u>	<u>0.85</u>	<u>0.03</u>
<u>CE02</u>	<u>45.81</u>	<u>7.52</u>	<u>1907140539</u>	<u>86.98</u>	<u>0.35</u>	<u>0.35</u>
<u>CE02</u>	<u>45.81</u>	<u>7.52</u>	<u>1907140943</u>	<u>67.97</u>	<u>-0.62</u>	<u>0.27</u>
<u>CE02</u>	<u>45.81</u>	<u>7.52</u>	<u>1908021203</u>	<u>89.90</u>	<u>0.01</u>	<u>0.12</u>
<u>CE02</u>	<u>45.81</u>	<u>7.52</u>	<u>1909190706</u>	<u>83.94</u>	<u>1.09</u>	<u>0.06</u>
<u>CE02</u>	<u>45.81</u>	<u>7.52</u>	<u>1910290104</u>	<u>65.08</u>	<u>1.86</u>	<u>0.18</u>
<u>CE03</u>	<u>45.79</u>	<u>7.60</u>	<u>1809281002</u>	<u>73.89</u>	<u>0.44</u>	<u>0.04</u>
<u>CE03</u>	<u>45.79</u>	<u>7.60</u>	<u>1812290339</u>	<u>64.19</u>	<u>0.65</u>	<u>0.03</u>
<u>CE03</u>	<u>45.79</u>	<u>7.60</u>	<u>1901181640</u>	<u>290.91</u>	<u>-0.85</u>	<u>0.17</u>
<u>CE03</u>	<u>45.79</u>	<u>7.60</u>	<u>1902020927</u>	<u>90.21</u>	<u>0.02</u>	<u>0.18</u>
<u>CE03</u>	<u>45.79</u>	<u>7.60</u>	<u>1902021059</u>	<u>90.19</u>	<u>0.02</u>	<u>0.22</u>
<u>CE03</u>	<u>45.79</u>	<u>7.60</u>	<u>1902021101</u>	<u>89.97</u>	<u>0.02</u>	<u>0.20</u>
<u>CE03</u>	<u>45.79</u>	<u>7.60</u>	<u>1903150503</u>	<u>246.00</u>	<u>-0.95</u>	<u>0.19</u>
<u>CE03</u>	<u>45.79</u>	<u>7.60</u>	<u>1904121140</u>	<u>72.86</u>	<u>0.65</u>	<u>0.23</u>
<u>CE03</u>	<u>45.79</u>	<u>7.60</u>	<u>1904230537</u>	<u>61.78</u>	<u>0.51</u>	<u>0.07</u>
<u>CE03</u>	<u>45.79</u>	<u>7.60</u>	<u>1905062119</u>	<u>55.46</u>	<u>1.18</u>	<u>0.17</u>
<u>CE03</u>	<u>45.79</u>	<u>7.60</u>	<u>1905311012</u>	<u>64.30</u>	<u>0.04</u>	<u>0.08</u>
<u>CE03</u>	<u>45.79</u>	<u>7.60</u>	<u>1906140019</u>	<u>241.68</u>	<u>0.82</u>	<u>0.17</u>
<u>CE03</u>	<u>45.79</u>	<u>7.60</u>	<u>1906240253</u>	<u>70.85</u>	<u>0.49</u>	<u>0.06</u>
<u>CE03</u>	<u>45.79</u>	<u>7.60</u>	<u>1907071508</u>	<u>68.38</u>	<u>0.53</u>	<u>0.04</u>
<u>CE03</u>	<u>45.79</u>	<u>7.60</u>	<u>1909141621</u>	<u>67.50</u>	<u>-0.01</u>	<u>0.18</u>
<u>CE03</u>	<u>45.79</u>	<u>7.60</u>	<u>1909290202</u>	<u>64.64</u>	<u>0.81</u>	<u>0.09</u>
<u>CE03</u>	<u>45.79</u>	<u>7.60</u>	<u>1910161137</u>	<u>65.18</u>	<u>0.02</u>	<u>0.13</u>

<u>CE03</u>	<u>45.79</u>	<u>7.60</u>	<u>1911141617</u>	<u>67.44</u>	<u>0.54</u>	<u>0.06</u>
<u>CE04</u>	<u>45.74</u>	<u>7.75</u>	<u>1809281002</u>	<u>74.01</u>	<u>0.90</u>	<u>0.08</u>
<u>CE04</u>	<u>45.74</u>	<u>7.75</u>	<u>1812290339</u>	<u>64.32</u>	<u>0.49</u>	<u>0.04</u>
<u>CE04</u>	<u>45.74</u>	<u>7.75</u>	<u>1901061727</u>	<u>66.87</u>	<u>1.22</u>	<u>0.13</u>
<u>CE04</u>	<u>45.74</u>	<u>7.75</u>	<u>1904220911</u>	<u>63.38</u>	<u>-0.06</u>	<u>0.13</u>
<u>CE04</u>	<u>45.74</u>	<u>7.75</u>	<u>1904230537</u>	<u>61.90</u>	<u>0.66</u>	<u>0.04</u>
<u>CE04</u>	<u>45.74</u>	<u>7.75</u>	<u>1905311012</u>	<u>64.42</u>	<u>0.62</u>	<u>0.04</u>
<u>CE04</u>	<u>45.74</u>	<u>7.75</u>	<u>1906240253</u>	<u>70.99</u>	<u>0.49</u>	<u>0.03</u>
<u>CE04</u>	<u>45.74</u>	<u>7.75</u>	<u>1907071508</u>	<u>68.51</u>	<u>0.82</u>	<u>0.08</u>
<u>CE04</u>	<u>45.74</u>	<u>7.75</u>	<u>1909190706</u>	<u>84.12</u>	<u>0.48</u>	<u>0.06</u>
<u>CE04</u>	<u>45.74</u>	<u>7.75</u>	<u>1909290202</u>	<u>64.76</u>	<u>1.31</u>	<u>0.12</u>
<u>CE04</u>	<u>45.74</u>	<u>7.75</u>	<u>1910290104</u>	<u>65.27</u>	<u>0.73</u>	<u>0.08</u>
<u>CE04</u>	<u>45.74</u>	<u>7.75</u>	<u>1910310111</u>	<u>65.04</u>	<u>-0.39</u>	<u>0.24</u>
<u>CE04</u>	<u>45.74</u>	<u>7.75</u>	<u>1911052052</u>	<u>189.30</u>	<u>0.79</u>	<u>0.21</u>
<u>CE04</u>	<u>45.74</u>	<u>7.75</u>	<u>1911150117</u>	<u>67.63</u>	<u>1.83</u>	<u>0.26</u>
<u>CE05</u>	<u>45.68</u>	<u>7.86</u>	<u>1810292017</u>	<u>216.72</u>	<u>0.37</u>	<u>0.12</u>
<u>CE05</u>	<u>45.68</u>	<u>7.86</u>	<u>1811040755</u>	<u>65.60</u>	<u>0.10</u>	<u>0.18</u>
<u>CE05</u>	<u>45.68</u>	<u>7.86</u>	<u>1812290339</u>	<u>64.42</u>	<u>0.34</u>	<u>0.05</u>
<u>CE05</u>	<u>45.68</u>	<u>7.86</u>	<u>1902081155</u>	<u>62.14</u>	<u>0.41</u>	<u>0.21</u>
<u>CE05</u>	<u>45.68</u>	<u>7.86</u>	<u>1903240437</u>	<u>67.67</u>	<u>0.50</u>	<u>0.31</u>
<u>CE05</u>	<u>45.68</u>	<u>7.86</u>	<u>1904121140</u>	<u>73.09</u>	<u>1.03</u>	<u>0.06</u>
<u>CE05</u>	<u>45.68</u>	<u>7.86</u>	<u>1904230537</u>	<u>61.99</u>	<u>1.00</u>	<u>0.05</u>
<u>CE05</u>	<u>45.68</u>	<u>7.86</u>	<u>1905311012</u>	<u>64.52</u>	<u>0.77</u>	<u>0.27</u>
<u>CE05</u>	<u>45.68</u>	<u>7.86</u>	<u>1906240253</u>	<u>71.10</u>	<u>0.75</u>	<u>0.04</u>
<u>CE05</u>	<u>45.68</u>	<u>7.86</u>	<u>1907071508</u>	<u>68.61</u>	<u>1.37</u>	<u>0.08</u>



<u>CE05</u>	<u>45.68</u>	<u>7.86</u>	<u>1909290202</u>	<u>64.86</u>	<u>1.55</u>	<u>0.14</u>
<u>CE05</u>	<u>45.68</u>	<u>7.86</u>	<u>1910310111</u>	<u>65.14</u>	<u>1.42</u>	<u>0.09</u>
<u>CE05</u>	<u>45.68</u>	<u>7.86</u>	<u>1911141617</u>	<u>67.68</u>	<u>0.28</u>	<u>0.15</u>
<u>CE06</u>	<u>45.63</u>	<u>7.98</u>	<u>1812290339</u>	<u>64.54</u>	<u>0.58</u>	<u>0.08</u>
<u>CE06</u>	<u>45.63</u>	<u>7.98</u>	<u>1901171506</u>	<u>53.37</u>	<u>1.42</u>	<u>0.22</u>
<u>CE06</u>	<u>45.63</u>	<u>7.98</u>	<u>1903010850</u>	<u>251.39</u>	<u>1.21</u>	<u>0.10</u>
<u>CE06</u>	<u>45.63</u>	<u>7.98</u>	<u>1904062155</u>	<u>74.88</u>	<u>-0.16</u>	<u>0.07</u>
<u>CE06</u>	<u>45.63</u>	<u>7.98</u>	<u>1904121140</u>	<u>73.20</u>	<u>0.68</u>	<u>0.06</u>
<u>CE06</u>	<u>45.63</u>	<u>7.98</u>	<u>1904230537</u>	<u>62.10</u>	<u>0.66</u>	<u>0.08</u>
<u>CE06</u>	<u>45.63</u>	<u>7.98</u>	<u>1906240253</u>	<u>71.23</u>	<u>1.27</u>	<u>0.03</u>
<u>CE06</u>	<u>45.63</u>	<u>7.98</u>	<u>1907011659</u>	<u>64.54</u>	<u>1.01</u>	<u>0.20</u>
<u>CE06</u>	<u>45.63</u>	<u>7.98</u>	<u>1907071508</u>	<u>68.73</u>	<u>1.48</u>	<u>0.05</u>
<u>CE06</u>	<u>45.63</u>	<u>7.98</u>	<u>1907081852</u>	<u>68.65</u>	<u>0.96</u>	<u>0.09</u>
<u>CE06</u>	<u>45.63</u>	<u>7.98</u>	<u>1907140943</u>	<u>68.41</u>	<u>1.43</u>	<u>0.37</u>
<u>CE06</u>	<u>45.63</u>	<u>7.98</u>	<u>1907141026</u>	<u>68.08</u>	<u>-1.18</u>	<u>0.07</u>
<u>CE06</u>	<u>45.63</u>	<u>7.98</u>	<u>1911141617</u>	<u>67.79</u>	<u>1.26</u>	<u>0.05</u>
<u>CE07</u>	<u>45.57</u>	<u>8.17</u>	<u>1809281002</u>	<u>74.38</u>	<u>0.77</u>	<u>0.11</u>
<u>CE07</u>	<u>45.57</u>	<u>8.17</u>	<u>1812110226</u>	<u>198.19</u>	<u>-0.23</u>	<u>0.06</u>
<u>CE07</u>	<u>45.57</u>	<u>8.17</u>	<u>1812290339</u>	<u>64.70</u>	<u>0.95</u>	<u>0.08</u>
<u>CE07</u>	<u>45.57</u>	<u>8.17</u>	<u>1904050956</u>	<u>41.09</u>	<u>0.61</u>	<u>0.26</u>
<u>CE07</u>	<u>45.57</u>	<u>8.17</u>	<u>1904230537</u>	<u>62.25</u>	<u>0.35</u>	<u>0.07</u>
<u>CE07</u>	<u>45.57</u>	<u>8.17</u>	<u>1906040439</u>	<u>41.36</u>	<u>-0.27</u>	<u>0.10</u>
<u>CE07</u>	<u>45.57</u>	<u>8.17</u>	<u>1907011659</u>	<u>64.70</u>	<u>0.20</u>	<u>0.44</u>
<u>CE07</u>	<u>45.57</u>	<u>8.17</u>	<u>1907071508</u>	<u>68.91</u>	<u>0.78</u>	<u>0.09</u>
<u>CE07</u>	<u>45.57</u>	<u>8.17</u>	<u>1907141026</u>	<u>68.25</u>	<u>1.83</u>	<u>0.13</u>

<u>CI01</u>	<u>46.50</u>	<u>4.72</u>	<u>1809281014</u>	<u>71.35</u>	<u>-1.19</u>	<u>0.12</u>
<u>CI01</u>	<u>46.50</u>	<u>4.72</u>	<u>1901221901</u>	<u>153.32</u>	<u>0.65</u>	<u>0.11</u>
<u>CI01</u>	<u>46.50</u>	<u>4.72</u>	<u>1902020927</u>	<u>88.08</u>	<u>0.90</u>	<u>0.14</u>
<u>CI02</u>	<u>46.44</u>	<u>4.82</u>	<u>1809181157</u>	<u>40.67</u>	<u>0.00</u>	<u>0.09</u>
<u>CI02</u>	<u>46.44</u>	<u>4.82</u>	<u>1809281014</u>	<u>71.45</u>	<u>-1.35</u>	<u>0.08</u>
<u>CI02</u>	<u>46.44</u>	<u>4.82</u>	<u>1810260905</u>	<u>37.16</u>	<u>1.27</u>	<u>0.46</u>
<u>CI02</u>	<u>46.44</u>	<u>4.82</u>	<u>1812011327</u>	<u>69.30</u>	<u>0.00</u>	<u>0.05</u>
<u>CI02</u>	<u>46.44</u>	<u>4.82</u>	<u>1812192137</u>	<u>47.80</u>	<u>0.46</u>	<u>0.12</u>
<u>CI02</u>	<u>46.44</u>	<u>4.82</u>	<u>1901221901</u>	<u>153.39</u>	<u>1.11</u>	<u>0.09</u>
<u>CI03</u>	<u>46.42</u>	<u>4.95</u>	<u>1809281002</u>	<u>71.64</u>	<u>0.28</u>	<u>0.04</u>
<u>CI03</u>	<u>46.42</u>	<u>4.95</u>	<u>1809281014</u>	<u>71.55</u>	<u>-1.57</u>	<u>0.22</u>
<u>CI03</u>	<u>46.42</u>	<u>4.95</u>	<u>1809281025</u>	<u>72.11</u>	<u>-1.37</u>	<u>0.18</u>
<u>CI03</u>	<u>46.42</u>	<u>4.95</u>	<u>1904091753</u>	<u>196.05</u>	<u>1.38</u>	<u>0.07</u>
<u>CI03</u>	<u>46.42</u>	<u>4.95</u>	<u>1904220911</u>	<u>61.24</u>	<u>-0.06</u>	<u>0.12</u>
<u>CI04</u>	<u>46.40</u>	<u>5.07</u>	<u>1901221901</u>	<u>153.56</u>	<u>-0.52</u>	<u>0.16</u>
<u>CI04</u>	<u>46.40</u>	<u>5.07</u>	<u>1902121234</u>	<u>38.50</u>	<u>1.47</u>	<u>0.24</u>
<u>CI05</u>	<u>46.28</u>	<u>5.33</u>	<u>1809281025</u>	<u>72.46</u>	<u>1.21</u>	<u>0.16</u>
<u>CI05</u>	<u>46.28</u>	<u>5.33</u>	<u>1903240437</u>	<u>65.43</u>	<u>0.03</u>	<u>0.12</u>
<u>CI05</u>	<u>46.28</u>	<u>5.33</u>	<u>1908272355</u>	<u>196.24</u>	<u>0.27</u>	<u>0.08</u>
<u>CI05</u>	<u>46.28</u>	<u>5.33</u>	<u>1910290242</u>	<u>63.18</u>	<u>-0.02</u>	<u>0.11</u>
<u>CI05</u>	<u>46.28</u>	<u>5.33</u>	<u>1911231211</u>	<u>60.00</u>	<u>0.24</u>	<u>0.13</u>
<u>CI06</u>	<u>46.28</u>	<u>5.45</u>	<u>1901212359</u>	<u>79.84</u>	<u>0.40</u>	<u>0.08</u>
<u>CI06</u>	<u>46.28</u>	<u>5.45</u>	<u>1906040439</u>	<u>39.28</u>	<u>0.34</u>	<u>0.05</u>
<u>CI06</u>	<u>46.28</u>	<u>5.45</u>	<u>1907141026</u>	<u>65.75</u>	<u>-0.92</u>	<u>0.42</u>
<u>CI06</u>	<u>46.28</u>	<u>5.45</u>	<u>1911042153</u>	<u>238.70</u>	<u>0.03</u>	<u>0.15</u>

<u>CI07</u>	<u>46.23</u>	<u>5.52</u>	<u>1810020016</u>	<u>79.26</u>	<u>-0.42</u>	<u>0.17</u>
<u>CI07</u>	<u>46.23</u>	<u>5.52</u>	<u>1810292326</u>	<u>282.59</u>	<u>-0.02</u>	<u>0.20</u>
<u>CI07</u>	<u>46.23</u>	<u>5.52</u>	<u>1812160942</u>	<u>57.14</u>	<u>0.55</u>	<u>0.10</u>
<u>CI07</u>	<u>46.23</u>	<u>5.52</u>	<u>1901181640</u>	<u>289.41</u>	<u>0.00</u>	<u>0.04</u>
<u>CI07</u>	<u>46.23</u>	<u>5.52</u>	<u>1901200132</u>	<u>240.02</u>	<u>0.03</u>	<u>0.33</u>
<u>CI07</u>	<u>46.23</u>	<u>5.52</u>	<u>1901212359</u>	<u>79.92</u>	<u>0.01</u>	<u>0.18</u>
<u>CI07</u>	<u>46.23</u>	<u>5.52</u>	<u>1901220510</u>	<u>80.09</u>	<u>0.01</u>	<u>0.18</u>
<u>CI07</u>	<u>46.23</u>	<u>5.52</u>	<u>1901221901</u>	<u>153.87</u>	<u>0.00</u>	<u>0.06</u>
<u>CI07</u>	<u>46.23</u>	<u>5.52</u>	<u>1901260812</u>	<u>64.23</u>	<u>0.03</u>	<u>0.34</u>
<u>CI07</u>	<u>46.23</u>	<u>5.52</u>	<u>1901301531</u>	<u>282.22</u>	<u>0.01</u>	<u>0.06</u>
<u>CI07</u>	<u>46.23</u>	<u>5.52</u>	<u>1902020927</u>	<u>88.69</u>	<u>0.01</u>	<u>0.13</u>
<u>CI07</u>	<u>46.23</u>	<u>5.52</u>	<u>1902021059</u>	<u>88.67</u>	<u>0.01</u>	<u>0.13</u>
<u>CI07</u>	<u>46.23</u>	<u>5.52</u>	<u>1902021101</u>	<u>88.44</u>	<u>0.01</u>	<u>0.13</u>
<u>CI07</u>	<u>46.23</u>	<u>5.52</u>	<u>1902081155</u>	<u>60.18</u>	<u>0.04</u>	<u>0.43</u>
<u>CI07</u>	<u>46.23</u>	<u>5.52</u>	<u>1904062155</u>	<u>72.64</u>	<u>0.20</u>	<u>0.05</u>
<u>CI07</u>	<u>46.23</u>	<u>5.52</u>	<u>1907141026</u>	<u>65.84</u>	<u>-0.70</u>	<u>0.24</u>
<u>CI07</u>	<u>46.23</u>	<u>5.52</u>	<u>1911042153</u>	<u>238.74</u>	<u>1.88</u>	<u>0.45</u>
<u>CI08</u>	<u>46.18</u>	<u>5.68</u>	<u>1810260905</u>	<u>38.00</u>	<u>0.47</u>	<u>0.08</u>
<u>CI08</u>	<u>46.18</u>	<u>5.68</u>	<u>1811011930</u>	<u>196.58</u>	<u>1.32</u>	<u>0.12</u>
<u>CI08</u>	<u>46.18</u>	<u>5.68</u>	<u>1901220510</u>	<u>80.24</u>	<u>-0.66</u>	<u>0.08</u>
<u>CI08</u>	<u>46.18</u>	<u>5.68</u>	<u>1901260351</u>	<u>42.14</u>	<u>0.83</u>	<u>0.30</u>
<u>CI08</u>	<u>46.18</u>	<u>5.68</u>	<u>1907141026</u>	<u>65.99</u>	<u>-0.54</u>	<u>0.29</u>
<u>CI08</u>	<u>46.18</u>	<u>5.68</u>	<u>1909290202</u>	<u>62.99</u>	<u>1.21</u>	<u>0.32</u>
<u>CI08</u>	<u>46.18</u>	<u>5.68</u>	<u>1911161019</u>	<u>65.86</u>	<u>0.26</u>	<u>0.19</u>
<u>CI09</u>	<u>46.19</u>	<u>5.82</u>	<u>1809230552</u>	<u>42.15</u>	<u>-0.47</u>	<u>0.19</u>

<u>CI09</u>	<u>46.19</u>	<u>5.82</u>	<u>1812011327</u>	<u>70.27</u>	<u>-0.60</u>	<u>0.10</u>
<u>CI09</u>	<u>46.19</u>	<u>5.82</u>	<u>1901220510</u>	<u>80.34</u>	<u>-0.85</u>	<u>0.08</u>
<u>CI09</u>	<u>46.19</u>	<u>5.82</u>	<u>1903060013</u>	<u>60.97</u>	<u>0.69</u>	<u>0.13</u>
<u>CI09</u>	<u>46.19</u>	<u>5.82</u>	<u>1904051614</u>	<u>198.90</u>	<u>-0.01</u>	<u>0.12</u>
<u>CI09</u>	<u>46.19</u>	<u>5.82</u>	<u>1911141845</u>	<u>66.04</u>	<u>-1.48</u>	<u>0.33</u>
<u>CI10</u>	<u>46.11</u>	<u>5.92</u>	<u>1809281002</u>	<u>72.50</u>	<u>0.17</u>	<u>0.04</u>
<u>CI10</u>	<u>46.11</u>	<u>5.92</u>	<u>1812110226</u>	<u>197.10</u>	<u>1.31</u>	<u>0.07</u>
<u>CI10</u>	<u>46.11</u>	<u>5.92</u>	<u>1812280303</u>	<u>61.53</u>	<u>0.21</u>	<u>0.15</u>
<u>CI10</u>	<u>46.11</u>	<u>5.92</u>	<u>1901200132</u>	<u>240.25</u>	<u>0.02</u>	<u>0.25</u>
<u>CI10</u>	<u>46.11</u>	<u>5.92</u>	<u>1909190732</u>	<u>82.63</u>	<u>-0.44</u>	<u>0.04</u>
<u>CI11</u>	<u>46.09</u>	<u>6.03</u>	<u>1809181157</u>	<u>42.41</u>	<u>0.02</u>	<u>0.10</u>
<u>CI11</u>	<u>46.09</u>	<u>6.03</u>	<u>1810292326</u>	<u>282.94</u>	<u>0.24</u>	<u>0.31</u>
<u>CI11</u>	<u>46.09</u>	<u>6.03</u>	<u>1811011930</u>	<u>196.75</u>	<u>0.75</u>	<u>0.30</u>
<u>CI11</u>	<u>46.09</u>	<u>6.03</u>	<u>1812110226</u>	<u>197.16</u>	<u>1.04</u>	<u>0.09</u>
<u>CI11</u>	<u>46.09</u>	<u>6.03</u>	<u>1901212359</u>	<u>80.37</u>	<u>0.09</u>	<u>0.07</u>
<u>CI11</u>	<u>46.09</u>	<u>6.03</u>	<u>1902021059</u>	<u>89.05</u>	<u>-0.90</u>	<u>0.19</u>
<u>CI11</u>	<u>46.09</u>	<u>6.03</u>	<u>1905162252</u>	<u>282.79</u>	<u>0.54</u>	<u>0.17</u>
<u>CI11</u>	<u>46.09</u>	<u>6.03</u>	<u>1906040439</u>	<u>39.73</u>	<u>0.68</u>	<u>0.24</u>
<u>CI11</u>	<u>46.09</u>	<u>6.03</u>	<u>1907071508</u>	<u>67.01</u>	<u>0.69</u>	<u>0.03</u>
<u>CI12</u>	<u>46.05</u>	<u>6.17</u>	<u>1812110226</u>	<u>197.23</u>	<u>1.06</u>	<u>0.11</u>
<u>CI12</u>	<u>46.05</u>	<u>6.17</u>	<u>1812290339</u>	<u>62.97</u>	<u>0.03</u>	<u>0.04</u>
<u>CI12</u>	<u>46.05</u>	<u>6.17</u>	<u>1901260351</u>	<u>42.81</u>	<u>0.93</u>	<u>0.17</u>
<u>CI12</u>	<u>46.05</u>	<u>6.17</u>	<u>1905162252</u>	<u>282.89</u>	<u>1.74</u>	<u>0.33</u>
<u>CI12</u>	<u>46.05</u>	<u>6.17</u>	<u>1906040439</u>	<u>39.84</u>	<u>0.67</u>	<u>0.07</u>
<u>CI12</u>	<u>46.05</u>	<u>6.17</u>	<u>1906240253</u>	<u>69.53</u>	<u>0.50</u>	<u>0.05</u>

<u>CI12</u>	<u>46.05</u>	<u>6.17</u>	<u>1907071508</u>	<u>67.13</u>	<u>0.70</u>	<u>0.03</u>
<u>CI12</u>	<u>46.05</u>	<u>6.17</u>	<u>1910290104</u>	<u>63.96</u>	<u>0.44</u>	<u>0.06</u>
<u>CI12</u>	<u>46.05</u>	<u>6.17</u>	<u>1910310111</u>	<u>63.72</u>	<u>1.00</u>	<u>0.13</u>
<u>CI13</u>	<u>45.99</u>	<u>6.26</u>	<u>1809281014</u>	<u>72.70</u>	<u>1.80</u>	<u>0.17</u>
<u>CI13</u>	<u>45.99</u>	<u>6.26</u>	<u>1810102200</u>	<u>46.90</u>	<u>-0.34</u>	<u>0.24</u>
<u>CI13</u>	<u>45.99</u>	<u>6.26</u>	<u>1812290339</u>	<u>63.06</u>	<u>0.01</u>	<u>0.09</u>
<u>CI13</u>	<u>45.99</u>	<u>6.26</u>	<u>1901260351</u>	<u>42.95</u>	<u>0.80</u>	<u>0.10</u>
<u>CI13</u>	<u>45.99</u>	<u>6.26</u>	<u>1906040439</u>	<u>39.90</u>	<u>1.02</u>	<u>0.08</u>
<u>CI14</u>	<u>46.00</u>	<u>6.39</u>	<u>1809281025</u>	<u>73.37</u>	<u>1.72</u>	<u>0.49</u>
<u>CI14</u>	<u>46.00</u>	<u>6.39</u>	<u>1811040755</u>	<u>64.40</u>	<u>0.89</u>	<u>0.18</u>
<u>CI14</u>	<u>46.00</u>	<u>6.39</u>	<u>1901061727</u>	<u>65.69</u>	<u>1.04</u>	<u>0.11</u>
<u>CI14</u>	<u>46.00</u>	<u>6.39</u>	<u>1901221901</u>	<u>154.45</u>	<u>-0.78</u>	<u>0.08</u>
<u>CI14</u>	<u>46.00</u>	<u>6.39</u>	<u>1904051614</u>	<u>199.19</u>	<u>-0.05</u>	<u>0.21</u>
<u>CI14</u>	<u>46.00</u>	<u>6.39</u>	<u>1904221449</u>	<u>198.79</u>	<u>0.10</u>	<u>0.17</u>
<u>CI14</u>	<u>46.00</u>	<u>6.39</u>	<u>1911141845</u>	<u>66.57</u>	<u>-0.04</u>	<u>0.20</u>
<u>CI15</u>	<u>46.01</u>	<u>6.54</u>	<u>1809281002</u>	<u>73.01</u>	<u>0.35</u>	<u>0.03</u>
<u>CI15</u>	<u>46.01</u>	<u>6.54</u>	<u>1810102200</u>	<u>47.20</u>	<u>-0.91</u>	<u>0.21</u>
<u>CI15</u>	<u>46.01</u>	<u>6.54</u>	<u>1810290654</u>	<u>216.44</u>	<u>0.07</u>	<u>0.15</u>
<u>CI15</u>	<u>46.01</u>	<u>6.54</u>	<u>1812290339</u>	<u>63.28</u>	<u>0.02</u>	<u>0.08</u>
<u>CI15</u>	<u>46.01</u>	<u>6.54</u>	<u>1901260812</u>	<u>65.24</u>	<u>0.46</u>	<u>0.12</u>
<u>CI15</u>	<u>46.01</u>	<u>6.54</u>	<u>1902081155</u>	<u>61.04</u>	<u>-0.48</u>	<u>0.21</u>
<u>CI15</u>	<u>46.01</u>	<u>6.54</u>	<u>1905062119</u>	<u>54.23</u>	<u>1.04</u>	<u>0.07</u>
<u>CI15</u>	<u>46.01</u>	<u>6.54</u>	<u>1905162252</u>	<u>283.15</u>	<u>0.81</u>	<u>0.20</u>
<u>CI15</u>	<u>46.01</u>	<u>6.54</u>	<u>1906191724</u>	<u>58.74</u>	<u>0.45</u>	<u>0.09</u>
<u>CI15</u>	<u>46.01</u>	<u>6.54</u>	<u>1906281551</u>	<u>40.68</u>	<u>1.15</u>	<u>0.03</u>

<u>CI15</u>	<u>46.01</u>	<u>6.54</u>	<u>1907071508</u>	<u>67.44</u>	<u>0.68</u>	<u>0.06</u>
<u>CI15</u>	<u>46.01</u>	<u>6.54</u>	<u>1908272355</u>	<u>196.79</u>	<u>0.85</u>	<u>0.03</u>
<u>CI15</u>	<u>46.01</u>	<u>6.54</u>	<u>1911141617</u>	<u>66.51</u>	<u>0.80</u>	<u>0.04</u>
<u>CI16</u>	<u>45.92</u>	<u>6.62</u>	<u>1809281002</u>	<u>73.09</u>	<u>0.62</u>	<u>0.04</u>
<u>CI16</u>	<u>45.92</u>	<u>6.62</u>	<u>1809281025</u>	<u>73.57</u>	<u>-0.49</u>	<u>0.16</u>
<u>CI16</u>	<u>45.92</u>	<u>6.62</u>	<u>1812190137</u>	<u>253.14</u>	<u>-0.03</u>	<u>0.25</u>
<u>CI16</u>	<u>45.92</u>	<u>6.62</u>	<u>1901221901</u>	<u>154.61</u>	<u>-0.01</u>	<u>0.06</u>
<u>CI16</u>	<u>45.92</u>	<u>6.62</u>	<u>1901260812</u>	<u>65.35</u>	<u>0.03</u>	<u>0.32</u>
<u>CI16</u>	<u>45.92</u>	<u>6.62</u>	<u>1901301531</u>	<u>282.96</u>	<u>0.01</u>	<u>0.06</u>
<u>CI16</u>	<u>45.92</u>	<u>6.62</u>	<u>1902020927</u>	<u>89.50</u>	<u>0.01</u>	<u>0.13</u>
<u>CI16</u>	<u>45.92</u>	<u>6.62</u>	<u>1902021059</u>	<u>89.48</u>	<u>0.01</u>	<u>0.13</u>
<u>CI16</u>	<u>45.92</u>	<u>6.62</u>	<u>1902021101</u>	<u>89.26</u>	<u>0.01</u>	<u>0.13</u>
<u>CI16</u>	<u>45.92</u>	<u>6.62</u>	<u>1902081155</u>	<u>61.11</u>	<u>0.05</u>	<u>0.40</u>
<u>CI16</u>	<u>45.92</u>	<u>6.62</u>	<u>1903081506</u>	<u>61.23</u>	<u>1.55</u>	<u>0.19</u>
<u>CI16</u>	<u>45.92</u>	<u>6.62</u>	<u>1904230537</u>	<u>60.99</u>	<u>1.01</u>	<u>0.05</u>
<u>CI16</u>	<u>45.92</u>	<u>6.62</u>	<u>1905062119</u>	<u>54.37</u>	<u>0.99</u>	<u>0.07</u>
<u>CI16</u>	<u>45.92</u>	<u>6.62</u>	<u>1905141258</u>	<u>45.78</u>	<u>0.87</u>	<u>0.19</u>
<u>CI16</u>	<u>45.92</u>	<u>6.62</u>	<u>1906040439</u>	<u>40.18</u>	<u>0.97</u>	<u>0.07</u>
<u>CI16</u>	<u>45.92</u>	<u>6.62</u>	<u>1906191724</u>	<u>58.85</u>	<u>1.38</u>	<u>0.11</u>
<u>CI16</u>	<u>45.92</u>	<u>6.62</u>	<u>1906240253</u>	<u>69.96</u>	<u>0.59</u>	<u>0.06</u>
<u>CI16</u>	<u>45.92</u>	<u>6.62</u>	<u>1906281551</u>	<u>40.76</u>	<u>1.33</u>	<u>0.05</u>
<u>CI16</u>	<u>45.92</u>	<u>6.62</u>	<u>1907071508</u>	<u>67.54</u>	<u>0.87</u>	<u>0.04</u>
<u>CI16</u>	<u>45.92</u>	<u>6.62</u>	<u>1907140910</u>	<u>66.78</u>	<u>1.30</u>	<u>0.11</u>
<u>CI16</u>	<u>45.92</u>	<u>6.62</u>	<u>1907141026</u>	<u>66.86</u>	<u>1.09</u>	<u>0.21</u>
<u>CI16</u>	<u>45.92</u>	<u>6.62</u>	<u>1908272355</u>	<u>196.83</u>	<u>1.32</u>	<u>0.05</u>

<u>CI16</u>	<u>45.92</u>	<u>6.62</u>	<u>1910290844</u>	<u>44.71</u>	<u>-0.28</u>	<u>0.10</u>
<u>CI17</u>	<u>45.95</u>	<u>6.72</u>	<u>1809281002</u>	<u>73.16</u>	<u>0.45</u>	<u>0.07</u>
<u>CI17</u>	<u>45.95</u>	<u>6.72</u>	<u>1810020016</u>	<u>80.31</u>	<u>1.45</u>	<u>0.23</u>
<u>CI17</u>	<u>45.95</u>	<u>6.72</u>	<u>1810101844</u>	<u>82.37</u>	<u>-0.09</u>	<u>0.11</u>
<u>CI17</u>	<u>45.95</u>	<u>6.72</u>	<u>1812290339</u>	<u>63.44</u>	<u>0.03</u>	<u>0.14</u>
<u>CI17</u>	<u>45.95</u>	<u>6.72</u>	<u>1901181640</u>	<u>290.27</u>	<u>-0.68</u>	<u>0.13</u>
<u>CI17</u>	<u>45.95</u>	<u>6.72</u>	<u>1901200132</u>	<u>240.73</u>	<u>0.38</u>	<u>0.11</u>
<u>CI17</u>	<u>45.95</u>	<u>6.72</u>	<u>1901221901</u>	<u>154.67</u>	<u>-0.92</u>	<u>0.10</u>
<u>CI17</u>	<u>45.95</u>	<u>6.72</u>	<u>1901301531</u>	<u>283.04</u>	<u>0.80</u>	<u>0.11</u>
<u>CI17</u>	<u>45.95</u>	<u>6.72</u>	<u>1902121234</u>	<u>40.02</u>	<u>0.45</u>	<u>0.26</u>
<u>CI17</u>	<u>45.95</u>	<u>6.72</u>	<u>1903041006</u>	<u>53.47</u>	<u>1.24</u>	<u>0.44</u>
<u>CI17</u>	<u>45.95</u>	<u>6.72</u>	<u>1903081506</u>	<u>61.30</u>	<u>0.65</u>	<u>0.09</u>
<u>CI17</u>	<u>45.95</u>	<u>6.72</u>	<u>1904091753</u>	<u>196.91</u>	<u>0.41</u>	<u>0.10</u>
<u>CI17</u>	<u>45.95</u>	<u>6.72</u>	<u>1906040439</u>	<u>40.25</u>	<u>0.73</u>	<u>0.07</u>
<u>CI17</u>	<u>45.95</u>	<u>6.72</u>	<u>1906281551</u>	<u>40.85</u>	<u>0.82</u>	<u>0.03</u>
<u>CI17</u>	<u>45.95</u>	<u>6.72</u>	<u>1907071508</u>	<u>67.61</u>	<u>0.70</u>	<u>0.03</u>
<u>CI17</u>	<u>45.95</u>	<u>6.72</u>	<u>1909190706</u>	<u>83.31</u>	<u>0.84</u>	<u>0.05</u>
<u>CI17</u>	<u>45.95</u>	<u>6.72</u>	<u>1910161137</u>	<u>64.44</u>	<u>0.37</u>	<u>0.08</u>
<u>CI18</u>	<u>45.90</u>	<u>6.77</u>	<u>1809281002</u>	<u>73.22</u>	<u>0.54</u>	<u>0.07</u>
<u>CI18</u>	<u>45.90</u>	<u>6.77</u>	<u>1810012359</u>	<u>80.36</u>	<u>0.55</u>	<u>0.15</u>
<u>CI18</u>	<u>45.90</u>	<u>6.77</u>	<u>1812110226</u>	<u>197.51</u>	<u>0.19</u>	<u>0.08</u>
<u>CI18</u>	<u>45.90</u>	<u>6.77</u>	<u>1901221901</u>	<u>154.71</u>	<u>-1.29</u>	<u>0.14</u>
<u>CI18</u>	<u>45.90</u>	<u>6.77</u>	<u>1901260351</u>	<u>43.62</u>	<u>-0.01</u>	<u>0.15</u>
<u>CI18</u>	<u>45.90</u>	<u>6.77</u>	<u>1901260812</u>	<u>65.50</u>	<u>-0.03</u>	<u>0.35</u>
<u>CI18</u>	<u>45.90</u>	<u>6.77</u>	<u>1901301531</u>	<u>283.07</u>	<u>0.03</u>	<u>0.47</u>

<u>CI18</u>	<u>45.90</u>	<u>6.77</u>	<u>1902121234</u>	<u>40.07</u>	<u>0.74</u>	<u>0.17</u>
<u>CI18</u>	<u>45.90</u>	<u>6.77</u>	<u>1902171435</u>	<u>46.02</u>	<u>0.20</u>	<u>0.31</u>
<u>CI18</u>	<u>45.90</u>	<u>6.77</u>	<u>1906191724</u>	<u>59.00</u>	<u>0.42</u>	<u>0.09</u>
<u>CI18</u>	<u>45.90</u>	<u>6.77</u>	<u>1907140910</u>	<u>66.91</u>	<u>1.34</u>	<u>0.18</u>
<u>CI19</u>	<u>45.94</u>	<u>6.90</u>	<u>1812192137</u>	<u>50.38</u>	<u>-0.86</u>	<u>0.19</u>
<u>CI19</u>	<u>45.94</u>	<u>6.90</u>	<u>1903010850</u>	<u>250.64</u>	<u>0.52</u>	<u>0.05</u>
<u>CI19</u>	<u>45.94</u>	<u>6.90</u>	<u>1904051614</u>	<u>199.46</u>	<u>1.10</u>	<u>0.08</u>
<u>CI19</u>	<u>45.94</u>	<u>6.90</u>	<u>1904062155</u>	<u>73.88</u>	<u>1.87</u>	<u>0.14</u>
<u>CI19</u>	<u>45.94</u>	<u>6.90</u>	<u>1904091753</u>	<u>197.00</u>	<u>0.26</u>	<u>0.20</u>
<u>CI19</u>	<u>45.94</u>	<u>6.90</u>	<u>1904121140</u>	<u>72.25</u>	<u>0.77</u>	<u>0.06</u>
<u>CI19</u>	<u>45.94</u>	<u>6.90</u>	<u>1906040439</u>	<u>40.39</u>	<u>1.24</u>	<u>0.13</u>
<u>CI19</u>	<u>45.94</u>	<u>6.90</u>	<u>1906191724</u>	<u>59.10</u>	<u>1.39</u>	<u>0.08</u>
<u>CI19</u>	<u>45.94</u>	<u>6.90</u>	<u>1907071508</u>	<u>67.76</u>	<u>0.94</u>	<u>0.04</u>
<u>CI19</u>	<u>45.94</u>	<u>6.90</u>	<u>1908272355</u>	<u>196.96</u>	<u>0.72</u>	<u>0.04</u>
<u>CI19</u>	<u>45.94</u>	<u>6.90</u>	<u>1909291557</u>	<u>237.91</u>	<u>0.79</u>	<u>0.07</u>
<u>CI19</u>	<u>45.94</u>	<u>6.90</u>	<u>1911141617</u>	<u>66.82</u>	<u>1.58</u>	<u>0.05</u>
<u>CI21</u>	<u>45.72</u>	<u>7.14</u>	<u>1809280659</u>	<u>73.71</u>	<u>0.41</u>	<u>0.34</u>
<u>CI21</u>	<u>45.72</u>	<u>7.14</u>	<u>1809281002</u>	<u>73.55</u>	<u>1.08</u>	<u>0.10</u>
<u>CI21</u>	<u>45.72</u>	<u>7.14</u>	<u>1809281014</u>	<u>73.46</u>	<u>1.54</u>	<u>0.09</u>
<u>CI21</u>	<u>45.72</u>	<u>7.14</u>	<u>1810141241</u>	<u>126.72</u>	<u>0.04</u>	<u>0.17</u>
<u>CI21</u>	<u>45.72</u>	<u>7.14</u>	<u>1812290339</u>	<u>63.84</u>	<u>0.84</u>	<u>0.08</u>
<u>CI21</u>	<u>45.72</u>	<u>7.14</u>	<u>1901181640</u>	<u>290.55</u>	<u>0.07</u>	<u>0.38</u>
<u>CI21</u>	<u>45.72</u>	<u>7.14</u>	<u>1901212359</u>	<u>81.37</u>	<u>0.15</u>	<u>0.23</u>
<u>CI21</u>	<u>45.72</u>	<u>7.14</u>	<u>1901220510</u>	<u>81.54</u>	<u>0.26</u>	<u>0.19</u>
<u>CI21</u>	<u>45.72</u>	<u>7.14</u>	<u>1901260351</u>	<u>44.17</u>	<u>0.94</u>	<u>0.26</u>



<u>CI21</u>	<u>45.72</u>	<u>7.14</u>	<u>1906240253</u>	<u>70.49</u>	<u>0.97</u>	<u>0.04</u>
<u>CI21</u>	<u>45.72</u>	<u>7.14</u>	<u>1907071508</u>	<u>68.03</u>	<u>1.11</u>	<u>0.05</u>
<u>CI21</u>	<u>45.72</u>	<u>7.14</u>	<u>1907140539</u>	<u>86.75</u>	<u>1.16</u>	<u>0.12</u>
<u>CI21</u>	<u>45.72</u>	<u>7.14</u>	<u>1909141621</u>	<u>67.14</u>	<u>-0.09</u>	<u>0.16</u>
<u>CI21</u>	<u>45.72</u>	<u>7.14</u>	<u>1909190732</u>	<u>83.64</u>	<u>1.50</u>	<u>0.26</u>
<u>CI21</u>	<u>45.72</u>	<u>7.14</u>	<u>1911150117</u>	<u>67.15</u>	<u>-1.21</u>	<u>0.14</u>
<u>CI22</u>	<u>45.68</u>	<u>7.14</u>	<u>1809281002</u>	<u>73.56</u>	<u>0.80</u>	<u>0.07</u>
<u>CI22</u>	<u>45.68</u>	<u>7.14</u>	<u>1809281014</u>	<u>73.47</u>	<u>1.94</u>	<u>0.20</u>
<u>CI22</u>	<u>45.68</u>	<u>7.14</u>	<u>1905162252</u>	<u>283.51</u>	<u>-0.04</u>	<u>0.16</u>
<u>CI22</u>	<u>45.68</u>	<u>7.14</u>	<u>1907011659</u>	<u>63.88</u>	<u>1.96</u>	<u>0.14</u>
<u>CI22</u>	<u>45.68</u>	<u>7.14</u>	<u>1907071508</u>	<u>68.04</u>	<u>0.97</u>	<u>0.09</u>
<u>CI22</u>	<u>45.68</u>	<u>7.14</u>	<u>1907140539</u>	<u>86.77</u>	<u>0.92</u>	<u>0.16</u>
<u>CI23</u>	<u>45.68</u>	<u>7.24</u>	<u>1809281002</u>	<u>73.64</u>	<u>1.07</u>	<u>0.07</u>
<u>CI23</u>	<u>45.68</u>	<u>7.24</u>	<u>1810020016</u>	<u>80.83</u>	<u>-0.37</u>	<u>0.17</u>
<u>CI23</u>	<u>45.68</u>	<u>7.24</u>	<u>1810141241</u>	<u>126.79</u>	<u>-1.21</u>	<u>0.16</u>
<u>CI23</u>	<u>45.68</u>	<u>7.24</u>	<u>1812160942</u>	<u>59.06</u>	<u>-0.01</u>	<u>0.06</u>
<u>CI23</u>	<u>45.68</u>	<u>7.24</u>	<u>1812161426</u>	<u>96.66</u>	<u>-0.02</u>	<u>0.25</u>
<u>CI23</u>	<u>45.68</u>	<u>7.24</u>	<u>1812290339</u>	<u>63.93</u>	<u>0.39</u>	<u>0.06</u>
<u>CI23</u>	<u>45.68</u>	<u>7.24</u>	<u>1901061727</u>	<u>66.48</u>	<u>0.46</u>	<u>0.10</u>
<u>CI23</u>	<u>45.68</u>	<u>7.24</u>	<u>1901181640</u>	<u>290.62</u>	<u>-0.91</u>	<u>0.21</u>
<u>CI23</u>	<u>45.68</u>	<u>7.24</u>	<u>1903060013</u>	<u>62.22</u>	<u>0.48</u>	<u>0.08</u>
<u>CI23</u>	<u>45.68</u>	<u>7.24</u>	<u>1904051614</u>	<u>199.61</u>	<u>0.04</u>	<u>0.14</u>
<u>CI23</u>	<u>45.68</u>	<u>7.24</u>	<u>1904230537</u>	<u>61.52</u>	<u>0.86</u>	<u>0.06</u>
<u>CI23</u>	<u>45.68</u>	<u>7.24</u>	<u>1905030725</u>	<u>39.67</u>	<u>1.39</u>	<u>0.16</u>
<u>CI23</u>	<u>45.68</u>	<u>7.24</u>	<u>1905311012</u>	<u>64.03</u>	<u>0.60</u>	<u>0.07</u>

<u>CI23</u>	<u>45.68</u>	<u>7.24</u>	<u>1906240253</u>	<u>70.60</u>	<u>0.95</u>	<u>0.04</u>
<u>CI23</u>	<u>45.68</u>	<u>7.24</u>	<u>1907071508</u>	<u>68.12</u>	<u>0.90</u>	<u>0.05</u>
<u>CI23</u>	<u>45.68</u>	<u>7.24</u>	<u>1910290104</u>	<u>64.89</u>	<u>0.79</u>	<u>0.08</u>
<u>CI23</u>	<u>45.68</u>	<u>7.24</u>	<u>1911141617</u>	<u>67.18</u>	<u>1.19</u>	<u>0.13</u>
<u>CI24</u>	<u>45.65</u>	<u>7.25</u>	<u>1809281002</u>	<u>73.66</u>	<u>1.07</u>	<u>0.09</u>
<u>CI24</u>	<u>45.65</u>	<u>7.25</u>	<u>1812290339</u>	<u>63.95</u>	<u>0.31</u>	<u>0.05</u>
<u>CI24</u>	<u>45.65</u>	<u>7.25</u>	<u>1902021101</u>	<u>89.73</u>	<u>-0.33</u>	<u>0.24</u>
<u>CI24</u>	<u>45.65</u>	<u>7.25</u>	<u>1904062155</u>	<u>74.29</u>	<u>0.19</u>	<u>0.09</u>
<u>CI24</u>	<u>45.65</u>	<u>7.25</u>	<u>1904230537</u>	<u>61.53</u>	<u>0.86</u>	<u>0.05</u>
<u>CI24</u>	<u>45.65</u>	<u>7.25</u>	<u>1905062119</u>	<u>55.19</u>	<u>0.07</u>	<u>0.30</u>
<u>CI24</u>	<u>45.65</u>	<u>7.25</u>	<u>1906240253</u>	<u>70.62</u>	<u>1.03</u>	<u>0.05</u>
<u>CI24</u>	<u>45.65</u>	<u>7.25</u>	<u>1907071508</u>	<u>68.14</u>	<u>0.90</u>	<u>0.05</u>
<u>CI24</u>	<u>45.65</u>	<u>7.25</u>	<u>1910142223</u>	<u>90.32</u>	<u>1.03</u>	<u>0.06</u>
<u>CI24</u>	<u>45.65</u>	<u>7.25</u>	<u>1910290104</u>	<u>64.90</u>	<u>0.92</u>	<u>0.06</u>
<u>CI24</u>	<u>45.65</u>	<u>7.25</u>	<u>1911052052</u>	<u>189.03</u>	<u>-0.24</u>	<u>0.25</u>
<u>CI24</u>	<u>45.65</u>	<u>7.25</u>	<u>1911231211</u>	<u>61.89</u>	<u>0.55</u>	<u>0.07</u>
<u>CI25</u>	<u>45.63</u>	<u>7.32</u>	<u>1809281002</u>	<u>73.72</u>	<u>0.97</u>	<u>0.07</u>
<u>CI25</u>	<u>45.63</u>	<u>7.32</u>	<u>1809281025</u>	<u>74.20</u>	<u>0.64</u>	<u>0.14</u>
<u>CI25</u>	<u>45.63</u>	<u>7.32</u>	<u>1812290339</u>	<u>64.01</u>	<u>0.44</u>	<u>0.04</u>
<u>CI25</u>	<u>45.63</u>	<u>7.32</u>	<u>1901220510</u>	<u>81.72</u>	<u>0.98</u>	<u>0.08</u>
<u>CI25</u>	<u>45.63</u>	<u>7.32</u>	<u>1902121234</u>	<u>40.60</u>	<u>-0.19</u>	<u>0.13</u>
<u>CI25</u>	<u>45.63</u>	<u>7.32</u>	<u>1903041006</u>	<u>54.27</u>	<u>-0.55</u>	<u>0.14</u>
<u>CI25</u>	<u>45.63</u>	<u>7.32</u>	<u>1904230537</u>	<u>61.59</u>	<u>0.57</u>	<u>0.05</u>
<u>CI25</u>	<u>45.63</u>	<u>7.32</u>	<u>1905311012</u>	<u>64.11</u>	<u>-1.80</u>	<u>0.38</u>
<u>CI25</u>	<u>45.63</u>	<u>7.32</u>	<u>1906240253</u>	<u>70.69</u>	<u>1.04</u>	<u>0.06</u>

<u>CI25</u>	<u>45.63</u>	<u>7.32</u>	<u>1907071508</u>	<u>68.21</u>	<u>0.91</u>	<u>0.10</u>
<u>CI25</u>	<u>45.63</u>	<u>7.32</u>	<u>1907141026</u>	<u>67.54</u>	<u>-0.92</u>	<u>0.19</u>
<u>CI25</u>	<u>45.63</u>	<u>7.32</u>	<u>1910290104</u>	<u>64.96</u>	<u>1.17</u>	<u>0.13</u>
<u>CI25</u>	<u>45.63</u>	<u>7.32</u>	<u>1911141617</u>	<u>67.27</u>	<u>0.27</u>	<u>0.08</u>
<u>CI26</u>	<u>45.60</u>	<u>7.39</u>	<u>1901220510</u>	<u>81.78</u>	<u>1.15</u>	<u>0.21</u>
<u>CI26</u>	<u>45.60</u>	<u>7.39</u>	<u>1903101248</u>	<u>51.72</u>	<u>0.71</u>	<u>0.28</u>
<u>CI26</u>	<u>45.60</u>	<u>7.39</u>	<u>1907071508</u>	<u>68.27</u>	<u>1.17</u>	<u>0.08</u>
<u>CI26</u>	<u>45.60</u>	<u>7.39</u>	<u>1907141026</u>	<u>67.61</u>	<u>1.75</u>	<u>0.45</u>
<u>CI27</u>	<u>45.60</u>	<u>7.49</u>	<u>1810020016</u>	<u>81.05</u>	<u>0.39</u>	<u>0.48</u>
<u>CI28</u>	<u>45.56</u>	<u>7.57</u>	<u>1904230537</u>	<u>61.79</u>	<u>0.45</u>	<u>0.11</u>
<u>CI28</u>	<u>45.56</u>	<u>7.57</u>	<u>1907140943</u>	<u>68.10</u>	<u>1.42</u>	<u>0.38</u>
<u>CI29</u>	<u>45.54</u>	<u>7.66</u>	<u>1905311012</u>	<u>64.41</u>	<u>0.44</u>	<u>0.24</u>
<u>CI29</u>	<u>45.54</u>	<u>7.66</u>	<u>1906240253</u>	<u>71.01</u>	<u>1.09</u>	<u>0.15</u>
<u>CI29</u>	<u>45.54</u>	<u>7.66</u>	<u>1907071508</u>	<u>68.51</u>	<u>0.79</u>	<u>0.39</u>
<u>CI29</u>	<u>45.54</u>	<u>7.66</u>	<u>1905311012</u>	<u>64.41</u>	<u>0.44</u>	<u>0.24</u>
<u>CI29</u>	<u>45.54</u>	<u>7.66</u>	<u>1906240253</u>	<u>71.01</u>	<u>1.09</u>	<u>0.15</u>
<u>CI29</u>	<u>45.54</u>	<u>7.66</u>	<u>1907071508</u>	<u>68.51</u>	<u>0.79</u>	<u>0.39</u>
<u>CI30</u>	<u>45.52</u>	<u>7.71</u>	<u>1812192137</u>	<u>51.51</u>	<u>-1.19</u>	<u>0.25</u>
<u>CI30</u>	<u>45.52</u>	<u>7.71</u>	<u>1902121234</u>	<u>40.95</u>	<u>-1.45</u>	<u>0.16</u>
<u>CI30</u>	<u>45.52</u>	<u>7.71</u>	<u>1907071508</u>	<u>68.55</u>	<u>1.23</u>	<u>0.11</u>
<u>CI30</u>	<u>45.52</u>	<u>7.71</u>	<u>1909141621</u>	<u>67.68</u>	<u>0.49</u>	<u>0.29</u>
<u>CI31</u>	<u>45.44</u>	<u>7.81</u>	<u>1903010850</u>	<u>251.27</u>	<u>0.58</u>	<u>0.05</u>
<u>CI31</u>	<u>45.44</u>	<u>7.81</u>	<u>1904220911</u>	<u>63.45</u>	<u>0.23</u>	<u>0.11</u>
<u>CI31</u>	<u>45.44</u>	<u>7.81</u>	<u>1906040439</u>	<u>41.09</u>	<u>-0.65</u>	<u>0.15</u>
<u>CI31</u>	<u>45.44</u>	<u>7.81</u>	<u>1910161137</u>	<u>65.42</u>	<u>0.49</u>	<u>0.08</u>

<u>CI32</u>	<u>45.36</u>	<u>7.91</u>	<u>1810102113</u>	<u>50.39</u>	<u>-0.81</u>	<u>0.23</u>
<u>CI32</u>	<u>45.36</u>	<u>7.91</u>	<u>1905311012</u>	<u>64.64</u>	<u>0.74</u>	<u>0.20</u>
<u>CI32</u>	<u>45.36</u>	<u>7.91</u>	<u>1907011659</u>	<u>64.53</u>	<u>-1.09</u>	<u>0.26</u>
<u>CI32</u>	<u>45.36</u>	<u>7.91</u>	<u>1910290104</u>	<u>65.48</u>	<u>0.46</u>	<u>0.14</u>
<u>CI33</u>	<u>45.29</u>	<u>7.94</u>	<u>1812161426</u>	<u>97.32</u>	<u>-0.93</u>	<u>0.12</u>
<u>CI33</u>	<u>45.29</u>	<u>7.94</u>	<u>1901200132</u>	<u>241.36</u>	<u>0.65</u>	<u>0.14</u>
<u>CI33</u>	<u>45.29</u>	<u>7.94</u>	<u>1902021101</u>	<u>90.25</u>	<u>1.85</u>	<u>0.19</u>
<u>CI33</u>	<u>45.29</u>	<u>7.94</u>	<u>1902081155</u>	<u>62.28</u>	<u>0.27</u>	<u>0.09</u>
<u>CI33</u>	<u>45.29</u>	<u>7.94</u>	<u>1906281551</u>	<u>41.99</u>	<u>-1.47</u>	<u>0.07</u>
<u>CI33</u>	<u>45.29</u>	<u>7.94</u>	<u>1907141026</u>	<u>68.17</u>	<u>0.08</u>	<u>0.40</u>
<u>CI34</u>	<u>45.19</u>	<u>8.02</u>	<u>1810102045</u>	<u>50.26</u>	<u>1.44</u>	<u>0.13</u>
<u>CI34</u>	<u>45.19</u>	<u>8.02</u>	<u>1901301531</u>	<u>283.79</u>	<u>0.19</u>	<u>0.18</u>
<u>CI34</u>	<u>45.19</u>	<u>8.02</u>	<u>1906040439</u>	<u>41.26</u>	<u>-0.86</u>	<u>0.13</u>
<u>CI35</u>	<u>45.11</u>	<u>8.11</u>	<u>1811040755</u>	<u>65.91</u>	<u>-0.89</u>	<u>0.11</u>
<u>CI35</u>	<u>45.11</u>	<u>8.11</u>	<u>1911021808</u>	<u>199.25</u>	<u>-0.63</u>	<u>0.14</u>
<u>CI36</u>	<u>45.03</u>	<u>8.18</u>	<u>1810020016</u>	<u>81.81</u>	<u>-1.17</u>	<u>0.24</u>
<u>CI36</u>	<u>45.03</u>	<u>8.18</u>	<u>1901220510</u>	<u>82.60</u>	<u>-0.71</u>	<u>0.07</u>
<u>CI36</u>	<u>45.03</u>	<u>8.18</u>	<u>1902020927</u>	<u>90.67</u>	<u>-0.09</u>	<u>0.23</u>
<u>CI36</u>	<u>45.03</u>	<u>8.18</u>	<u>1904230537</u>	<u>62.34</u>	<u>0.38</u>	<u>0.07</u>
<u>CI36</u>	<u>45.03</u>	<u>8.18</u>	<u>1905311012</u>	<u>64.94</u>	<u>0.82</u>	<u>0.12</u>
<u>CI37</u>	<u>44.95</u>	<u>8.25</u>	<u>1812161426</u>	<u>97.69</u>	<u>-1.46</u>	<u>0.41</u>
<u>CI37</u>	<u>44.95</u>	<u>8.25</u>	<u>1902121234</u>	<u>41.51</u>	<u>0.00</u>	<u>0.13</u>
<u>CI37</u>	<u>44.95</u>	<u>8.25</u>	<u>1903150503</u>	<u>246.43</u>	<u>-0.63</u>	<u>0.14</u>
<u>CI37</u>	<u>44.95</u>	<u>8.25</u>	<u>1905311012</u>	<u>65.01</u>	<u>0.37</u>	<u>0.18</u>
<u>CI37</u>	<u>44.95</u>	<u>8.25</u>	<u>1907150821</u>	<u>52.80</u>	<u>-0.92</u>	<u>0.11</u>

<u>CI37</u>	<u>44.95</u>	<u>8.25</u>	<u>1909141621</u>	<u>68.34</u>	<u>0.77</u>	<u>0.30</u>
<u>CI37</u>	<u>44.95</u>	<u>8.25</u>	<u>1910161137</u>	<u>65.87</u>	<u>0.04</u>	<u>0.09</u>
<u>CI38</u>	<u>44.76</u>	<u>8.41</u>	<u>1810290654</u>	<u>216.76</u>	<u>0.00</u>	<u>0.02</u>
<u>CI38</u>	<u>44.76</u>	<u>8.41</u>	<u>1810292017</u>	<u>216.62</u>	<u>0.00</u>	<u>0.02</u>
<u>CI38</u>	<u>44.76</u>	<u>8.41</u>	<u>1810292326</u>	<u>284.31</u>	<u>-0.02</u>	<u>0.16</u>
<u>CI38</u>	<u>44.76</u>	<u>8.41</u>	<u>1903010850</u>	<u>251.66</u>	<u>-0.51</u>	<u>0.05</u>
<u>CI38</u>	<u>44.76</u>	<u>8.41</u>	<u>1904230537</u>	<u>62.56</u>	<u>0.04</u>	<u>0.11</u>
<u>CI38</u>	<u>44.76</u>	<u>8.41</u>	<u>1905311012</u>	<u>65.18</u>	<u>-1.31</u>	<u>0.20</u>
<u>CI38</u>	<u>44.76</u>	<u>8.41</u>	<u>1906250601</u>	<u>127.59</u>	<u>0.01</u>	<u>0.06</u>
<u>CI38</u>	<u>44.76</u>	<u>8.41</u>	<u>1906281551</u>	<u>42.47</u>	<u>-0.01</u>	<u>0.09</u>
<u>CI38</u>	<u>44.76</u>	<u>8.41</u>	<u>1907011659</u>	<u>65.02</u>	<u>-0.02</u>	<u>0.24</u>
<u>CI38</u>	<u>44.76</u>	<u>8.41</u>	<u>1907071508</u>	<u>69.35</u>	<u>-0.02</u>	<u>0.24</u>
<u>CI38</u>	<u>44.76</u>	<u>8.41</u>	<u>1907081852</u>	<u>69.27</u>	<u>-0.02</u>	<u>0.23</u>
<u>CI38</u>	<u>44.76</u>	<u>8.41</u>	<u>1907122042</u>	<u>63.50</u>	<u>-0.02</u>	<u>0.18</u>
<u>CI38</u>	<u>44.76</u>	<u>8.41</u>	<u>1907140910</u>	<u>68.66</u>	<u>-0.02</u>	<u>0.23</u>
<u>CI38</u>	<u>44.76</u>	<u>8.41</u>	<u>1907140943</u>	<u>69.06</u>	<u>-0.02</u>	<u>0.23</u>
<u>CI38</u>	<u>44.76</u>	<u>8.41</u>	<u>1907141026</u>	<u>68.73</u>	<u>-0.02</u>	<u>0.23</u>
<u>CI38</u>	<u>44.76</u>	<u>8.41</u>	<u>1907150821</u>	<u>53.09</u>	<u>-0.01</u>	<u>0.12</u>
<u>CI38</u>	<u>44.76</u>	<u>8.41</u>	<u>1910290104</u>	<u>66.01</u>	<u>-0.06</u>	<u>0.37</u>
<u>CI38</u>	<u>44.76</u>	<u>8.41</u>	<u>1910290242</u>	<u>65.95</u>	<u>-0.03</u>	<u>0.37</u>
<u>CI38</u>	<u>44.76</u>	<u>8.41</u>	<u>1910310111</u>	<u>65.77</u>	<u>-0.02</u>	<u>0.36</u>
<u>CI38</u>	<u>44.76</u>	<u>8.41</u>	<u>1911021808</u>	<u>199.38</u>	<u>0.00</u>	<u>0.04</u>
<u>CI38</u>	<u>44.76</u>	<u>8.41</u>	<u>1911042153</u>	<u>240.19</u>	<u>-0.02</u>	<u>0.21</u>
<u>CI38</u>	<u>44.76</u>	<u>8.41</u>	<u>1911052052</u>	<u>189.62</u>	<u>0.00</u>	<u>0.03</u>
<u>CI38</u>	<u>44.76</u>	<u>8.41</u>	<u>1911141845</u>	<u>68.58</u>	<u>-0.03</u>	<u>0.42</u>

<u>CI38</u>	<u>44.76</u>	<u>8.41</u>	<u>1911142112</u>	<u>68.46</u>	<u>-0.38</u>	<u>0.41</u>
<u>CI38</u>	<u>44.76</u>	<u>8.41</u>	<u>1911150117</u>	<u>68.46</u>	<u>-0.03</u>	<u>0.43</u>
<u>CI38</u>	<u>44.76</u>	<u>8.41</u>	<u>1911161019</u>	<u>68.50</u>	<u>-0.02</u>	<u>0.42</u>
<u>CI38</u>	<u>44.76</u>	<u>8.41</u>	<u>1911231211</u>	<u>63.20</u>	<u>-0.03</u>	<u>0.31</u>
<u>CI38</u>	<u>44.76</u>	<u>8.41</u>	<u>1912030846</u>	<u>249.30</u>	<u>-0.03</u>	<u>0.34</u>
<u>CI39</u>	<u>44.67</u>	<u>8.47</u>	<u>1810290654</u>	<u>216.75</u>	<u>-1.12</u>	<u>0.15</u>
<u>CI39</u>	<u>44.67</u>	<u>8.47</u>	<u>1810292326</u>	<u>284.33</u>	<u>1.74</u>	<u>0.24</u>
<u>CI39</u>	<u>44.67</u>	<u>8.47</u>	<u>1902020927</u>	<u>90.90</u>	<u>0.09</u>	<u>0.30</u>
<u>CI39</u>	<u>44.67</u>	<u>8.47</u>	<u>1907140943</u>	<u>69.14</u>	<u>1.87</u>	<u>0.44</u>
<u>CI39</u>	<u>44.67</u>	<u>8.47</u>	<u>1908272355</u>	<u>197.59</u>	<u>0.92</u>	<u>0.03</u>
<u>CI39</u>	<u>44.67</u>	<u>8.47</u>	<u>1911231211</u>	<u>63.28</u>	<u>-0.20</u>	<u>0.15</u>
<u>CI40</u>	<u>44.60</u>	<u>8.52</u>	<u>1902020927</u>	<u>90.94</u>	<u>-1.97</u>	<u>0.25</u>
<u>CI40</u>	<u>44.60</u>	<u>8.52</u>	<u>1904221449</u>	<u>199.78</u>	<u>0.30</u>	<u>0.38</u>
<u>CI40</u>	<u>44.60</u>	<u>8.52</u>	<u>1906191724</u>	<u>61.22</u>	<u>-0.75</u>	<u>0.07</u>
<u>CI40</u>	<u>44.60</u>	<u>8.52</u>	<u>1907140539</u>	<u>88.35</u>	<u>-0.78</u>	<u>0.23</u>
<u>CI40</u>	<u>44.60</u>	<u>8.52</u>	<u>1909141621</u>	<u>68.68</u>	<u>0.27</u>	<u>0.22</u>
<u>CI41</u>	<u>44.53</u>	<u>8.53</u>	<u>1903010850</u>	<u>251.73</u>	<u>-1.10</u>	<u>0.07</u>
<u>CI41</u>	<u>44.53</u>	<u>8.53</u>	<u>1904062155</u>	<u>75.78</u>	<u>-0.43</u>	<u>0.06</u>
<u>CI41</u>	<u>44.53</u>	<u>8.53</u>	<u>1906140019</u>	<u>241.98</u>	<u>-0.57</u>	<u>0.04</u>
<u>CI41</u>	<u>44.53</u>	<u>8.53</u>	<u>1906240253</u>	<u>72.19</u>	<u>-0.45</u>	<u>0.08</u>
<u>CI41</u>	<u>44.53</u>	<u>8.53</u>	<u>1906281551</u>	<u>42.61</u>	<u>-0.73</u>	<u>0.04</u>
<u>CI41</u>	<u>44.53</u>	<u>8.53</u>	<u>1908272355</u>	<u>197.60</u>	<u>0.78</u>	<u>0.02</u>
<u>CI41</u>	<u>44.53</u>	<u>8.53</u>	<u>1909291557</u>	<u>238.46</u>	<u>-0.77</u>	<u>0.04</u>
<u>CI42</u>	<u>44.46</u>	<u>8.58</u>	<u>1901220510</u>	<u>83.12</u>	<u>1.14</u>	<u>0.23</u>
<u>CI42</u>	<u>44.46</u>	<u>8.58</u>	<u>1901221901</u>	<u>155.96</u>	<u>0.87</u>	<u>0.05</u>

<u>CI42</u>	<u>44.46</u>	<u>8.58</u>	<u>1903150503</u>	<u>246.65</u>	<u>-1.35</u>	<u>0.20</u>
<u>CI42</u>	<u>44.46</u>	<u>8.58</u>	<u>1906240253</u>	<u>72.26</u>	<u>-0.60</u>	<u>0.10</u>
<u>CI42</u>	<u>44.46</u>	<u>8.58</u>	<u>1909291557</u>	<u>238.47</u>	<u>-1.21</u>	<u>0.07</u>
<u>CI42</u>	<u>44.46</u>	<u>8.58</u>	<u>1911142112</u>	<u>68.69</u>	<u>-0.49</u>	<u>0.05</u>
<u>CI43</u>	<u>44.40</u>	<u>8.62</u>	<u>1811011930</u>	<u>197.91</u>	<u>-0.01</u>	<u>0.12</u>
<u>CI43</u>	<u>44.40</u>	<u>8.62</u>	<u>1811040755</u>	<u>66.44</u>	<u>0.03</u>	<u>0.27</u>
<u>CI43</u>	<u>44.40</u>	<u>8.62</u>	<u>1901221901</u>	<u>155.98</u>	<u>0.95</u>	<u>0.07</u>
<u>CI43</u>	<u>44.40</u>	<u>8.62</u>	<u>1902171435</u>	<u>48.88</u>	<u>-0.70</u>	<u>0.10</u>
<u>CI43</u>	<u>44.40</u>	<u>8.62</u>	<u>1903010850</u>	<u>251.79</u>	<u>-0.70</u>	<u>0.09</u>
<u>CI43</u>	<u>44.40</u>	<u>8.62</u>	<u>1906240253</u>	<u>72.32</u>	<u>-0.32</u>	<u>0.06</u>
<u>CI43</u>	<u>44.40</u>	<u>8.62</u>	<u>1908011828</u>	<u>238.95</u>	<u>-0.88</u>	<u>0.07</u>
<u>CI43</u>	<u>44.40</u>	<u>8.62</u>	<u>1909190706</u>	<u>85.08</u>	<u>-1.42</u>	<u>0.09</u>
<u>CI43</u>	<u>44.40</u>	<u>8.62</u>	<u>1909291557</u>	<u>238.47</u>	<u>-1.08</u>	<u>0.08</u>
<u>CW01</u>	<u>45.43</u>	<u>7.26</u>	<u>1810292017</u>	<u>216.40</u>	<u>-0.22</u>	<u>0.40</u>
<u>CW01</u>	<u>45.43</u>	<u>7.26</u>	<u>1811040755</u>	<u>65.19</u>	<u>1.35</u>	<u>0.32</u>
<u>CW01</u>	<u>45.43</u>	<u>7.26</u>	<u>1812161426</u>	<u>96.79</u>	<u>-0.72</u>	<u>0.17</u>
<u>CW01</u>	<u>45.43</u>	<u>7.26</u>	<u>1901221901</u>	<u>155.05</u>	<u>0.39</u>	<u>0.12</u>
<u>CW01</u>	<u>45.43</u>	<u>7.26</u>	<u>1903041006</u>	<u>54.32</u>	<u>0.19</u>	<u>0.27</u>
<u>CW01</u>	<u>45.43</u>	<u>7.26</u>	<u>1903150503</u>	<u>245.75</u>	<u>1.23</u>	<u>0.15</u>
<u>CW01</u>	<u>45.43</u>	<u>7.26</u>	<u>1907071508</u>	<u>68.22</u>	<u>0.89</u>	<u>0.05</u>
<u>CW01</u>	<u>45.43</u>	<u>7.26</u>	<u>1907141026</u>	<u>67.56</u>	<u>0.47</u>	<u>0.10</u>
<u>CW02</u>	<u>45.43</u>	<u>7.37</u>	<u>1810290654</u>	<u>216.58</u>	<u>1.77</u>	<u>0.12</u>
<u>CW02</u>	<u>45.43</u>	<u>7.37</u>	<u>1810292017</u>	<u>216.45</u>	<u>-0.22</u>	<u>0.10</u>
<u>CW02</u>	<u>45.43</u>	<u>7.37</u>	<u>1901181640</u>	<u>290.69</u>	<u>-1.46</u>	<u>0.48</u>
<u>CW02</u>	<u>45.43</u>	<u>7.37</u>	<u>1902121234</u>	<u>40.67</u>	<u>-0.78</u>	<u>0.12</u>

<u>CW02</u>	<u>45.43</u>	<u>7.37</u>	<u>1906250601</u>	<u>126.80</u>	<u>-1.91</u>	<u>0.19</u>
<u>CW02</u>	<u>45.43</u>	<u>7.37</u>	<u>1907071508</u>	<u>68.31</u>	<u>1.07</u>	<u>0.09</u>
<u>CW02</u>	<u>45.43</u>	<u>7.37</u>	<u>1908142135</u>	<u>302.99</u>	<u>-0.04</u>	<u>0.36</u>
<u>CW02</u>	<u>45.43</u>	<u>7.37</u>	<u>1909141621</u>	<u>67.44</u>	<u>0.04</u>	<u>0.19</u>
<u>CW03</u>	<u>45.41</u>	<u>7.51</u>	<u>1901061727</u>	<u>66.77</u>	<u>1.73</u>	<u>0.20</u>
<u>CW03</u>	<u>45.41</u>	<u>7.51</u>	<u>1904230537</u>	<u>61.76</u>	<u>0.59</u>	<u>0.08</u>
<u>CW03</u>	<u>45.41</u>	<u>7.51</u>	<u>1907071508</u>	<u>68.42</u>	<u>0.86</u>	<u>0.10</u>
<u>CW03</u>	<u>45.41</u>	<u>7.51</u>	<u>1910290104</u>	<u>65.16</u>	<u>-0.58</u>	<u>0.20</u>
<u>CW04</u>	<u>45.37</u>	<u>7.61</u>	<u>1810292326</u>	<u>283.91</u>	<u>-1.01</u>	<u>0.31</u>
<u>CW04</u>	<u>45.37</u>	<u>7.61</u>	<u>1903060013</u>	<u>62.58</u>	<u>0.44</u>	<u>0.09</u>
<u>CW04</u>	<u>45.37</u>	<u>7.61</u>	<u>1907071508</u>	<u>68.52</u>	<u>1.08</u>	<u>0.09</u>
<u>CW05</u>	<u>45.32</u>	<u>7.73</u>	<u>1901260812</u>	<u>66.63</u>	<u>0.87</u>	<u>0.11</u>
<u>CW05</u>	<u>45.32</u>	<u>7.73</u>	<u>1910290104</u>	<u>65.35</u>	<u>-0.71</u>	<u>0.09</u>
<u>CW05</u>	<u>45.32</u>	<u>7.73</u>	<u>1911052052</u>	<u>189.28</u>	<u>1.43</u>	<u>0.38</u>

553

554

555

556

557

558



559 | **Supplementary Material**

560 |

561 |

562 |

563 |

564

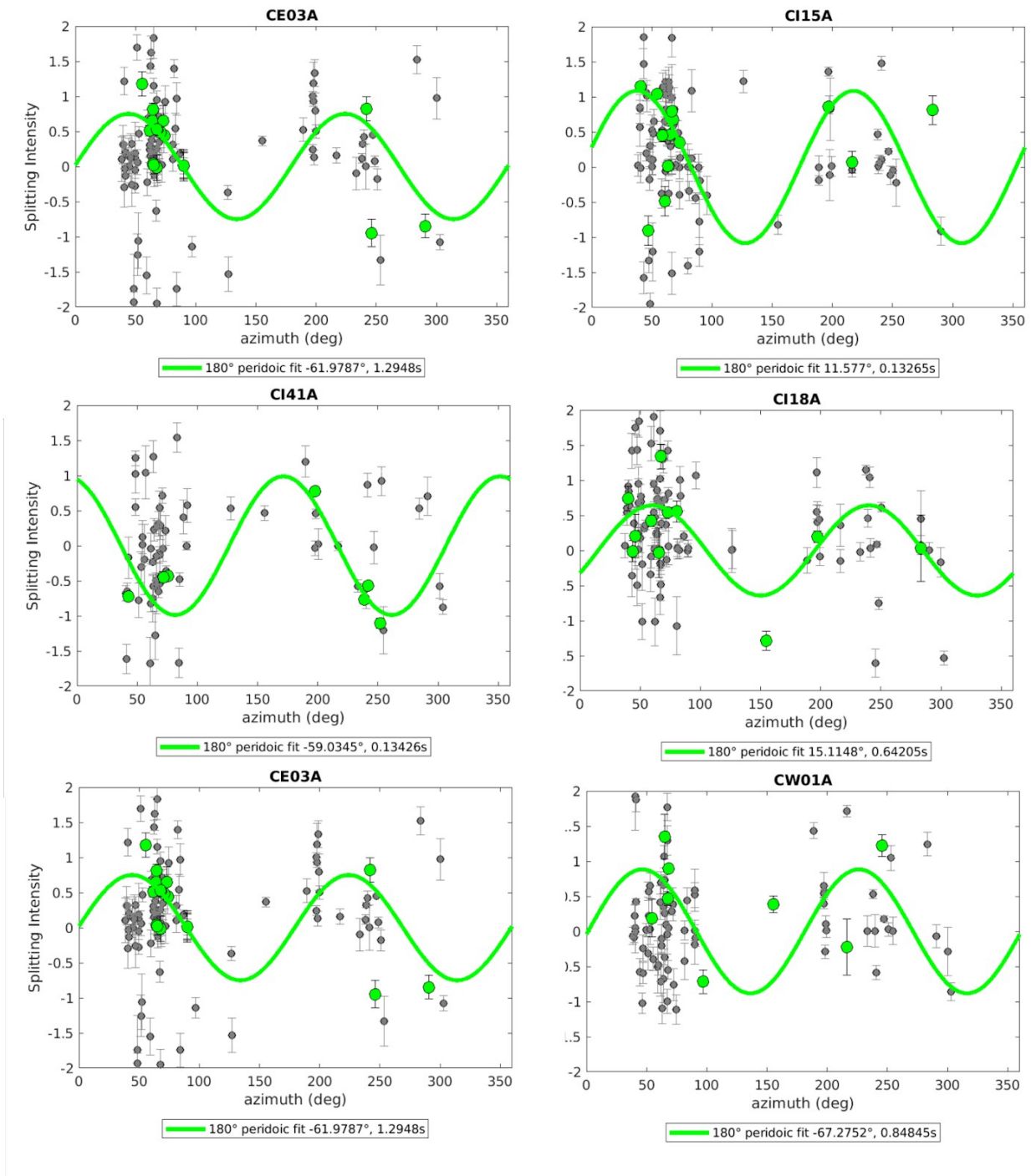
565

566 | ~~Figure S1—Map of null measurements plotted at the piercing point of 150 km depth, marked with crosses, rotated in the~~  
567 | ~~back azimuth direction; in red from CIFALPS2 stations, in light blue all previous data.~~

568 |

569

570 | \_\_\_\_\_



571

572 **Figure S2—**Splitting intensity measurements for a few example stations. Grey dots: all measurements; green circles: only573 **measurements that fit the criteria and the sinusoidal curve (fast polarisation direction and time delay written below).**

575 Table S2 - Splitting parameters for stations with good SI measurements from at least four different  
 576 back-azimuthal bin directions. Header: Station | Station latitude (Lat) | Station longitude (Lon) | FPD |  
 577 FPDerr | TD | TDerr | RMS | Number of Measurements (#) | ~~Single Splitting Intensity (SI)~~  
 578 measurements

<u>Station</u>	<u>Lat</u>	<u>Lon</u>	<u>FPD</u>	<u>FPDerr</u>	<u>TD</u>	<u>TDerr</u>	<u>RMS</u>	<u>#</u>
<u>CE03</u>	<u>45.79</u>	<u>7.60</u>	<u>-0.78</u>	<u>2.35</u>	<u>0.75</u>	<u>0.06</u>	<u>12.64</u>	<u>18</u>
<u>CI07</u>	<u>46.23</u>	<u>5.52</u>	<u>11.58</u>	<u>6.57</u>	<u>0.13</u>	<u>0.04</u>	<u>8.05</u>	<u>17</u>
<u>CI11</u>	<u>46.09</u>	<u>6.03</u>	<u>-0.33</u>	<u>1.56</u>	<u>0.83</u>	<u>0.05</u>	<u>13.30</u>	<u>9</u>
<u>CI15</u>	<u>46.01</u>	<u>6.54</u>	<u>-7.45</u>	<u>0.57</u>	<u>1.08</u>	<u>0.02</u>	<u>18.86</u>	<u>13</u>
<u>CI16</u>	<u>45.92</u>	<u>6.62</u>	<u>-2.58</u>	<u>0.66</u>	<u>1.09</u>	<u>0.02</u>	<u>27.78</u>	<u>23</u>
<u>CI17</u>	<u>45.95</u>	<u>6.72</u>	<u>11.48</u>	<u>0.96</u>	<u>0.79</u>	<u>0.02</u>	<u>17.21</u>	<u>17</u>
<u>CI18</u>	<u>45.90</u>	<u>6.77</u>	<u>15.11</u>	<u>2.53</u>	<u>0.64</u>	<u>0.06</u>	<u>8.29</u>	<u>11</u>
<u>CI19</u>	<u>45.94</u>	<u>6.90</u>	<u>0.98</u>	<u>0.61</u>	<u>1.32</u>	<u>0.03</u>	<u>20.85</u>	<u>12</u>
<u>CI21</u>	<u>45.72</u>	<u>7.14</u>	<u>37.08</u>	<u>2.27</u>	<u>1.04</u>	<u>0.07</u>	<u>18.74</u>	<u>15</u>
<u>CI23</u>	<u>45.68</u>	<u>7.24</u>	<u>22.22</u>	<u>1.97</u>	<u>0.74</u>	<u>0.05</u>	<u>20.34</u>	<u>17</u>
<u>CI24</u>	<u>45.65</u>	<u>7.25</u>	<u>37.75</u>	<u>1.59</u>	<u>0.93</u>	<u>0.05</u>	<u>14.58</u>	<u>12</u>
<u>CI37</u>	<u>44.95</u>	<u>8.25</u>	<u>87.15</u>	<u>12.30</u>	<u>0.32</u>	<u>0.09</u>	<u>9.52</u>	<u>7</u>
<u>CI38</u>	<u>44.76</u>	<u>8.41</u>	<u>-59.03</u>	<u>3.69</u>	<u>0.13</u>	<u>0.02</u>	<u>10.61</u>	<u>28</u>
<u>CI39</u>	<u>44.67</u>	<u>8.47</u>	<u>-43.54</u>	<u>2.80</u>	<u>1.01</u>	<u>0.07</u>	<u>16.59</u>	<u>6</u>
<u>CI41</u>	<u>44.53</u>	<u>8.53</u>	<u>-53.46</u>	<u>0.62</u>	<u>0.99</u>	<u>0.02</u>	<u>19.35</u>	<u>7</u>
<u>CI42</u>	<u>44.46</u>	<u>8.58</u>	<u>76.64</u>	<u>1.76</u>	<u>2.18</u>	<u>0.13</u>	<u>5.75</u>	<u>6</u>
<u>CI43</u>	<u>44.40</u>	<u>8.62</u>	<u>-67.28</u>	<u>1.86</u>	<u>0.85</u>	<u>0.06</u>	<u>12.82</u>	<u>9</u>
<u>CW01</u>	<u>45.43</u>	<u>7.26</u>	<u>1.35</u>	<u>3.98</u>	<u>0.88</u>	<u>0.13</u>	<u>12.19</u>	<u>8</u>
<u>CW02</u>	<u>45.43</u>	<u>7.37</u>	<u>22.80</u>	<u>2.92</u>	<u>0.78</u>	<u>0.08</u>	<u>19.64</u>	<u>8</u>

STA	STA LAT	STA LON	-EV LAT	EV LON	-DEP	-BAZ	INC	SI	SIerr	EQ_ID (yy,mm,dd,hh,m m)
CE01A	45.850	-7.3820	-0.26	119.90	-19.5	73.7	7.74	-0.5633	0.0405	1809281002
CE01A	45.850	-7.3820	-5.86	126.89	-83.2	64.0	7.74	-0.0601	0.0928	1812290339
CE01A	45.850	-7.3820	-2.27	126.85	-66.8	66.5	7.38	-0.6501	0.0388	1901061727
CE01A	45.850	-7.3820	-3.47	146.07	-10.2	52.6	5.52	-0.7454	0.2563	1901171506
CE01A	45.850	-7.3820	-5.52	133.85	-9.8	66.0	6.14	-0.1614	0.1787	1901260812
CE01A	45.850	-7.3820	-1.81	122.63	-19.5	72.6	7.34	-0.4412	0.0684	1904121140
CE01A	45.850	-7.3820	-11.71	125.30	-84.8	61.5	8.53	-0.4253	0.0563	1904230537
CE01A	45.850	-7.3820	-4.10	152.61	-19.5	46.6	5.11	-1.2355	0.0936	1905141258
CE01A	45.850	-7.3820	-6.26	126.61	-98.0	64.1	7.80	-0.3064	0.1287	1905311012
CE01A	45.850	-7.3820	-0.49	126.18	-19.5	68.1	7.27	-0.2399	0.2292	1907071508
CE01A	45.850	-7.3820	-3.44	128.44	-19.5	69.1	6.72	-0.3207	0.1676	1909252346
CE01A	45.850	-7.3820	-6.80	125.20	-19.5	64.9	8.00	-1.8302	0.1558	1910290104
CE01A	45.850	-7.3820	-1.56	126.39	-59.0	67.2	7.35	-1.1091	0.0626	1911141617
CE02A	45.809	-7.5183	-1.06	119.96	-10.0	74.3	7.67	-1.9190	0.2833	1809281025
CE02A	45.809	-7.5183	-10.34	119.05	-19.5	81.6	6.89	-0.5372	0.2347	1901212359
CE02A	45.809	-7.5183	-1.81	122.63	-19.5	72.7	7.35	-0.7407	0.3568	1904121140
CE02A	45.809	-7.5183	-6.38	129.17	226.4	70.7	6.38	-0.8537	0.0250	1906240253
CE02A	45.809	-7.5183	-18.05	120.33	-9.8	86.9	6.15	-0.3457	0.3510	1907140539
CE02A	45.809	-7.5183	-7.31	104.81	-19.5	89.9	8.50	-0.0089	0.1153	1908021203
CE02A	45.809	-7.5183	-6.80	125.20	-19.5	65.0	8.01	-1.8607	0.1805	1910290104
CE03A	45.786	-7.6024	-0.26	119.90	-19.5	73.8	7.75	-0.4436	0.0433	1809281002
CE03A	45.786	-7.6024	-5.86	126.89	-83.2	64.1	7.75	-0.6473	0.0336	1812290339
CE03A	45.786	-7.6024	-2.72	100.20	-19.5	90.2	9.54	-0.0166	0.1762	1902020927

STA	STA LAT	STA LON	EV LAT	EV LON	DEP	BAZ	INC	SI	SIerr	EQ_ID (yy,mm,dd,hh,m m)
CE03A	45.786	-7.6024	-2.78	100.26	-19.5	90.1	9.53	-0.0174	0.2243	1902021059
CE03A	45.786	-7.6024	-1.81	122.63	-19.5	72.8	7.36	-0.6455	0.2272	1904121140
CE03A	45.786	-7.6024	-11.71	125.30	-84.8	61.7	8.55	-0.5141	0.0685	1904230537
CE03A	45.786	-7.6024	-6.94	146.46	-139.5	55.4	5.20	-1.1786	0.1737	1905062119
CE03A	45.786	-7.6024	-6.26	126.61	-98.0	64.2	7.82	-0.0370	0.0817	1905311012
CE03A	45.786	-7.6024	-30.00	-72.11	9.8	241.6	7.90	-0.8227	0.1711	1906140019
CE03A	45.786	-7.6024	-6.38	129.17	226.4	70.8	6.39	-0.4875	0.0605	1906240253
CE03A	45.786	-7.6024	-0.49	126.18	-19.5	68.3	7.29	-0.5261	0.0354	1907071508
CE03A	45.786	-7.6024	-0.92	128.60	-9.8	67.4	6.95	-0.0136	0.1784	1909141621
CE03A	45.786	-7.6024	-5.69	126.66	-91.0	64.6	7.75	-0.8130	0.0916	1909290202
CE03A	45.786	-7.6024	-6.80	125.15	-19.5	65.1	8.02	-0.0234	0.1278	1910161137
CE03A	45.786	-7.6024	-1.56	126.39	-59.0	67.4	7.36	-0.5351	0.0624	1911141617
CE04A	45.740	-7.7453	-0.26	119.90	-19.5	74.0	7.76	-0.9002	0.0797	1809281002
CE04A	45.740	-7.7453	-5.86	126.89	-83.2	64.3	7.76	-0.4851	0.0445	1812290339
CE04A	45.740	-7.7453	-2.27	126.85	-66.8	66.8	7.41	-1.2227	0.1311	1901061727
CE04A	45.740	-7.7453	-11.71	125.30	-84.8	61.8	8.56	-0.6598	0.0393	1904230537
CE04A	45.740	-7.7453	-6.26	126.61	-98.0	64.4	7.83	-0.6234	0.0394	1905311012
CE04A	45.740	-7.7453	-6.38	129.17	226.4	70.9	6.39	-0.4874	0.0283	1906240253
CE04A	45.740	-7.7453	-0.49	126.18	-19.5	68.5	7.30	-0.8205	0.0843	1907071508
CE04A	45.740	-7.7453	-5.69	126.66	-91.0	64.7	7.76	-1.3103	0.1227	1909290202
CE04A	45.740	-7.7453	-6.80	125.20	-19.5	65.2	8.03	-0.7340	0.0793	1910290104
CE04A	45.740	-7.7453	-6.94	125.31	-19.9	65.0	8.03	-0.3912	0.2440	1910310111
CE05A	45.685	-7.8551	-57.49	-66.29	33.6	216.7	5.99	-0.3681	0.1224	1810292017

STA	STA LAT	STA LON	EV LAT	EV LON	DEP	BAZ	INC	SI	SIerr	EQ_ID (yy,mm,dd,hh,m m)
CE05A	45.685	-7.8551	-5.86	126.89	-83.2	64.4	7.77	-0.3449	0.0544	1812290339
CE05A	45.685	-7.8551	-9.78	126.60	-19.5	62.1	8.24	-0.4057	0.2107	1902081155
CE05A	45.685	-7.8551	-1.65	126.44	-65.2	67.6	7.39	-0.5038	0.3057	1903240437
CE05A	45.685	-7.8551	-1.81	122.63	-19.5	73.0	7.38	-1.0346	0.0606	1904121140
CE05A	45.685	-7.8551	-11.71	125.30	-84.8	61.9	8.56	-1.0035	0.0526	1904230537
CE05A	45.685	-7.8551	-6.26	126.61	-98.0	64.5	7.84	-0.7699	0.2665	1905311012
CE05A	45.685	-7.8551	-6.38	129.17	226.4	71.1	6.40	-0.7452	0.0435	1906240253
CE05A	45.685	-7.8551	-0.49	126.18	-19.5	68.6	7.30	-1.3720	0.0813	1907071508
CE05A	45.685	-7.8551	-5.69	126.66	-91.0	64.8	7.77	-1.5481	0.1440	1909290202
CE05A	45.685	-7.8551	-6.94	125.31	-19.9	65.1	8.04	-1.4171	0.0876	1910310111
CE05A	45.685	-7.8551	-1.56	126.39	-59.0	67.6	7.38	-0.2845	0.1529	1911141617
CE06A	45.627	-7.9818	-5.86	126.89	-83.2	64.5	7.78	-0.5776	0.0807	1812290339
CE06A	45.627	-7.9818	-3.47	146.07	-10.2	53.3	5.54	-1.4210	0.2191	1901171506
CE06A	45.627	-7.9818	-14.62	-70.10	258.6	251.3	9.71	-1.2115	0.1033	1903010850
CE06A	45.627	-7.9818	-6.85	125.03	549.6	74.8	6.62	-0.1637	0.0712	1904062155
CE06A	45.627	-7.9818	-1.81	122.63	-19.5	73.2	7.39	-0.6756	0.0601	1904121140
CE06A	45.627	-7.9818	-11.71	125.30	-84.8	62.0	8.57	-0.6584	0.0794	1904230537
CE06A	45.627	-7.9818	-6.38	129.17	226.4	71.2	6.41	-1.2692	0.0288	1906240253
CE06A	45.627	-7.9818	-0.49	126.18	-19.5	68.7	7.31	-1.4828	0.0455	1907071508
CE06A	45.627	-7.9818	-1.56	126.39	-59.0	67.7	7.39	-1.2550	0.0529	1911141617
CE07A	45.567	-8.1720	-0.26	119.90	-19.5	74.3	7.80	-0.7674	0.1094	1809281002
CE07A	45.567	-8.1720	-58.42	-26.33	164.8	198.1	7.42	-0.2332	0.0613	1812110226
CE07A	45.567	-8.1720	-5.86	126.89	-83.2	64.7	7.79	-0.9517	0.0782	1812290339

STA	STA LAT	STA LON	-EV LAT	EV LON	-DEP	-BAZ	INC	-SI	SIerr	EQ_ID (yy,mm,dd,hh,m m)
-CE07A	45.567	-8.1720	-11.71	125.30	-84.8	62.2	8.58	-0.3496	0.0663	1904230537
-CE07A	45.567	-8.1720	-29.00	139.37	434.8	41.3	9.47	-0.2703	0.1049	1906040439
-CE07A	45.567	-8.1720	-0.49	126.18	-19.5	68.9	7.33	-0.7826	0.0851	1907071508
-CI01A	46.504	-4.7212	-0.00	119.76	-10.0	71.3	7.57	-1.1948	0.1183	1809281014
-CI01A	46.504	-4.7212	-42.87	-42.28	19.5	153.3	9.28	-0.6481	0.1108	1901221901
-CI01A	46.504	-4.7212	-2.72	100.20	-19.5	88.0	9.22	-0.8975	0.1411	1902020927
-CI02A	46.439	-4.8174	-0.00	119.76	-10.0	71.4	7.58	-1.3547	0.0757	1809281014
-CI02A	46.439	-4.8174	-17.29	147.87	-10.2	37.1	7.42	-1.2665	0.4633	1810260905
-CI02A	46.439	-4.8174	-7.43	128.75	159.0	69.2	6.16	-0.0045	0.0479	1812011327
-CI02A	46.439	-4.8174	-6.04	149.90	-19.5	47.8	4.99	-0.4637	0.1208	1812192137
-CI02A	46.439	-4.8174	-42.87	-42.28	19.5	153.3	9.29	-1.1079	0.0936	1901221901
-CI03A	46.421	-4.9455	-0.26	119.90	-19.5	71.6	7.54	-0.2770	0.0378	1809281002
-CI03A	46.421	-4.9455	-0.00	119.76	-10.0	71.5	7.59	-1.5665	0.2224	1809281014
-CI03A	46.421	-4.9455	-1.06	119.96	-10.0	72.1	7.47	-1.3681	0.1830	1809281025
-CI04A	46.402	-5.0743	-42.87	-42.28	19.5	153.5	9.31	-0.5223	0.1560	1901221901
-CI05A	46.277	-5.3345	-1.06	119.96	-10.0	72.4	7.49	-1.2095	0.1553	1809281025
-CI05A	46.277	-5.3345	-1.65	126.44	-65.2	65.4	7.21	-0.0324	0.1228	1903240437
-CI05A	46.277	-5.3345	-60.03	-26.63	124.2	196.2	7.22	-0.2716	0.0822	1908272355
-CI05A	46.277	-5.3345	-6.87	125.24	-34.8	63.1	7.86	-0.0161	0.1148	1910290242
-CI05A	46.277	-5.3345	-1.64	132.86	-9.8	60.0	6.74	-0.2371	0.1292	1911231211
-CI06A	46.282	-5.4496	-10.34	119.05	-19.5	79.8	6.72	-0.3987	0.0763	1901212359
-CI06A	46.282	-5.4496	-29.00	139.37	434.8	39.2	9.36	-0.3377	0.0487	1906040439
-CI06A	46.282	-5.4496	-31.80	-71.45	55.9	238.7	7.92	-0.0303	0.1514	1911042153

STA	STA LAT	STA LON	-EV LAT	EV LON	-DEP	-BAZ	INC	SI	SIerr	EQ_ID (yy,mm,dd,hh,m m)
-CI07A	46.231	-5.5241	-10.46	120.17	-10.0	79.2	6.62	-0.4238	0.1723	1810020016
-CI07A	46.231	-5.5241	-30.11	-71.58	61.3	240.0	8.07	-0.0305	0.3285	1901200132
-CI07A	46.231	-5.5241	-10.34	119.05	-19.5	79.9	6.73	-0.0121	0.1786	1901212359
-CI07A	46.231	-5.5241	-10.37	119.05	-19.5	80.0	6.73	-0.0144	0.1773	1901220510
-CI07A	46.231	-5.5241	-42.87	-42.28	19.5	153.8	9.36	-0.0046	0.0551	1901221901
-CI07A	46.231	-5.5241	-5.52	133.85	-9.8	64.2	6.03	-0.0272	0.3418	1901260812
-CI07A	46.231	-5.5241	-2.72	100.20	-19.5	88.6	9.30	-0.0113	0.1311	1902020927
-CI07A	46.231	-5.5241	-2.78	100.26	-19.5	88.6	9.29	-0.0097	0.1310	1902021059
-CI07A	46.231	-5.5241	-9.78	126.60	-19.5	60.1	8.08	-0.0419	0.4250	1902081155
-CI07A	46.231	-5.5241	-6.85	125.03	549.6	72.6	6.46	-0.1952	0.0530	1904062155
-CI07A	46.231	-5.5241	-31.80	-71.45	55.9	238.7	7.91	-1.8757	0.4471	1911042153
-CI08A	46.185	-5.6842	-17.29	147.87	-10.2	37.9	7.44	-0.4694	0.0833	1810260905
-CI08A	46.185	-5.6842	-10.37	119.05	-19.5	80.2	6.74	-0.6585	0.0788	1901220510
-CI08A	46.185	-5.6842	-7.00	156.40	384.4	42.1	4.58	-0.8294	0.3038	1901260351
-CI08A	46.185	-5.6842	-5.69	126.66	-91.0	62.9	7.62	-1.2057	0.3176	1909290202
-CI09A	46.193	-5.8187	-12.22	146.24	-10.0	42.1	6.97	-0.4719	0.1859	1809230552
-CI09A	46.193	-5.8187	-7.43	128.75	159.0	70.2	6.22	-0.6023	0.1002	1812011327
-CI09A	46.193	-5.8187	-10.37	119.05	-19.5	80.3	6.75	-0.8538	0.0843	1901220510
-CI09A	46.193	-5.8187	-8.52	127.04	-15.6	60.9	7.92	-0.6865	0.1300	1903060013
-CI09A	46.193	-5.8187	-55.76	-27.85	74.2	198.9	7.71	-0.0111	0.1160	1904051614
-CH0A	46.105	-5.9172	-0.26	119.90	-19.5	72.4	7.62	-0.1711	0.0390	1809281002
-CH0A	46.105	-5.9172	-58.42	-26.33	164.8	197.1	7.42	-1.3135	0.0682	1812110226
-CH0A	46.105	-5.9172	-30.11	-71.58	61.3	240.2	8.05	-0.0236	0.2471	1901200132



STA	STA LAT	STA LON	EV LAT	EV LON	DEP	BAZ	INC	SI	SIerr	EQ_ID (yy,mm,dd,hh,m m)
CH1A	46.087	-6.0314	-58.42	-26.33	164.8	197.1	7.42	-1.0427	0.0921	1812110226
CH1A	46.087	-6.0314	-10.34	119.05	-19.5	80.3	6.76	-0.0942	0.0732	1901212359
CH1A	46.087	-6.0314	-2.78	100.26	-19.5	89.0	9.35	-0.8960	0.1927	1902021059
CH1A	46.087	-6.0314	-29.00	139.37	434.8	39.7	9.38	-0.6820	0.2361	1906040439
CH1A	46.087	-6.0314	-0.49	126.18	-19.5	67.0	7.17	-0.6936	0.0319	1907071508
CH2A	46.053	-6.1727	-58.42	-26.33	164.8	197.2	7.42	-1.0550	0.1108	1812110226
CH2A	46.053	-6.1727	-5.86	126.89	-83.2	62.9	7.65	-0.0273	0.0413	1812290339
CH2A	46.053	-6.1727	-7.00	156.40	384.4	42.8	4.59	-0.9258	0.1733	1901260351
CH2A	46.053	-6.1727	-29.00	139.37	434.8	39.8	9.38	-0.6696	0.0703	1906040439
CH2A	46.053	-6.1727	-6.38	129.17	226.4	69.5	6.29	-0.5003	0.0529	1906240253
CH2A	46.053	-6.1727	-0.49	126.18	-19.5	67.1	7.18	-0.7010	0.0255	1907071508
CH2A	46.053	-6.1727	-6.80	125.20	-19.5	63.9	7.91	-0.4365	0.0629	1910290104
CH2A	46.053	-6.1727	-6.94	125.31	-19.9	63.7	7.92	-0.9995	0.1303	1910310111
CH3A	45.994	-6.2554	-0.00	119.76	-10.0	72.6	7.69	-1.8037	0.1709	1809281014
CH3A	45.994	-6.2554	-4.94	151.71	139.8	46.8	5.02	-0.3421	0.2386	1810102200
CH3A	45.994	-6.2554	-5.86	126.89	-83.2	63.0	7.66	-0.0133	0.0877	1812290339
CH3A	45.994	-6.2554	-7.00	156.40	384.4	42.9	4.59	-0.7991	0.0959	1901260351
CH3A	45.994	-6.2554	-29.00	139.37	434.8	39.9	9.38	-1.0184	0.0821	1906040439
CH4A	46.004	-6.3926	-1.06	119.96	-10.0	73.3	7.57	-1.7214	0.4915	1809281025
CH4A	46.004	-6.3926	-2.27	126.85	-66.8	65.6	7.31	-1.0425	0.1084	1901061727
CH4A	46.004	-6.3926	-42.87	-42.28	19.5	154.4	9.44	-0.7778	0.0786	1901221901
CH4A	46.004	-6.3926	-55.76	-27.85	74.2	199.1	7.72	-0.0462	0.2071	1904051614
CH5A	46.005	-6.5370	-0.26	119.90	-19.5	73.0	7.67	-0.3478	0.0340	1809281002

STA	STA LAT	STA LON	EV LAT	EV LON	DEP	BAZ	INC	SI	SIerr	EQ_ID (yy,mm,dd,hh,m m)
CH5A	46.005	-6.5370	-4.94	151.71	139.8	47.2	5.03	-0.9066	0.2099	1810102200
CH5A	46.005	-6.5370	-57.30	-66.37	63.3	216.4	6.03	-0.0711	0.1547	1810290654
CH5A	46.005	-6.5370	-5.86	126.89	83.2	63.2	7.68	-0.0152	0.0767	1812290339
CH5A	46.005	-6.5370	-5.52	133.85	9.8	65.2	6.08	-0.4599	0.1246	1901260812
CH5A	46.005	-6.5370	-9.78	126.60	19.5	61.0	8.15	-0.4844	0.2110	1902081155
CH5A	46.005	-6.5370	-6.94	146.46	139.5	54.2	5.15	-1.0375	0.0683	1905062119
CH5A	46.005	-6.5370	-2.16	138.50	19.5	58.7	6.06	-0.4506	0.0900	1906191724
CH5A	46.005	-6.5370	-19.79	144.47	409.8	40.6	7.87	-1.1455	0.0290	1906281551
CH5A	46.005	-6.5370	-0.49	126.18	19.5	67.4	7.21	-0.6778	0.0558	1907071508
CH5A	46.005	-6.5370	-60.03	-26.63	124.2	196.7	7.23	-0.8547	0.0277	1908272355
CH5A	46.005	-6.5370	-1.56	126.39	59.0	66.5	7.29	-0.7970	0.0410	1911141617
CH6A	45.925	-6.6170	-0.26	119.90	19.5	73.0	7.67	-0.6229	0.0386	1809281002
CH6A	45.925	-6.6170	-1.06	119.96	10.0	73.5	7.59	-0.4874	0.1644	1809281025
CH6A	45.925	-6.6170	-35.87	101.03	18	253.1	5.33	-0.0334	0.2491	1812190137
CH6A	45.925	-6.6170	-42.87	-42.28	19.5	154.6	9.46	-0.0054	0.0569	1901221901
CH6A	45.925	-6.6170	-5.52	133.85	9.8	65.3	6.09	-0.0277	0.3249	1901260812
CH6A	45.925	-6.6170	-2.72	100.20	19.5	89.5	9.43	-0.0097	0.1283	1902020927
CH6A	45.925	-6.6170	-2.78	100.26	19.5	89.4	9.42	-0.0110	0.1277	1902021059
CH6A	45.925	-6.6170	-9.78	126.60	19.5	61.1	8.15	-0.0456	0.4047	1902081155
CH6A	45.925	-6.6170	-10.35	126.12	62.1	61.2	8.24	-1.5484	0.1891	1903081506
CH6A	45.925	-6.6170	-11.71	125.30	84.8	60.9	8.47	-1.0051	0.0516	1904230537
CH6A	45.925	-6.6170	-6.94	146.46	139.5	54.3	5.15	-0.9850	0.0723	1905062119
CH6A	45.925	-6.6170	-4.10	152.61	19.5	45.7	5.08	-0.8694	0.1868	1905141258

STA	STA LAT	STA LON	EV LAT	EV LON	DEP	BAZ	INC	SI	SIerr	EQ_ID (yy,mm,dd,hh,m m)
CH6A	45.925	-6.6170	-29.00	139.37	434.8	40.1	9.40	-0.9680	0.0709	1906040439
CH6A	45.925	-6.6170	-2.16	138.50	19.5	58.8	6.06	-1.3793	0.1107	1906191724
CH6A	45.925	-6.6170	-6.38	129.17	226.4	69.9	6.32	-0.5927	0.0624	1906240253
CH6A	45.925	-6.6170	-19.79	144.47	409.8	40.7	7.87	-1.3315	0.0520	1906281551
CH6A	45.925	-6.6170	-0.49	126.18	19.5	67.5	7.21	-0.8738	0.0392	1907071508
CH6A	45.925	-6.6170	-0.64	128.02	9.8	66.7	6.95	-1.3038	0.1065	1907140910
CH6A	45.925	-6.6170	-60.03	-26.63	124.2	196.8	7.23	-1.3241	0.0545	1908272355
CH7A	45.947	-6.7180	-0.26	119.90	19.5	73.1	7.69	-0.4495	0.0705	1809281002
CH7A	45.947	-6.7180	-10.46	120.17	10.0	80.3	6.72	-1.4507	0.2269	1810020016
CH7A	45.947	-6.7180	-7.45	114.43	19.5	82.3	7.48	-0.0878	0.1087	1810101844
CH7A	45.947	-6.7180	-5.86	126.89	83.2	63.4	7.69	-0.0272	0.1362	1812290339
CH7A	45.947	-6.7180	-30.11	-71.58	61.3	240.7	7.99	-0.3770	0.1061	1901200132
CH7A	45.947	-6.7180	-42.87	-42.28	19.5	154.6	9.46	-0.9240	0.1025	1901221901
CH7A	45.947	-6.7180	-10.35	126.12	-62.1	61.3	8.25	-0.6499	0.0917	1903081506
CH7A	45.947	-6.7180	-29.00	139.37	434.8	40.2	9.41	-0.7326	0.0746	1906040439
CH7A	45.947	-6.7180	-19.79	144.47	409.8	40.8	7.88	-0.8229	0.0342	1906281551
CH7A	45.947	-6.7180	-0.49	126.18	19.5	67.6	7.22	-0.6969	0.0281	1907071508
CH7A	45.947	-6.7180	-6.80	125.15	19.5	64.4	7.95	-0.3724	0.0796	1910161137
CH8A	45.900	-6.7699	-0.26	119.90	19.5	73.2	7.69	-0.5447	0.0679	1809281002
CH8A	45.900	-6.7699	-10.51	120.24	19.5	80.3	6.71	-0.5548	0.1480	1810012359
CH8A	45.900	-6.7699	-58.42	-26.33	164.8	197.5	7.42	-0.1933	0.0836	1812110226
CH8A	45.900	-6.7699	-42.87	-42.28	19.5	154.7	9.47	-1.2876	0.1389	1901221901
CH8A	45.900	-6.7699	-7.00	156.40	384.4	43.6	4.61	-0.0103	0.1471	1901260351

STA	STA LAT	STA LON	-EV LAT	EV LON	-DEP	-BAZ	INC	-SI	SIerr	EQ_ID (yy,mm,dd,hh,m m)
-CH8A	45.900	-6.7699	-5.52	133.85	-9.8	65.5	6.10	-0.0302	0.3543	1901260812
-CH8A	45.900	-6.7699	-3.35	152.23	358.6	46.0	5.13	-0.2036	0.3078	1902171435
-CH8A	45.900	-6.7699	-2.16	138.50	-19.5	59.0	6.07	-0.4230	0.0856	1906191724
-CH8A	45.900	-6.7699	-0.64	128.02	-9.8	66.9	6.97	-1.3366	0.1783	1907140910
-CH9A	45.945	-6.8987	-6.04	149.90	-19.5	50.3	5.07	-0.8620	0.1875	1812192137
-CH9A	45.945	-6.8987	-14.62	-70.10	258.6	250.6	9.81	-0.5240	0.0502	1903010850
-CH9A	45.945	-6.8987	-55.76	-27.85	74.2	199.4	7.71	-1.1017	0.0813	1904051614
-CH9A	45.945	-6.8987	-6.85	125.03	549.6	73.8	6.55	-1.8740	0.1424	1904062155
-CH9A	45.945	-6.8987	-1.81	122.63	-19.5	72.2	7.31	-0.7696	0.0560	1904121140
-CH9A	45.945	-6.8987	-29.00	139.37	434.8	40.3	9.42	-1.2433	0.1255	1906040439
-CH9A	45.945	-6.8987	-2.16	138.50	-19.5	59.0	6.08	-1.3913	0.0837	1906191724
-CH9A	45.945	-6.8987	-0.49	126.18	-19.5	67.7	7.24	-0.9356	0.0420	1907071508
-CH9A	45.945	-6.8987	-60.03	-26.63	124.2	196.9	7.22	-0.7249	0.0415	1908272355
-CH9A	45.945	-6.8987	-35.41	-73.17	13.1	237.9	7.35	-0.7925	0.0687	1909291557
-CH9A	45.945	-6.8987	-1.56	126.39	-59.0	66.8	7.32	-1.5790	0.0520	1911141617
-CI21A	45.724	-7.1389	-0.26	119.90	-19.5	73.5	7.71	-1.0832	0.0989	1809281002
-CI21A	45.724	-7.1389	-0.00	119.76	-10.0	73.4	7.75	-1.5397	0.0906	1809281014
-CI21A	45.724	-7.1389	-5.86	126.89	-83.2	63.8	7.72	-0.8406	0.0842	1812290339
-CI21A	45.724	-7.1389	-10.34	119.05	-19.5	81.3	6.85	-0.1473	0.2306	1901212359
-CI21A	45.724	-7.1389	-10.37	119.05	-19.5	81.5	6.85	-0.2566	0.1864	1901220510
-CI21A	45.724	-7.1389	-7.00	156.40	384.4	44.1	4.62	-0.9413	0.2628	1901260351
-CI21A	45.724	-7.1389	-6.38	129.17	226.4	70.4	6.35	-0.9671	0.0372	1906240253
-CI21A	45.724	-7.1389	-0.49	126.18	-19.5	68.0	7.25	-1.1114	0.0520	1907071508

STA	STA LAT	STA LON	-EV LAT	EV LON	-DEP	-BAZ	INC	SI	SIerr	EQ_ID (yy,mm,dd,hh,m m)
-CI21A	45.724	-7.1389	-18.05	120.33	-9.8	86.7	6.12	-1.1557	0.1200	1907140539
-CI21A	45.724	-7.1389	-0.92	128.60	-9.8	67.1	6.92	-0.0895	0.1605	1909141621
-CI22A	45.684	-7.1415	-0.26	119.90	-19.5	73.5	7.71	-0.7957	0.0723	1809281002
-CI22A	45.684	-7.1415	-0.00	119.76	-10.0	73.4	7.75	-1.9444	0.1960	1809281014
-CI22A	45.684	-7.1415	-0.49	126.18	-19.5	68.0	7.24	-0.9683	0.0948	1907071508
-CI22A	45.684	-7.1415	-18.05	120.33	-9.8	86.7	6.12	-0.9249	0.1636	1907140539
-CI23A	45.678	-7.2388	-0.26	119.90	-19.5	73.6	7.72	-1.0696	0.0717	1809281002
-CI23A	45.678	-7.2388	-10.46	120.17	-10.0	80.8	6.75	-0.3726	0.1663	1810020016
-CI23A	45.678	-7.2388	-23.04	112.66	-10.2	96.6	6.36	-0.0229	0.2452	1812161426
-CI23A	45.678	-7.2388	-5.86	126.89	-83.2	63.9	7.72	-0.3909	0.0632	1812290339
-CI23A	45.678	-7.2388	-2.27	126.85	-66.8	66.4	7.36	-0.4645	0.0964	1901061727
-CI23A	45.678	-7.2388	-8.52	127.04	-15.6	62.2	8.01	-0.4764	0.0846	1903060013
-CI23A	45.678	-7.2388	-55.76	-27.85	74.2	199.6	7.73	-0.0351	0.1391	1904051614
-CI23A	45.678	-7.2388	-11.71	125.30	-84.8	61.5	8.51	-0.8582	0.0591	1904230537
-CI23A	45.678	-7.2388	-6.91	160.18	-19.5	39.6	4.49	-1.3872	0.1619	1905030725
-CI23A	45.678	-7.2388	-6.26	126.61	-98.0	64.0	7.78	-0.5985	0.0725	1905311012
-CI23A	45.678	-7.2388	-6.38	129.17	226.4	70.5	6.36	-0.9549	0.0367	1906240253
-CI23A	45.678	-7.2388	-0.49	126.18	-19.5	68.1	7.25	-0.8975	0.0462	1907071508
-CI23A	45.678	-7.2388	-6.80	125.20	-19.5	64.8	7.98	-0.7865	0.0844	1910290104
-CI23A	45.678	-7.2388	-1.56	126.39	-59.0	67.1	7.33	-1.1949	0.1322	1911141617
-CI24A	45.650	-7.2530	-0.26	119.90	-19.5	73.6	7.72	-1.0694	0.0929	1809281002
-CI24A	45.650	-7.2530	-5.86	126.89	-83.2	63.9	7.72	-0.3099	0.0539	1812290339
-CI24A	45.650	-7.2530	-6.85	125.03	549.6	74.2	6.57	-0.1893	0.0861	1904062155

STA	STA LAT	STA LON	-EV LAT	EV LON	-DEP	-BAZ	INC	SI	SIerr	EQ_ID (yy,mm,dd,hh,m m)
-CI24A	45.650	-7.2530	-11.71	125.30	-84.8	61.5	8.50	-0.8582	0.0459	1904230537
-CI24A	45.650	-7.2530	-6.94	146.46	139.5	55.1	5.17	-0.0734	0.2975	1905062119
-CI24A	45.650	-7.2530	-6.38	129.17	226.4	70.6	6.36	-1.0258	0.0482	1906240253
-CI24A	45.650	-7.2530	-0.49	126.18	-19.5	68.1	7.25	-0.9026	0.0457	1907071508
-CI24A	45.650	-7.2530	-4.44	101.28	-19.5	90.3	9.18	-1.0278	0.0605	1910142223
-CI24A	45.650	-7.2530	-6.80	125.20	-19.5	64.9	7.98	-0.9197	0.0646	1910290104
-CI24A	45.650	-7.2530	-1.64	132.86	-9.8	61.8	6.84	-0.5526	0.0733	1911231211
-CI25A	45.629	-7.3243	-0.26	119.90	-19.5	73.7	7.73	-0.9740	0.0663	1809281002
-CI25A	45.629	-7.3243	-1.06	119.96	-10.0	74.2	7.64	-0.6391	0.1449	1809281025
-CI25A	45.629	-7.3243	-5.86	126.89	-83.2	64.0	7.72	-0.4368	0.0366	1812290339
-CI25A	45.629	-7.3243	-10.37	119.05	-19.5	81.7	6.86	-0.9757	0.0780	1901220510
-CI25A	45.629	-7.3243	-11.71	125.30	-84.8	61.5	8.51	-0.5712	0.0546	1904230537
-CI25A	45.629	-7.3243	-6.26	126.61	-98.0	64.1	7.78	-1.7950	0.3814	1905311012
-CI25A	45.629	-7.3243	-6.38	129.17	226.4	70.6	6.36	-1.0434	0.0566	1906240253
-CI25A	45.629	-7.3243	-0.49	126.18	-19.5	68.2	7.26	-0.9086	0.0999	1907071508
-CI25A	45.629	-7.3243	-6.80	125.20	-19.5	64.9	7.98	-1.1708	0.1304	1910290104
-CI25A	45.629	-7.3243	-1.56	126.39	-59.0	67.2	7.34	-0.2650	0.0838	1911141617
-CI26A	45.596	-7.3907	-10.37	119.05	-19.5	81.7	6.87	-1.1453	0.2121	1901220510
-CI26A	45.596	-7.3907	-10.09	152.09	-10.2	51.7	4.62	-0.7148	0.2772	1903101248
-CI26A	45.596	-7.3907	-0.49	126.18	-19.5	68.2	7.26	-1.1745	0.0782	1907071508
-CI27A	45.596	-7.4880	-10.46	120.17	-10.0	81.0	6.77	-0.3866	0.4755	1810020016
-CI28A	45.556	-7.5737	-11.71	125.30	-84.8	61.7	8.53	-0.4497	0.1141	1904230537
-CI29A	45.538	-7.6631	-6.26	126.61	-98.0	64.4	7.81	-0.4439	0.2432	1905311012

STA	STA LAT	STA LON	-EV LAT	EV LON	-DEP	-BAZ	INC	SI	SIerr	EQ_ID (yy,mm,dd,hh,m m)
-CI29A	45.538	-7.6631	-6.38	129.17	226.4	71.0	6.38	-1.0928	0.1515	1906240253
-CI29A	45.538	-7.6631	-0.49	126.18	-19.5	68.5	7.28	-0.7900	0.3852	1907071508
-CI29A	45.538	-7.6631	-6.26	126.61	-98.0	64.4	7.81	-0.4439	0.2432	1905311012
-CI29A	45.538	-7.6631	-6.38	129.17	226.4	71.0	6.38	-1.0928	0.1515	1906240253
-CI29A	45.538	-7.6631	-0.49	126.18	-19.5	68.5	7.28	-0.7900	0.3852	1907071508
-CI30A	45.524	-7.7104	-6.04	149.90	-19.5	51.5	5.08	-1.1889	0.2453	1812192137
-CI30A	45.524	-7.7104	-0.49	126.18	-19.5	68.5	7.28	-1.2315	0.1096	1907071508
-CI30A	45.524	-7.7104	-0.92	128.60	-9.8	67.6	6.95	-0.4890	0.2897	1909141621
-CI31A	45.441	-7.8122	-14.62	-70.10	258.6	251.2	9.74	-0.5816	0.0492	1903010850
-CI31A	45.441	-7.8122	-29.00	139.37	434.8	41.0	9.43	-0.6504	0.1497	1906040439
-CI31A	45.441	-7.8122	-6.80	125.15	-19.5	65.4	8.02	-0.4940	0.0762	1910161137
-CI32A	45.359	-7.9062	-6.26	126.61	-98.0	64.6	7.82	-0.7431	0.1956	1905311012
-CI32A	45.359	-7.9062	-6.80	125.20	-19.5	65.4	8.02	-0.4591	0.1371	1910290104
-CI33A	45.288	-7.9447	-23.04	112.66	-10.2	97.3	6.42	-0.9293	0.1217	1812161426
-CI33A	45.288	-7.9447	-30.11	-71.58	61.3	241.3	7.93	-0.6535	0.1378	1901200132
-CI33A	45.288	-7.9447	-9.78	126.60	-19.5	62.2	8.22	-0.2719	0.0948	1902081155
-CI33A	45.288	-7.9447	-19.79	144.47	409.8	41.9	7.89	-1.4684	0.0720	1906281551
-CI34A	45.191	-8.0221	-29.00	139.37	434.8	41.2	9.42	-0.8557	0.1315	1906040439
-CI36A	45.031	-8.1833	-10.46	120.17	-10.0	81.8	6.82	-1.1712	0.2383	1810020016
-CI36A	45.031	-8.1833	-10.37	119.05	-19.5	82.6	6.93	-0.7112	0.0744	1901220510
-CI36A	45.031	-8.1833	-2.72	100.20	-19.5	90.6	9.62	-0.0929	0.2266	1902020927
-CI36A	45.031	-8.1833	-11.71	125.30	-84.8	62.3	8.55	-0.3814	0.0714	1904230537
-CI36A	45.031	-8.1833	-6.26	126.61	-98.0	64.9	7.83	-0.8216	0.1222	1905311012

STA	STA LAT	STA LON	EV LAT	EV LON	DEP	BAZ	INC	SI	SIerr	EQ_ID (yy,mm,dd,hh,m m)
-C137A	44.952	-8.2530	-23.04	112.66	-10.2	97.6	6.45	-1.4554	0.4135	1812161426
-C137A	44.952	-8.2530	-6.26	126.61	-98.0	65.0	7.83	-0.3742	0.1807	1905311012
-C137A	44.952	-8.2530	-5.97	149.59	-77.3	52.8	5.10	-0.9196	0.1089	1907150821
-C137A	44.952	-8.2530	-0.92	128.60	-9.8	68.3	6.97	-0.7664	0.2996	1909141621
-C137A	44.952	-8.2530	-6.80	125.15	-19.5	65.8	8.03	-0.0407	0.0936	1910161137
-C138A	44.762	-8.4124	-57.30	-66.37	63.3	216.7	6.05	-0.0020	0.0200	1810290654
-C138A	44.762	-8.4124	-57.49	-66.29	33.6	216.6	6.04	-0.0013	0.0212	1810292017
-C138A	44.762	-8.4124	-14.62	-70.10	258.6	251.6	9.71	-0.5057	0.0510	1903010850
-C138A	44.762	-8.4124	-11.71	125.30	-84.8	62.5	8.55	-0.0356	0.1141	1904230537
-C138A	44.762	-8.4124	-6.26	126.61	-98.0	65.1	7.83	-1.3133	0.1998	1905311012
-C138A	44.762	-8.4124	-19.79	144.47	409.8	42.4	7.87	-0.0079	0.0850	1906281551
-C138A	44.762	-8.4124	-0.49	126.18	-19.5	69.3	7.31	-0.0235	0.2395	1907071508
-C138A	44.762	-8.4124	-0.64	128.02	-9.8	68.6	7.05	-0.0216	0.2307	1907140910
-C138A	44.762	-8.4124	-5.97	149.59	-77.3	53.0	5.09	-0.0113	0.1240	1907150821
-C138A	44.762	-8.4124	-6.80	125.20	-19.5	66.0	8.03	-0.0554	0.3688	1910290104
-C138A	44.762	-8.4124	-6.87	125.24	-34.8	65.9	8.03	-0.0287	0.3667	1910290242
-C138A	44.762	-8.4124	-6.94	125.31	-19.9	65.7	8.03	-0.0234	0.3639	1910310111
-C138A	44.762	-8.4124	-31.80	-71.45	55.9	240.1	7.77	-0.0203	0.2100	1911042153
-C138A	44.762	-8.4124	-1.64	132.86	-9.8	63.1	6.88	-0.0321	0.3138	1911231211
-C138A	44.762	-8.4124	-18.35	-70.45	9.8	249.3	9.30	-0.0295	0.3405	1912030846
-C139A	44.674	-8.4731	-57.30	-66.37	63.3	216.7	6.05	-1.1151	0.1490	1810290654
-C139A	44.674	-8.4731	-2.72	100.20	-19.5	90.8	9.66	-0.0927	0.2980	1902020927
-C139A	44.674	-8.4731	-60.03	-26.63	124.2	197.5	7.34	-0.9247	0.0259	1908272355



STA	STA LAT	STA LON	EV LAT	EV LON	DEP	BAZ	INC	SI	SIerr	EQ_ID (yy,mm,dd,hh,m m)
CI39A	44.674	-8.4731	-1.64	132.86	-9.8	63.2	6.88	-0.1997	0.1510	1911231211
CI40A	44.605	-8.5230	-2.72	100.20	-19.5	90.9	9.66	-1.9685	0.2516	1902020927
CI40A	44.605	-8.5230	-2.16	138.50	-19.5	61.2	6.12	-0.7546	0.0745	1906191724
CI40A	44.605	-8.5230	-18.05	120.33	-9.8	88.3	6.22	-0.7765	0.2318	1907140539
CI40A	44.605	-8.5230	-0.92	128.60	-9.8	68.6	6.97	-0.2667	0.2197	1909141621
CI41A	44.530	-8.5343	-14.62	-70.10	258.6	251.7	9.71	-1.1041	0.0740	1903010850
CI41A	44.530	-8.5343	-6.85	125.03	549.6	75.7	6.64	-0.4293	0.0606	1904062155
CI41A	44.530	-8.5343	-30.00	-72.11	9.8	241.9	7.90	-0.5665	0.0411	1906140019
CI41A	44.530	-8.5343	-6.38	129.17	226.4	72.1	6.41	-0.4470	0.0766	1906240253
CI41A	44.530	-8.5343	-19.79	144.47	409.8	42.6	7.85	-0.7258	0.0398	1906281551
CI41A	44.530	-8.5343	-60.03	-26.63	124.2	197.6	7.35	-0.7816	0.0243	1908272355
CI41A	44.530	-8.5343	-35.41	-73.17	13.1	238.4	7.33	-0.7712	0.0424	1909291557
CI42A	44.462	-8.5805	-10.37	119.05	-19.5	83.1	6.95	-1.1350	0.2285	1901220510
CI42A	44.462	-8.5805	-42.87	-42.28	19.5	155.9	9.78	-0.8690	0.0501	1901221901
CI42A	44.462	-8.5805	-6.38	129.17	226.4	72.2	6.41	-0.6015	0.0986	1906240253
CI42A	44.462	-8.5805	-35.41	-73.17	13.1	238.4	7.33	-1.2119	0.0655	1909291557
CI43A	44.397	-8.6165	-42.87	-42.28	19.5	155.9	9.80	-0.9450	0.0675	1901221901
CI43A	44.397	-8.6165	-3.35	152.23	358.6	48.8	5.12	-0.6969	0.0964	1902171435
CI43A	44.397	-8.6165	-14.62	-70.10	258.6	251.7	9.70	-0.6959	0.0911	1903010850
CI43A	44.397	-8.6165	-6.38	129.17	226.4	72.3	6.41	-0.3171	0.0641	1906240253
CI43A	44.397	-8.6165	-34.17	-72.38	19.7	238.9	7.50	-0.8792	0.0723	1908011828
CI43A	44.397	-8.6165	-35.41	-73.17	13.1	238.4	7.33	-1.0847	0.0803	1909291557
CW01A	45.433	-7.2591	-57.49	-66.29	33.6	216.4	6.04	-0.2244	0.4004	1810292017

STA	STA LAT	STA LON	-EV LAT	EV LON	-DEP	-BAZ	INC	SI	SIerr	EQ_ID (yy,mm,dd,hh,m m)
-CW01A	45.433	-7.2591	-23.04	112.66	-10.2	96.7	6.37	-0.7174	0.1679	1812161426
-CW01A	45.433	-7.2591	-42.87	-42.28	-19.5	155.0	9.57	-0.3877	0.1196	1901221901
-CW01A	45.433	-7.2591	-0.49	126.18	-19.5	68.2	7.24	-0.8938	0.0544	1907071508
-CW02A	45.433	-7.3747	-57.30	-66.37	63.3	216.5	6.04	-1.7705	0.1204	1810290654
-CW02A	45.433	-7.3747	-57.49	-66.29	33.6	216.4	6.03	-0.2153	0.0996	1810292017
-CW02A	45.433	-7.3747	-0.49	126.18	-19.5	68.3	7.25	-1.0730	0.0886	1907071508
-CW02A	45.433	-7.3747	-0.92	128.60	-9.8	67.4	6.93	-0.0417	0.1917	1909141621
-CW03A	45.407	-7.5053	-2.27	126.85	-66.8	66.7	7.37	-1.7258	0.1987	1901061727
-CW03A	45.407	-7.5053	-11.71	125.30	-84.8	61.7	8.51	-0.5868	0.0836	1904230537
-CW03A	45.407	-7.5053	-0.49	126.18	-19.5	68.4	7.26	-0.8621	0.1016	1907071508
-CW03A	45.407	-7.5053	-6.80	125.20	-19.5	65.1	7.99	-0.5815	0.2034	1910290104
-CW04A	45.367	-7.6128	-8.52	127.04	-15.6	62.5	8.02	-0.4399	0.0883	1903060013
-CW04A	45.367	-7.6128	-0.49	126.18	-19.5	68.5	7.27	-1.0816	0.0850	1907071508
-CW05A	45.324	-7.7318	-5.52	133.85	-9.8	66.6	6.14	-0.8727	0.1121	1901260812
-CW05A	45.324	-7.7318	-6.80	125.20	-19.5	65.3	8.00	-0.7146	0.0854	1910290104
-CT03A	44.324	-5.0275	-46.33	-35.07	33	159.7	9.43	-1.0060	0.0652	1307220701
-CT04A	44.371	-5.1477	-46.33	-35.07	33	159.7	9.42	-1.4409	0.0996	1307220701
-CT05A	44.370	-5.2677	-46.33	-35.07	33	159.8	9.43	-1.4937	0.0686	1307220701
-CT06A	44.382	-5.3872	-3.23	100.59	-23.5	88.7	9.18	-0.8362	0.1189	1307060505
-CT08A	44.412	-5.6051	-18.79	145.27	598.0	39.9	7.44	-0.6962	0.0466	1305140032
-CT09A	44.429	-5.7144	-46.33	-35.07	33	160.1	9.44	-1.6600	0.0938	1307220701
-CT10A	44.437	-5.7940	-46.33	-35.07	33	160.2	9.44	-1.9193	0.0602	1307220701
-CT11A	44.454	-5.9026	-10.03	107.18	-11.1	89.3	7.83	-0.9164	0.0895	1306131647

STA	STA LAT	STA LON	-EV LAT	EV LON	-DEP	-BAZ	-INC	-SI	SIerr	EQ_ID (yy,mm,dd,hh,m m)
CT11A	44.454	-5.9026	-5.43	-81.99	5	264.6	9.80	-1.6904	0.0501	1308120949
CT12A	44.475	-5.9826	-46.33	-35.07	33	160.3	9.44	-1.8337	0.0526	1307220701
CT13A	44.460	-6.0559	-46.33	-35.07	33	160.3	9.45	-1.9759	0.0929	1307220701
CT20A	44.585	-6.5389	-46.33	-35.07	33	160.6	9.45	-1.3514	0.0864	1307220701
CT21A	44.654	-6.5686	-3.23	100.59	-23.5	89.5	9.31	-0.3706	0.1366	1307060505
CT21A	44.654	-6.5686	-46.33	-35.07	33	160.7	9.44	-1.1207	0.0477	1307220701

580

581 Table S2 - Anisotropy parameters obtained from SI measurements

STA	ST LAT	ST LON	-FPD	Time Delay (s)	-FPDerr	-TDerr
CE03A	45.786	7.6024	-0.78	0.74992	-11.2	0,639
CI07A	46.231	5.5241	-11.58	0.13265	-14.3	0,203
CI11A	46.087	6.0314	-0.32	0.83092	-12.8	1,75
CI15A	46.005	6.5370	-7.45	1.08421	-7.0	1,101
CI16A	45.925	6.6170	-2.58	1.09206	-2.1	1,304
CI17A	45.947	6.7180	-11.48	0.79153	-12.3	0,709
CI18A	45.900	6.7699	-15.11	0.64205	-21.3	1,154
CI19A	45.945	6.8987	-0.99	1.32372	-4.1	1,079
CI21A	45.724	7.1389	-37.08	1.03633	-36.2	0,871
CI23A	45.678	7.2388	-22.22	0.73735	-22.8	1,026
CI24A	45.650	7.2530	-37.75	0.92882	-32.4	0,781
CI38A	44.762	8.4124	-59.03	0.13426	-45.1	0,187
CI39A	44.674	8.4731	-43.54	1.00657	-79.8	1,005
CI41A	44.530	8.5343	-53.46	0.98773	-66.8	0,707
CI42A	44.462	8.5805	-76.64	2.17814	-79.3	1,755

STA	STLAT	STLON	FPD	Time Delay (s)	FPDerr	TDerr
CI43A	44.397	8.6165	-67.27	0.84845	-63.6	0,865
CW01A	45.433	7.2591	-1.35	0.88253	-5.7	1,428
CW02A	45.433	7.3747	-22.80	0.77871	-35.3	1,92